N O T I C E

THIS DOCUMENT HAS BEEN REPRODUCED FROM MICROFICHE. ALTHOUGH IT IS RECOGNIZED THAT CERTAIN PORTIONS ARE ILLEGIBLE, IT IS BEING RELEASED IN THE INTEREST OF MAKING AVAILABLE AS MUCH INFORMATION AS POSSIBLE

NI

NASA Technical Memorandum 83221

(NASA-TM-83221) RESEARCH AND TECHNOLOGY Annual Report (NASA) 68 p HC A04/MF A01 CSCL 05B
N82-13043
Unclas G3/99 08386

# Research and Technology

## 1981 Annual Report of the Langley Research Center


NASA
National Aeronautics and Space Administration

**Langley Research Center**
Hampton, Virginia 23665

## FOREWORD

The role of the Langley Research Center is to engage in the basic and applied research necessary for the advancement of aeronautics and space flight, to generate new and advanced concepts for the accomplishment of related national goals, and to provide research advice, technological support, and assistance to other NASA installations, other government agencies, and industry. This Langley Research Center 1981 Annual Report on Research and Technology contains highlights of our major accomplishments and applications made during the past year. The highlights illustrate both the broad range of the research and technology activities at the Langley Research Center and the contributions of this work toward maintaining United States leadership in aeronautics and space research. For further information about the report contact Dr. Frank Hohl or Ed Prior, Mail Stop 103, Langley Research Center, Hampton, Virginia 23665 (827-2664).

Results of Langley research and technology are also made available to users through the NASA scientific and technical information system. The research output of the Langley Research Center is listed by title in an annual compilation entitled "Scientific and Technical Information Output of the Langley Research Center." The compilation for calendar year 1980 contains 1428 items and is available on request from The Report and Manuscript Control Office, Mail Stop 180A, Langley Research Center, Hampton, Virginia 23665 (827-2301).

Donald P. Hearth
Director

## AVAILABILITY INFORMATION

The research and technology accomplishments in this report are arranged according to the NASA program office sponsoring the work and the Agencywide Research and Technology Objectives and Plans (RTOP) work breakdown structure. For additional information on any summary, contact the individual identified with the highlight. Commercial telephone users may dial the listed extension preceded by (804) 827. Telephone users with access to the Federal Telecommunications System (FTS) may dial the extension preceded by 928.

## CONTENTS



### Aeronautics and Space Technology

## Space and Terrestrial Applications



## Space Transportation Systems

# Aeronautics and Space Technology

## Viscous/Inviscid Flow Past Wing-Body Configurations

Interaction schemes coupling an accurate and efficient three-dimensional integral-boundary-layer method with a number of three-dimensional transonic full-potential wing-alone and wing-body codes have been under development since 1979. The present procedure uses the wing-body code FLO-30, an integral-boundary-layer method, and a full viscous wake model which accounts for displacement and curvature effects. It was found, in the course of this study, that inclusion of both body and wake effects is essential for good agreement with experiment.

The computed spanwise lift distribution is shown for a difficult supercritical wing transport configuration test case. The two curves show results from a purely inviscid calculation and a calculation using the present interaction procedure; experimental values are shown as symbols. The agreement is excellent (the scale is deleted because of FEDD restrictions). Chordwise pressure distributions predicted from the interaction procedure are compared with experimental values for another test case. This configuration also had supercritical airfoil wing sections. A strong shock wave can be seen across the upper wing surface.

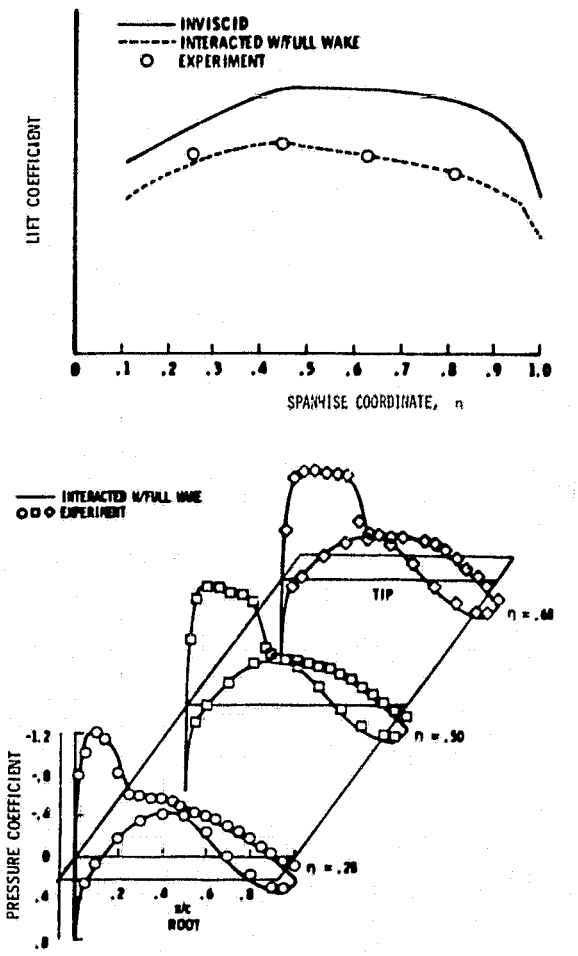


*Comparison of predicted and measured wing lift and pressures*

Craig L. Streett, 2627 (505-31-13)

## Transonic Flow Past Bodies in a Wind Tunnel

An accurate method for analysis of transonic flow about two-dimensional and axisymmetric bodies in wind tunnels has been developed. This required a robust computational algorithm and suitable boundary-fitted coordinates applicable to the full-potential equation and tunnel geometry. A coordinate system generated by a combination of conformal mappings and simple shearings suitable for two-dimensional axisymmetric bodies in a tunnel was developed in 1980. An accurate, conservative, finite-volume method has now been developed to solve the transonic full-potential equation. The artificial viscosity necessary to stabilize the scheme and to capture shocks is introduced by use of the artificial density method. The flow code has been written independently of the coordinate generation method so that it can accommodate general grids, including the above-described wind-tunnel coordinates. The prediction of free air flows using this code is accomplished by moving the tunnel wall far from the body.

The scheme was carefully checked against exact incompressible solutions for free air and tunnel wall flows. Comparisons have also been made with existing transonic potential and

Euler codes. In all cases examined, agreement has been excellent. The computed Mach contours are illustrated for a flow with free-stream Mach number of 0.73. In the computation, the tunnel walls were treated as being solid. The sonic line is indicated by the heavier line. The solution shows that the supersonic zone intersects the top tunnel wall and that there is a strong normal shock near the trailing edge.

Jerry C. South, Jr., 2627 (505-31-13)

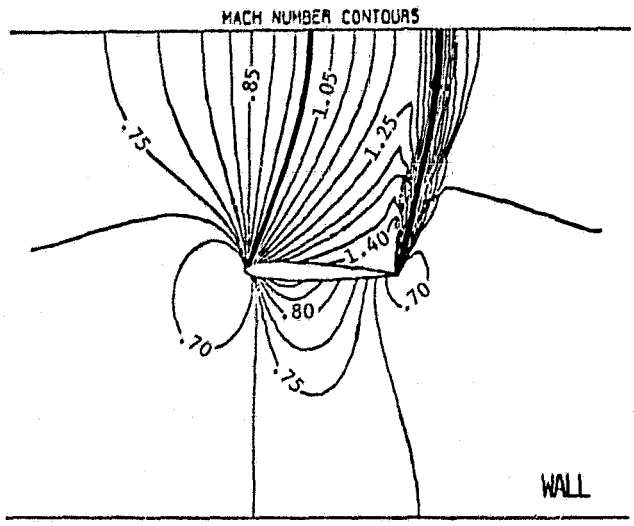


*Mach number contours for transonic potential flow past an airfoil*

## Flow in the Tile Gaps of the Space Shuttle TPS

Accurate prediction of the pressure distribution in the strain isolation pad (SIP) and the tiles of the Space Shuttle Orbiter thermal protection system (TPS) is necessary in order to calculate tile loads. Pressures in the porous tiles and SIP can be affected by the Shuttle surface pressure distribution communicating through the gaps between the tiles. Thus, a model for the tile-gap flow field is required before SIP and tile pressures can be predicted from a given Shuttle surface pressure distribution. In the present investigation, a Stokes flow (low Reynolds number) model was derived to predict the pressure and velocity in the tile gap. The model predicts that the mass flow rate through the tile gap is proportional to the cube of the gap width; thus the entire TPS flow field can be very sensitive to tile motion due to this flow metering effect.

A comparison of the pressure in the tile gap predicted by the present method with experimentally measured values is presented in the figure for a case in which a shock is impinging on the upper surface of the tile. Side loads calculated from these pressures indicate that the tile should move forward toward the low-pressure side and completely close the gap on that side. This would indicate that the SIP pressure should be biased to the high-pressure side of the tile, and this high-pressure air should flow forward under the adjacent tile. A complete model interacting the present analysis with a porous medium flow model for SIP and tile flows was developed by personnel in the Langley Systems Engineering Division; these results also show good agreement with experiment.

Douglas L. Dwoyer, 2627 (505-31-13)

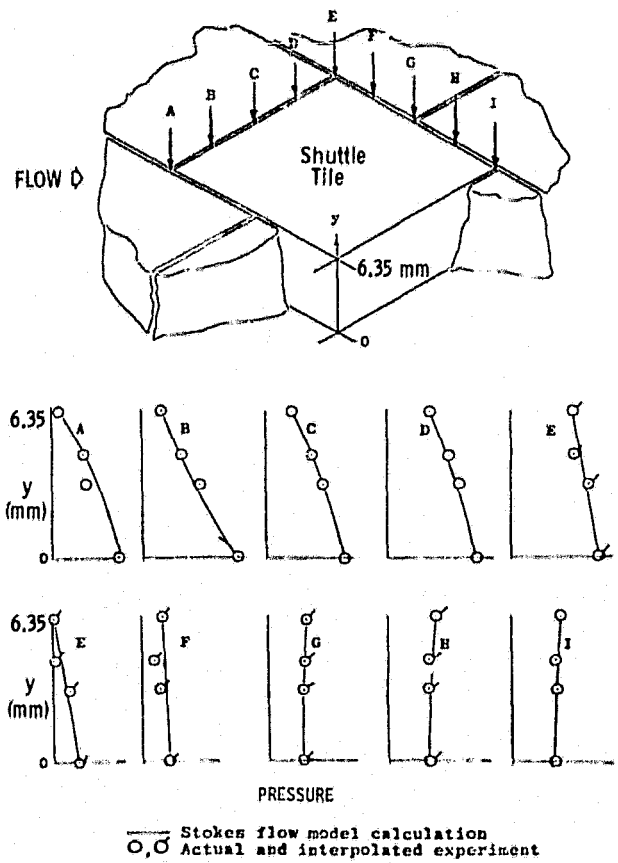


*Comparison of calculated and measured vertical pressure distribution in tile gap*

## Rotational Effects in Transonic Aerodynamics

For the past 10 years transonic aerodynamics theory has focused on the numerical solution of the potential flow equation. As a natural outgrowth of this effort, research is now being directed towards the numerical solution of the Euler equations which include rotational effects. During 1980 a technique for solving the Euler equations for transonic flow was developed which has been used to study a variety of rotational inviscid two-dimensional transonic flows.

Perhaps the most startling phenomenon discovered thus far is the possibility of inviscid separation induced by vorticity. An example of this phenomenon is illustrated for transonic flow over a circular cylinder. The vorticity, introduced by the recompression shock which forms at the top of the cylinder, retards the flow and induces a stagnation point and, hence, separation ahead of the usual rearward stagnation point. Theoretical evidence indicates that this is indeed a valid Euler solution, not a numerical effect. In addition to separation, the shock wave created a vortical layer at the rear of the cylinder, which is clearly indicated by the Mach contours. Perhaps inviscid theory alone can account for some effects traditionally associated with viscous flows. Clearly, vorticity can produce large-scale effects not predicted by the potential theory, and some of the ideas which have been developed on the basis of potential theory will have to be reformulated for the Euler equations.

Manuel D. Salas, 2627 (505-31-13)

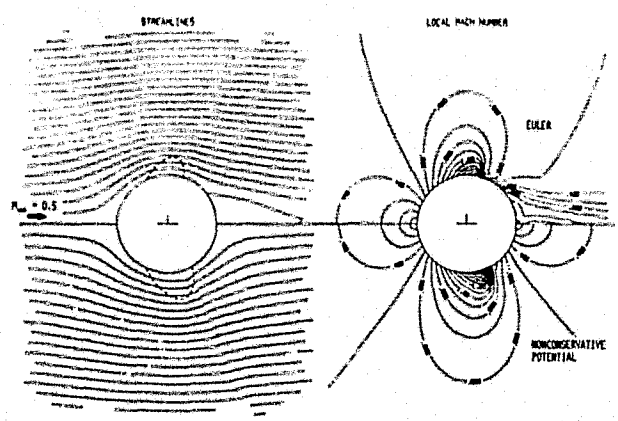


*Flow over a circular cylinder*

## Turbulent Drag Reduction Research for Energy Conservation

Turbulent skin friction drag is an important factor in the design and energy efficiency of many systems. For example, nearly one-half of an aircraft's fuel is burned to overcome turbulent friction drag, and in the pipeline transmission of such products as natural gas, oil, and coal slurries, the pumping energy is needed solely to overcome friction drag. A concept developed at Langley can possibly reduce this turbulent friction drag by creating a lower energy turbulent state. Basic turbulence research over the past 10 years has identified the detailed nature of the turbulence production process, and the new concept is designed to interfere with a portion of this process. The large-eddy break-up (LEBU) device is a thin flat surface submerged within the boundary layer at the appropriate location. The LEBU concept severely reduces the scale of the turbulent motions in the boundary layer, and results indicate a possible net drag reduction of up to 20 percent.

Jerry N. Hefner, 4546 (505-31-23)

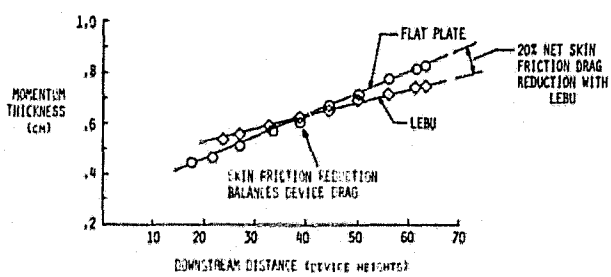


*Comparison of flat plate and LEBU devices*

## Frequency Scattering by a Turbulent Shear Layer

Sound propagation through a turbulent shear layer is important due to increased use of open-jet-flow facilities for aeroacoustic testing. Of concern are the effects of the shear layer between source and receiver on intensity, directivity, and spectra of the noise source compared to those which would be measured if the source were in flight. One

phenomenon observed in such acoustic testing is the spectral broadening of a tonal or narrowband source in the jet. Sound power radiated at a given frequency is received outside the jet as a band of frequencies scattered about the original frequency. Classical theories of sound propagation contain no mechanism to explain such an effect. It has been speculated that this frequency scattering may be caused by a Doppler shift produced as the sound traverses turbulent eddies in the flow. Recent in-house research has shown, however, that the apparent frequency shift is merely an artifact of amplitude modulation of the acoustic signal by the time-varying shear layer. A high-impedance harmonic acoustic source was placed in a large low-velocity jet. The sound was measured outside the jet after propagating through the shear layer. The power spectral density of the acoustic signal contains acoustic power in bands of considerable width about the source frequency and its harmonics. However, when the data are analyzed as the ratio of far-field autocorrelation to source autocorrelation, as illustrated, the modulation of the acoustic signal by the passage of large-scale structures (LSS) in the shear layer is observed. This modulation results in the generation of sidebands, which produces the observed spectra.

Jay C. Hardin, 2617 (505-31-23)

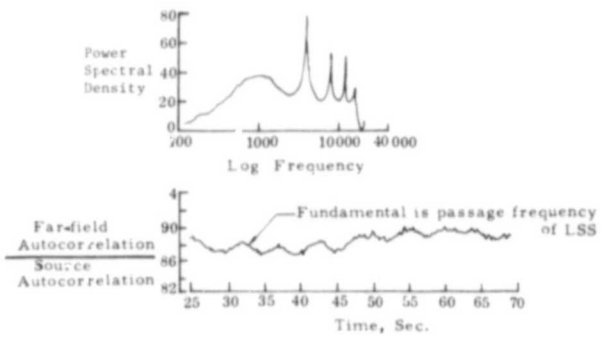


*Frequency scattering by a shear layer*

## Wind-Tunnel Wall Interference

Wind-tunnel data obtained on wing-section models have always required certain corrections for the interference of the tunnel walls on the flow about the model. In the past, most of these corrections concerned distortions in the flow caused by the walls above and below the model. This top- and bottom-wall interference required corrections to the lift, drag, and Mach number measured in the tunnel.

Another source of wind-tunnel interference on wing-section models is caused by the boundary layer on the sidewalls of the tunnel. The air flowing close to the surface of the sidewall is retarded due to its friction with the sidewall, and this thin layer of decelerated air is called the boundary layer. The pressures in the flow about the model cause variations in the thickness of the boundary layer, and these thickness variations in turn add a variation to the flow velocities induced by the model. With some simplifying assumptions, a mathematical model of the interference from the sidewall boundary layers was developed to determine the error in Mach number, lift, and drag measured in the tunnel due to the sidewall boundary layer. To evaluate this mathematical model, a wing-section model was tested in the Langley 6- by 19-Inch Transonic Tunnel with various thicknesses of sidewall boundary layers. The mathematical model used to predict boundary-layer interference worked satisfactorily for sidewall boundary layers with a thickness of up to 50 percent of the tunnel width.

John S. Peterson, 4514 (505-31-33)

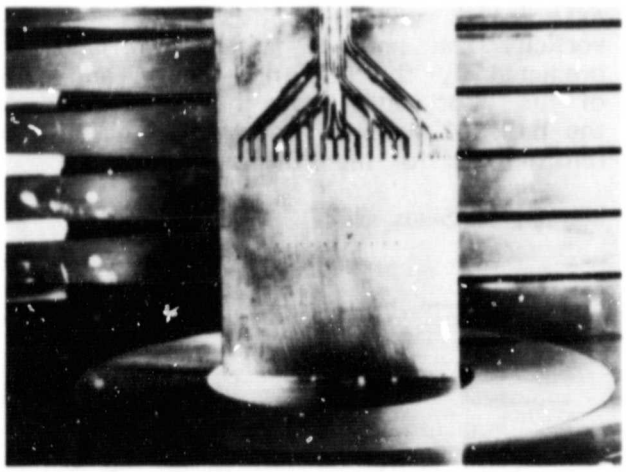

*Airfoil model in Langley 6- by 19-Inch Transonic Tunnel*

## Estimation of Vortex Flow Aerodynamics

In recent years interest has increased in slender-wing aircraft which incorporate higher sweep angles and thinner wing sections, and

which usually develop separation-induced vortex flows during some portion of their operational envelope. Whether by design or default, these vortical flow fields have significant induced effects on structural loads as well as on aerodynamic performance, stability, and control. It is important to understand, predict, and control the vortex for advantage in aircraft design.

The free vortex sheet (FVS) theory is one method presently under development for the estimation of the subject loads. The method is fully three-dimensional and models the flow with networks of higher-order doublet and source panels. Because the strength of the free vortex sheet as well as its shape and position are unknown, the problem is inherently nonlinear and requires an iterative solution procedure. The theory has been applied successfully to a variety of configurations. These include a cropped delta wing which has strong interactions between the leading-edge and side-edge vortex flows, an arrow wing which exhibits substantial trailing-edge notch effects, and a delta wing which incorporated leading-edge vortex flaps. All results were converged with a quasi-Newton iteration scheme so that the sum of the squares of the residuals was equal to or less than 0.000001.

In this example of the delta wing solution the wing has an inverse-taper leading-edge "vortex flap" deflected to achieve thrust recovery and, therefore, reduce drag while maintaining some vortex lift. This research is related to the development of maneuver capability for the supercruiser class of tactical fighters. The panel formulation for the converged solution is shown with wake panels removed for clarity. This visualization capability was achieved by interfacing the FVS code with an existing interactive graphics package. Also shown is the rotational nature of the field velocities near the vortex cores. These were obtained using grid generation techniques developed as part of an effort to evaluate off-body flow properties. Also illustrated is a spanwise pressure distribution at 44-percent root chord with the vortex-induced suction peak acting on the flap. This feature was exhibited along the entire flap.

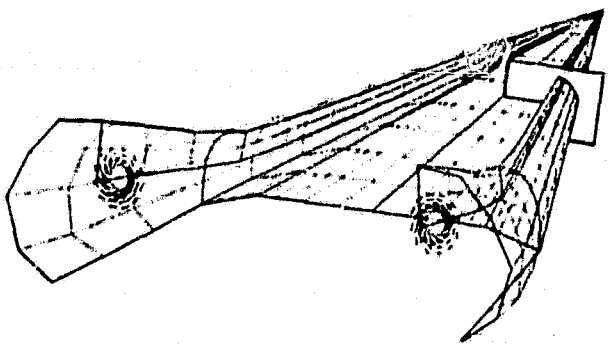

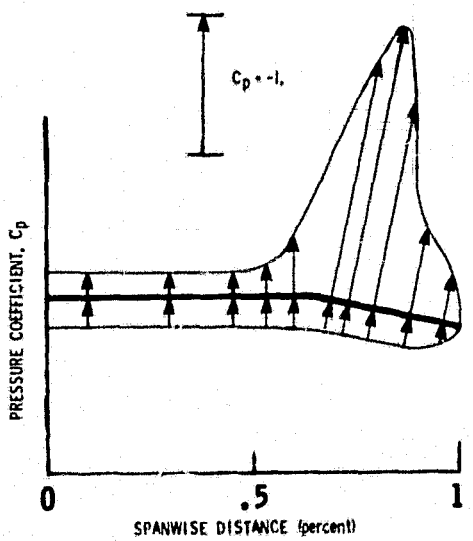


*Free vortex sheet solution for vortex flap*

James M. Luckring, 2601 (505-31-43)

## Coaxial Three-Component Laser Velocimeter

Three-component laser velocimeter measurements have been performed in small facilities by using a two-component fringe system mounted on the side of the facility to measure the axial (u) and vertical (v) components, and a second, one-component fringe system mounted on the top of the facility to measure the crossflow (w) component. This concept can not be utilized in large facilities due to the limitations of the mechanical traversing systems to achieve the positional accuracies required by a laser velocimeter system.

The three-component coaxial measurement concept presently under development at Langley utilizes a five-laser/two-color technique which generates four fringe patterns. The two fringe patterns generated by the four outside beams provide a measurement of the u- and v-components in

ORIGINAL PAGE IS
OF POOR QUALITY

the manner of a standard two-component laser velocimeter. The fringe pattern generated by the fifth beam (located to pass along the optical axis) and an outside beam is at a slight angle with respect to the u-component, thus containing information from the w-component. The final fringe pattern, generated by the fifth beam and the opposite outside beam, is also at a slight angle with respect to the u-component, but with the opposite sense. Thus, if the measurements from these two fringe patterns were vectorially subtracted, the result would be a measure of the crossflow or w-component. The measurements from the four fringe patterns are separated using color and frequency separation, and the vectorial subtraction is performed using electronic mixers. This concept was first tested in the Langley 4- by 7-Meter Tunnel to measure the downwash flow field behind an NACA 0012 airfoil. The test verified the concept and provided the information necessary to further develop the technique.

James F. Meyers, 4618 (Code 531)

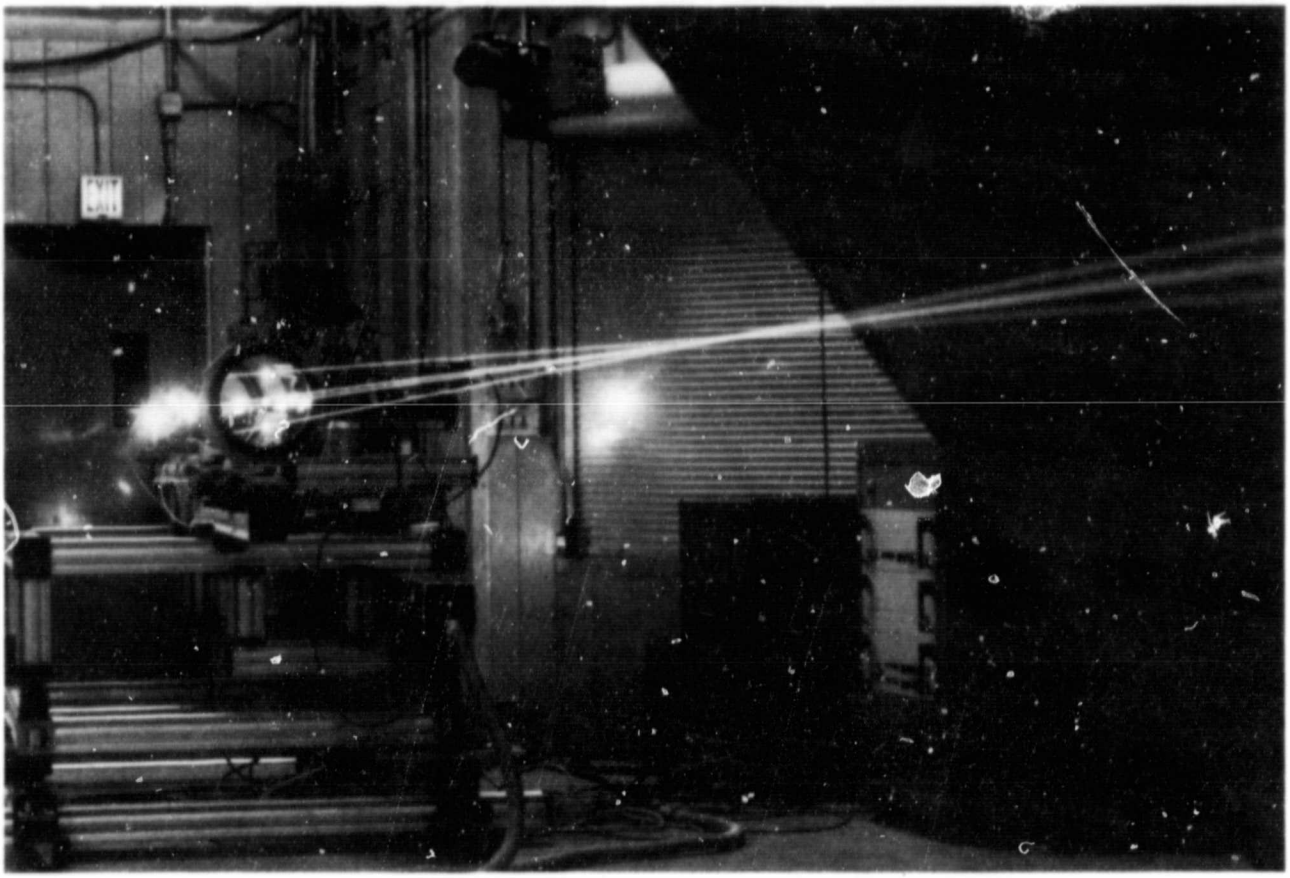

*Three-component laser velocimeter setup*

## Laser Velocimeter (Autocovariance) Buffer Interface

A laser velocimeter (LV), when used in wind-tunnel applications, can generate large amounts of data arriving randomly at a high average rate. Data acquisition by state-of-the-art laser velocimeter instrumentation and data handling by minicomputers are not adequate, since the full potential of the laser velocimeter is not realized. Loss of data can occur when using a minicomputer because of the incompatibility between computer operational speed and laser velocimeter instrumentation output rate. Further, advanced measurement concepts, such as vectorial flow-field analysis, turbulence power-spectral-density studies, and conditional sampling of other phenomena relating to the

laser velocimeter data, cannot be undertaken unless additional instrumentation is used. Current methods of processing laser velocimeter data determine the velocity statistics of an independent component of the flow field. These methods do not assure the researcher that each data point is based upon multicomponent measurements of each seeding particle.

An instrument known as the laser velocimeter (autocovariance) buffer interface (LVABI) has been developed which accepts data from laser velocimeter high-speed burst counters, determines the interarrival time between velocity measurements, sets a coincidence requirement on the data, and permits the conditional sampling of other phenomena. The LVABI will accept data from three counters, each capable of data transfer rates of up to one million data points per second. It will determine the interarrival times of velocity data up to 655.35 msec with a resolution of 100 nsec. The coincidence requirement may be set for any combination of two or all three input channels with the coincidence condition being satisfied if the measured events occur within 1 $\mu$sec. The instrument may also be set to conditionally sample nonvelocity data being acquired by any channel.

James F. Meyers, 4618 (505-31-53)

## Vacuum-Brazed Joints for Cryogenic Wind-Tunnel Models

Nitronic 40 is an austenitic stainless steel containing approximately 9 percent manganese and approximately 6 percent nickel, and which is nitrogen-strengthened to give properties generally superior to those of the 300-series stainless steels. It has been chosen for the construction of pilot models to be used in the National Transonic Facility (NTF) cryogenic tunnel because of its optimum combination of strength and toughness at low temperatures. The ability to form bonded joints in Nitronic 40 will be a very significant advantage in the construction of models that will follow the pilot models in the NTF.

Initial samples of Nitronic 40 were coated with 7.6-$\mu$m-thick electrodeposited copper layers, and bonds were formed by holding in a vacuum oven for 30 minutes at a temperature of 1180°C. Subsequent samples utilized 25.4-$\mu$m-thick copper foil and a holding temperature of 1200°C. A polished and etched metallurgical section taken through the joint formed using the copper foil shows that the copper is virtually continuous and the joint is of a brazed nature, but other sections indicated that there were also diffusion-bonded regions present.

A steroscan photograph was made of the tensile face of a small sample deformed through a 60° angle in a three-point bend test at room temperature. The surface had been polished to a 1-$\mu$m diamond finish prior to testing in order to show up the slip lines formed when a metal is stressed beyond its yield point. Within a grain, the lines produced by a single slip system are parallel to each other, and their direction changes at the boundaries due to the differing orientations of the slip planes in the various grains. Close examination shows that slip lines are visible not only in the parent metal but also within the copper-rich phase in the bond line. A similar three-point bend test carried out in liquid nitrogen showed that the bond strength still exceeded that of the parent metal.

Pierce L. Lawing, 3711 (505-31-53)

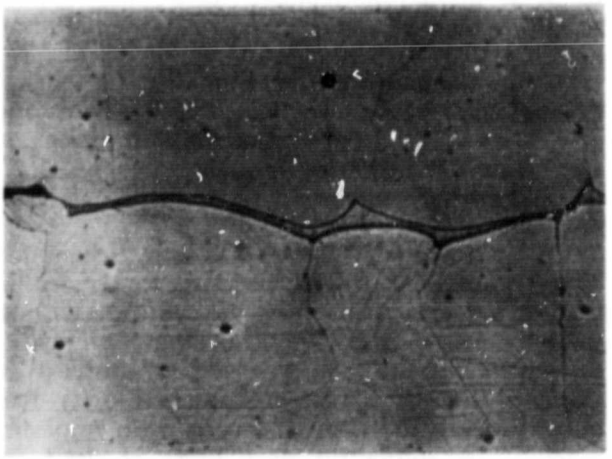

*Metallographic section through brazed joint*

*Stereoscan view of sliplines on sample*

## Precision Drilling Method for Airfoil Models

Drilling of the orifice holes in two-dimensional airfoils should be the last operation performed in the manufacturing process if smooth, sharp-edged holes are desired. All machining, tube installation, and hand finishing must be completed prior to drilling. The quality of the completed hole is directly related to the surface finish of the airfoil prior to drilling. Best results can be obtained only if the surface is finished to 25.4 μm (10 μin) rms or better.

A temporary air supply (140 to 170 kPa) is attached to all orifice tubes to prevent the buildup of oil, chips, abrasive particles, etc., and blockage of tubes during drilling and final polishing operations. Best quality results are produced when a similar metal strip is bonded over the airfoil and used to start the drill and function as a guide. The thickness of the metal strip should be two to three times the drill diameter. The hole is started using a 0.203-mm-diameter pivot drill, which should only be advanced deep enough into the work to produce a 0.13- to 0.18-mm-diameter indentation in the surface of the shim stock. The pivot drill serves only the function that would normally be performed by a center drill in a larger-diameter precision hole-drilling method.

A number 87 (0.254-mm diameter) high-speed twist drill is used to finish drilling the hole. The drill must be withdrawn and cleared every 0.5 to 0.8 mm of depth advancement. Short-flute drill bits should be used to prevent excessive flexing. Slower feed rates and light hand pressure will minimize burring. A miniature drill press is used for all drilling operations with the speed control set at 1840 rpm. A half-and-half mixture of sulfur oil and colloidal sulfur oil is used for a lubricant and applied by brush. The airfoil surface is then lightly polished using 600-grit paper backed with a metal block to remove any surface burr on the holes. The inside hole surface is lightly burnished using a 0.229- to 0.254-mm-diameter hardened steel pin. The polishing and burnishing operations may be repeated if inspection using a 100-power microscope indicates any remaining hole imperfections.

Dwight D. Stroupe, 3141 (505-31-63)

## A New Technique for Manufacturing Large-Diameter Seals

Seals are frequently required for very large diameter orifices, but the access for installation is very limited. A technique for fabricating a nonmetallic seal which is easily handled, occupies small volume, and is highly reliable was developed.

The seal is fabricated by peeling a thin continuous strip from the circumference of a disk of the material from which the seal is to be made. The disk is prepared by planing both surfaces to a smooth, parallel finish. A lathe turns the disk and the lathe crossfeed is adjusted to provide the required thickness for the strip. A special tool was developed which not only provides the proper thickness but simultaneously configures both sides of the strip to provide an interlocking design. This tool carves a notch on one side and a corresponding raised notch on the opposite side.

The seal is installed by simply wrapping it spirally in a premachined groove until the desired seal thickness is acquired. The width of the disk provides the depth desired. Closing the joint compresses the gasket, forming a tight seal. This concept eliminates several design weaknesses of large-diameter seals. It is not fabricated to the final diameter by the manufacturer, as are conventional gaskets; therefore problems of shipping, storing, and installation are minimized. The interlocking design eliminates radical leak paths and is very tolerant of thermal stresses.

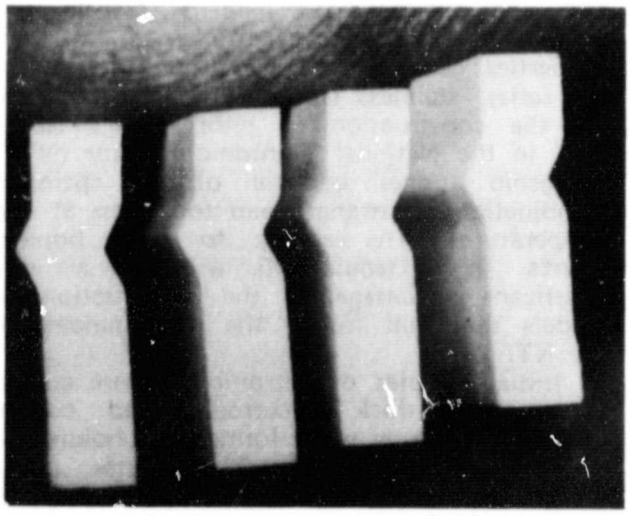

*Cross sections of seal strips*

This concept was used to fabricate a seal made of Teflon to be used on a 4.572-m-diameter gate valve at temperatures between -196°C and 77°C and pressures up to 3.4 MPa (500 psia).

A variation of the basic seal has an adhesive between the strips, resulting in a bonded solid piece of material. Other forms are a tubular strip with ends which allow for pressurization after assembly and a thermally controlled seal with a heated wire embedded in the strip. Large-diameter bearings could also be constructed in the same way using a suitable material. The strip seal can be custom-fitted to irregular flange surfaces and to different flange shapes. Additionally, the strip material has been used as a bearing. The material is etched on one side, bonded to a surface, and machined, if required, to fit.

S. C. Irick, 4621 (505-31-63)

## New Airfoil Model Fabrication Process

Two-dimensional airfoil models have been fabricated using a nylon-epoxy film adhesive to join the cover plates to the models. Attachment by bonding offers several advantages over furnace brazing or electron-beam welding as used in previous models. Material selection is increased because welding or brazing is no longer required, orifice tubing can be installed by low-temperature soldering rather than by furnace brazing or silver soldering, distortion due to joining method temperature is minimized, and the model can be disassembled by reheating to 204°C, if required, to repair inoperative orifices. Briefly, the process requires a simple cleaning and degreasing of the mating surfaces, application of adhesive film to one surface, assembly of the mating parts and curing for 1 hour at 176°C under 34.5 to 345 kPa (5 to 50 psi). The airfoil models fabricated using this process exceed strength requirements for testing in the Langley 0.3-Meter Transonic Cryogenic Tunnel, and the bond retained integrity after repeated cryogenic cycling.

George C. Firth, 4666 (505-31-63)

## Implicit Navier-Stokes Solver for the CYBER-203

Implicit finite difference methods such as the approximate factorization technique, used to solve complex partial differential equations, often offer significant advantages over explicit methods due to the size of the time step they can achieve. However, on the Control Data CYBER-203 explicit methods have more commonly been used due to the relative complexity of vectorizing the implicit methods to take advantage of the unique vector-processing capabilities of that computer.

A vectorized version of a computer code which uses the approximate factorization method to solve the two-dimensional Navier-Stokes equations has been developed for the CYBER-203. Efficient use of vector processing is achieved by first applying the solution process to all of the block tridiagonal sets of equations simultaneously. There is one system for each column of the grid. The matrices of grid values at each point are then efficiently transposed within memory. Finally, the implicit equations along each row of the grid are solved in a similar manner. This technique permits vectors which either span the entire grid or are the size of one grid dimension.

The vectorized code executes an iteration on a 100 × 100 grid in 1.35 seconds, which is seven times faster than the original serial code on the CYBER-175. The data transposition, crucial to the vectorization technique, adds only a 2 percent overhead penalty. Grids as large as 130 × 130 can be used.

Jules J. Lambiotte, Jr., 4612 (505-31-83)

## New Approach to Grid Spacing Control

A major problem encountered in computational fluid dynamics is the specification and control of grids on which numerical solutions are obtained. Algebraic approaches to grid generation require that explicit equations be derived to determine the boundary and interior distribution of grid points. There are many considerations for

this, but the overriding one is that the change in the grid point spacing be smooth.

A new approach to grid control which is highly flexible and can be applied in an interactive manner from a graphics terminal is a curve-drawing technique based on cubic spline smoothing. This grid control procedure has been incorporated into the "two-boundary technique" for algebraic grid generation and applied on the Langley Interactive Processing System. The grid control technique is coded in FORTRAN using the PLOT 10 interactive graphics package, and offers a higher degree of flexibility in the generation of two-dimensional grids than has previously been available.

Robert E. Smith, 3978 (505-31-83)

## Arbitrary Geometry Definition

In recent years, the ability to numerically define an aircraft concept for analysis and manufacture for wind-tunnel testing has progressed to the point that very complex and detailed numerical models can be generated easily and quickly with the aid of computer codes and interactive modeling techniques. Many of the analysis computer codes in use today in research institutions and throughout the aircraft industry were developed in the 1960's and were written to accept simple numerical models as input. Often this tends to be restrictive when applied to exotic and unconventional aircraft concepts currently being designed and evaluated.

Recently a more arbitrary type of geometry input has been designed and implemented into the Harris Wave Drag Computer Program. Wave drag analysis can now be performed on more true representations of numerical models without first having to manipulate the geometry of the concepts to meet the strict input requirements of the old programs. The geometry definition no longer requires that fuselage-shaped components be described with parallel sections which are perpendicular to the X axis. Other shapes for components can be described by nonintersecting contours in any direction rather than contours which are parallel to the XZ plane, as was formerly required. This arbitrary geometry definition is flexible enough to describe almost any complex concept, and is being used by members of the aircraft industry and various research groups as a guide for current and future applications.

Charlotte B. Craidon, 2385 (505-31-83)

## Sound Absorption in Moist Nitrogen

For proper evaluation of aircraft noise certification measurements, it is necessary to establish standard values of sound absorption in air under a wide variety of meteorological conditions. Only recently has the significance of nitrogen ($N_2$) as a sound-absorbing constituent of the Earth's atmosphere been appreciated, for $N_2$ dominates the absorption spectrum at frequencies up to about 2 kHz. However, measurement of sound absorption in $N_2$ is difficult for two reasons. First, the molecular relaxation peak of $N_2$ is extraordinarily small, and second, at atmospheric pressure the peak in dry $N_2$ appears at very low frequencies, shifting into the audio range with increasing relative humidity. An 18.288-m-long (60-ft) acoustic resonant tube developed at Langley Research Center has proved capable of permitting measurement of the elusive $N_2$ peak over hitherto unattainable ranges of pertinent parameters.

The first standard for sound absorption in air, SAE document ARP866A, ignores the $N_2$ contribution altogether. A more recent standard, ANSI Standard S1.26/ASA23-1978, includes the effect of $N_2$ but shows substantial disagreement with the experimental results of the present research. Consequently, both standards are subject to errors of up to several dB per 304.8 m (1000 ft). In the accompanying table, sound absorption values in air as specified by each standard and the present investigation are compared at various frequencies for a typical temperature of 20°C and relative humidity of 80 percent. In a sideline measurement of aircraft noise, where the prescribed propagation distance is 610 m (2000 ft), the error in both standards in several 1/3-octave bands between 2000 and 5000 Hz would exceed 2 dB. To illustrate the effect of temperature, the error in the ANSI standard in the 3150-Hz band would increase to 5.3 dB at 30°C and 10.3 dB at 40°C.

Allan J. Zuckerwar, 3446 (505-32-03)

| Frequency (Hz) | Sound Absorption in Air (dB per 304.8 m) | | |
|---|---|---|---|
| | ANSI | ARP866A | Present Work |
| 50 | 0.01 | 0.1 | 0.03 |
| 100 | 0.05 | 0.2 | 0.10 |
| 200 | 0.18 | 0.3 | 0.30 |
| 500 | 0.81 | 0.8 | 0.73 |
| 1000 | 1.69 | 1.6 | 1.09 |
| 2000 | 2.95 | 3.3 | 1.99 |
| 3150 | 4.77 | 5.4 | 3.71 |
| 4000 | 6.50 | 7.0 | 5.42 |
| 5000 | 9.07 | 7.9 | 7.97 |

*Sound absorption in air at 20°C and 80 percent relative humidity.*

## Flight Effects Theory for Jet Exhaust Noise

A new theory proposed by researchers at DFVRL (a German aerospace research establishment) for flight effects on jet exhaust noise is being evaluated for inclusion in Langley's Aircraft Noise Prediction Program (ANOPP). The theory is an analytical extension of the Lighthill theory of jet noise under static conditions to include flight effects. The new theory differs from commonly used empirical methods in that it recognizes the alteration of the jet mixing process in flight and rationally analyzes the dynamics of jet noise emission. Predictions have compared very favorably with a number of experiments. A typical comparison is shown for an RB-211 high-bypass-ratio engine in flight. The prediction from this new theory is very close to the flight data at all directivity angles and is significantly better than the empirical method.

Paul Pao, 2617 (505-32-03)

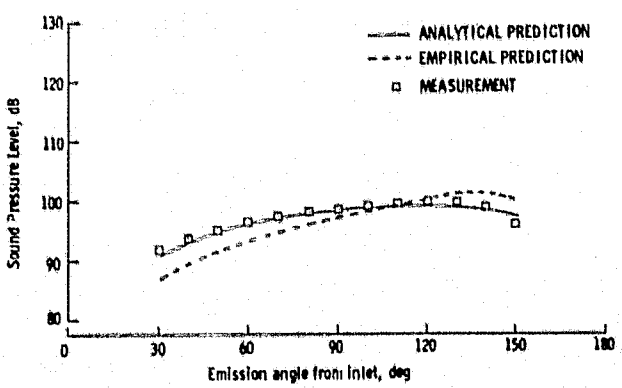


*Improved prediction of jet noise directivity*

## Lateral Sound Attenuation Model

A Boeing 747 lateral attenuation experiment was conducted to gather data needed to validate lateral attenuation prediction methods. Lateral attenuation is largest for sound propagation close to the ground; therefore, the experiment required the aircraft to fly at low altitudes perpendicular to an array of microphones on the ground. The measured results from the experiment are compared with the best available analytical model, which was developed at Langley. Lateral attenuation results are given as a function of elevation angle, which is defined as the angle between the ground and the line of sight from the observer to the aircraft, for the 150-Hz 1/3-octave band. Although the experimental data show some scatter, agreement between the measured and predicted results is considered to be excellent; even the small rise near 20° is matched.

W. L. Willshire, Jr., 2645 (505-32-03)

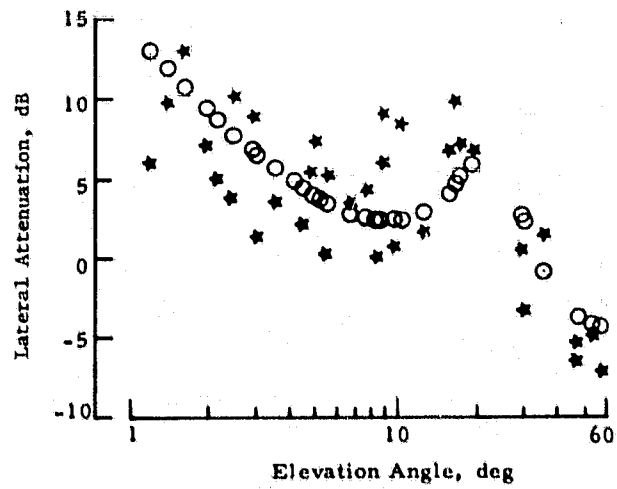


*Comparison of experimental (★) and predicted (○) results*

## A New Aircraft Noise Prediction Program

A new version of the NASA Aircraft Noise Prediction Program (ANOPP) is available which makes noise predictions for typical transport aircraft for less than half the computer cost of predictions using the previous version of ANOPP. In addition,

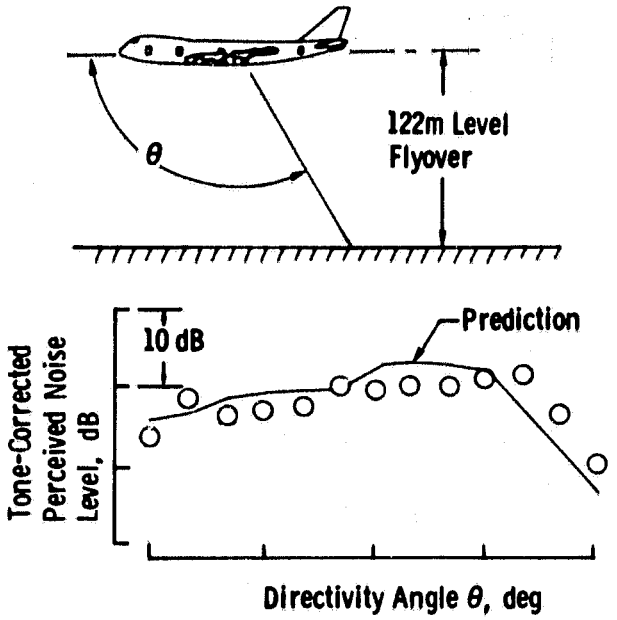


*Prediction and experiment compared for B-747*

improvements in the prediction methods produce more accurate predictions of flyover noise. The principal improvement is in the propagation model, which incorporates attenuation effects on a narrowband basis instead of in 1/3-octave bands. Another improvement is a group of modules which extract noise-critical parameters directly from engine cycle data. The capability of the new version is illustrated for a Boeing 747 in level flyover at approach power. These predictions were made by summing the noise from five individual noise sources – jet, fan, combustion, turbine, and airframe. For this case, the directivity of the prediction compares very favorably with the data, and noise level at any observer angle is predicted to within 3 to 5 dB.

William E. Zorumski, 2645 (505-32-03)

## Improved Jet Noise Reduction

The porous-plug jet nozzle suppressor has been previously demonstrated to be effective in reducing noise. Shock, screech, and mixing noise reductions of about 10 dB have been obtained at model scale in unheated flows. More recently, acoustic performance of the concept has been enhanced by injecting small amounts of cryogenic nitrogen through the porous center body. The cryogenic flow acts as a wave guide for sound generated in the surrounding shear layer by the annular jet flow. Noise reductions are realized mainly in the rear quadrant in the direction of maximum jet noise radiation.

An indication of the acoustic performance of the porous plug with and without cryogenic flow is shown in the figure. The spectra are taken at 30° from the jet axis at a pressure ratio of 1.9. Also shown for reference is the measured acoustic spectrum at the same angle for a standard convergent nozzle at the same mass flow and pressure ratio. The mass flow of cryogenic nitrogen is about 1 percent of the main jet mass flow. The results indicate that the porous plug nozzle provides about 8 dB noise reduction for 1.9 pressure ratio at the spectrum peak relative to the reference convergent nozzle. An additional noise reduction of 2 to 4 dB is provided by the cryogenic flow.

L. Maestrello, 2617 (505-32-03)

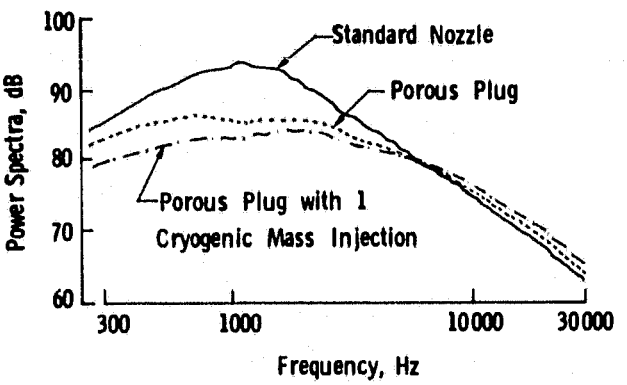


*Noise reduction with porous plug*

## Computation of a Scramjet Engine Flow Field

Interest in the development of a supersonic combustion ramjet (scramjet) propulsion system for hypersonic cruise aircraft and missiles dates back a number of years. A current program is underway at Langley to develop an airframe-integrated hydrogen-fueled scramjet for hypersonic cruise applications in the atmosphere. Scramjet design requires a detailed understanding of the internal flow field in the engine over a

range of operating conditions. Computational tools are attractive for studying such flows since the calculations can be economically carried out over a wide range of conditions.

A computer program has been developed to analyze the turbulent reacting flow in a scramjet. The program numerically solves the full two-dimensional Navier-Stokes and species equations in the engine inlet and combustor, allowing consideration of flow separation and possible inlet-combustor interactions. The current work represents an intermediate step toward development of a three-dimensional program.

The figures show the computed steady-state velocity field and water distribution formed from the reaction of hydrogen fuel and air in an engine model problem. Note the predicted flow separations (indicated by reversal of the arrows in the vector plot) in the engine inlet and combustor and the chemical reaction (forming water) taking place in the combustor. Accurate prediction of these and other phenomena in the engine flow field is critical to the successful design of a scramjet engine.

J. Philip Drummond, 3171 (505-32-93)

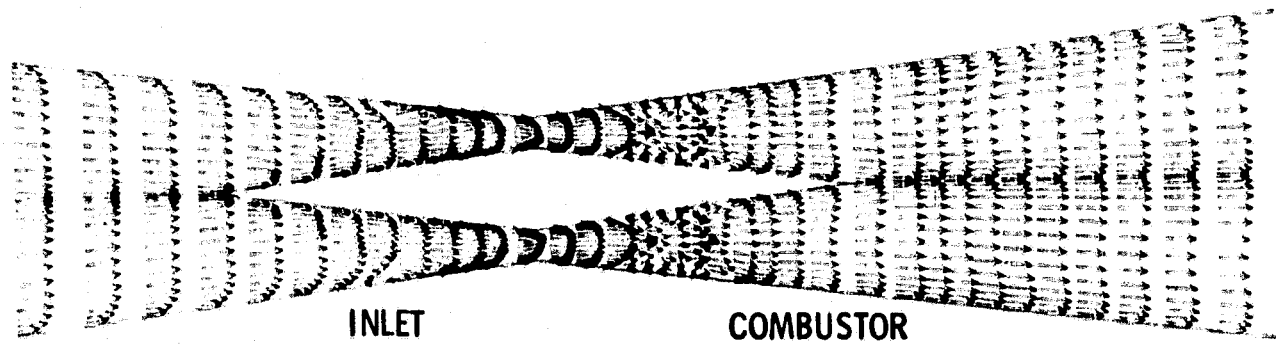


*Computed velocity field*

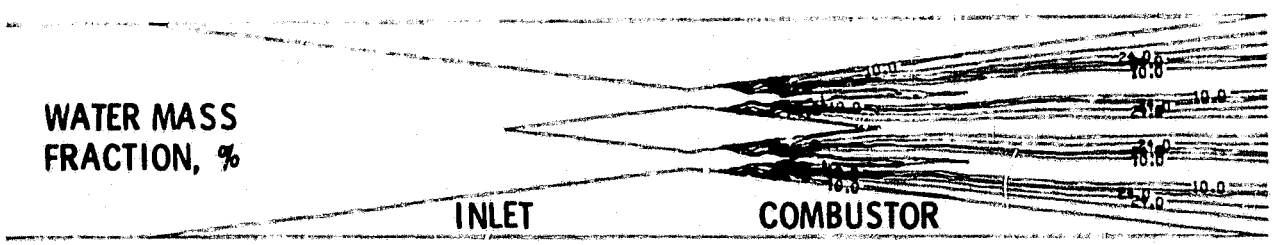


*Computed water mass fraction distribution*

## Numerical Analysis of a Scramjet Inlet Flow Field

A computer code has been developed to solve the full two-dimensional Navier-Stokes equations in the inlet of a supersonic combustion ramjet (scramjet) engine. The analysis uses a numerical coordinate transformation which generates a set of boundary-fitted curvilinear coordinates. It transforms the physical domain into a rectangular domain with uniform mesh spacing. The embedded bodies in the flow field are transformed into slits. MacCormack's unsplit, explicit finite-difference method is used to solve the governing equations. The code in its present form can analyze both inviscid and viscous (laminar or turbulent) flows with no strut, one strut, or multiple struts in the flow field.

The code was verified by solving several complex supersonic flow model problems. It was then used in a quasi-three-dimensional sense to analyze actual scramjet inlets. The sideview of a scramjet module illustrates the

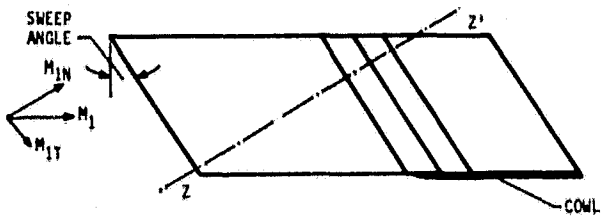


*Sideview of a scramjet module*

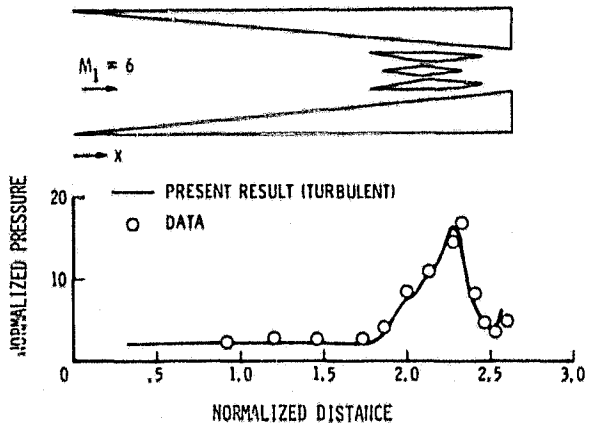


*Comparison of sidewall pressure distribution for three-strut inlet*

basic idea. The Mach number at the face of the inlet is $M_1$, with components $M_{1N}$ and $M_{1T}$ normal and tangential, respectively, to the sweep line. If the shock waves in the inlet do not detach and if the end effects are neglected, the flow disturbances should occur in the plane ZZ' normal to the sweep line, and the velocity component parallel to the sweep should remain unchanged. The flow can be solved using the two-dimensional code in the ZZ' plane with Mach number $M_{1N}$. The solution in the plane parallel to the cowl can be obtained by projecting the two-dimensional solution and properly superimposing the constant velocity component.

The preceding approach was verified by analyzing a three-strut inlet for which experimental results were available. Computer-generated predictions were compared with the measured sidewall pressure distribution in a plane parallel to the cowl. The agreement obtained for this inlet gives credibility to the code in its use as a tool for parametric studies in inlet design. It can be used to modify or eliminate those designs of flow conditions which are not expected to perform well, and thus can help reduce the experimental testing required in scramjet inlet design.

Ajay Kumar, 3171 (505-32-93)

# Scramjet Technology

A broad and comprehensive research program is currently underway to develop the technology for hydrogen-fueled, airframe-integrated, supersonic combustion ramjet engines for application in the Mach number 4 to 7 speed regime. It is clear that good performance in the Mach 4 to 5 range is dependent on the utilization of a dual-mode, supersonic/subsonic combustion process. Past experience has indicated that dual-mode combustion is very likely to be accompanied by severe inlet/combustion interactions which can destroy performance.

Recent combustor development tests using swept-strut hardware have demonstrated dual-mode operation of the airframe-integrated combustor concept without such severe combustor/inlet interactions. This was accomplished by the addition of 7.5 percent physical area blockage in the form of corner fillets near the downstream end of the combustor. At a simulated flight Mach number of 7 and a stoichiometric fuel-air ratio of one, the combustor operated in an all-supersonic mode. When the test stream condition was reduced to that corresponding to a flight Mach number of 4 and the fuel injection was altered to delay the mixing of fuel and air, the model operated in a subsonic combustion mode. In this case, the expected distribution of high pressure down the diverging combustor to the fillets was followed by an expansion back to supersonic. The area distribution and typical pressure distributions for the supersonic and subsonic combustion modes are illustrated; note that the combustor entrance pressures are not affected by the combustion processes.

These results are very encouraging because they indicate that the engine concept has good combustor performance potential over a

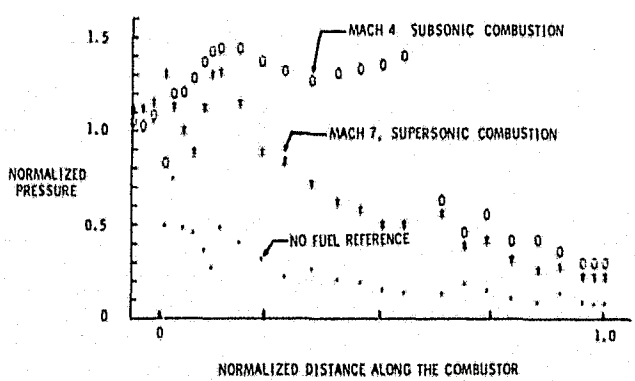


*Dual-mode combustor operation*

wide range of Mach numbers. They also imply that the combustion process can be decoupled from the inlet over the entire Mach number range.

H. L. Beach, Jr., 3772 (505-32-93)

## Nondestructive Imaging of Composites

An ultrasonic measurement technique originally developed at Washington University was successfully applied to nondestructive imaging of composites at Langley Research Center. In contrast to the more conventional ultrasonic imaging measurement of specular reflection amplitude (C-scan), this new method is based on the temporal integration of the ultrasonic backscatter from regions internal to the composite material. Significant internal delamination and cracking due to impact may be disguised by relatively minor structural variations in the outer surfaces of the fiber/epoxy composite plate. Therefore measurements of the amplitude of ultrasonic specular reflection may be only indirectly related to the extent of damage in the interior of the sample. However, an increase in the ultrasonic backscatter from between the surfaces of the plate results directly from voids and cracks related to the impact damage. The amplitude of the integrated ultrasonic backscatter is directly related to regions of impact damage in the composite plates, as the integrated ultrasonic backscatter scan illustrates.

This new measurement parameter exhibits significant improvement in the signal-to-noise ratio when compared with conventional specular reflection measurements on the same sample. Integrated backscatter imaging has found important applications in research on the underlying mechanisms of impact damage in composites. This technique also shows promise for other applications in ultrasonic nondestructive testing of materials for many aerospace applications.

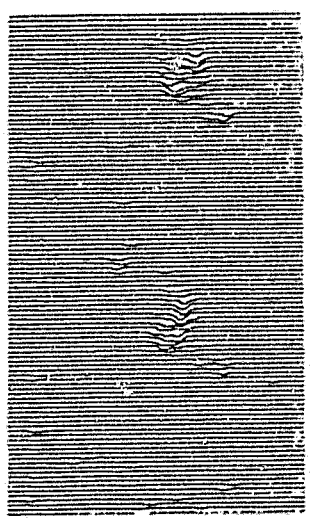

*Integrated ultrasonic backscatter scan*

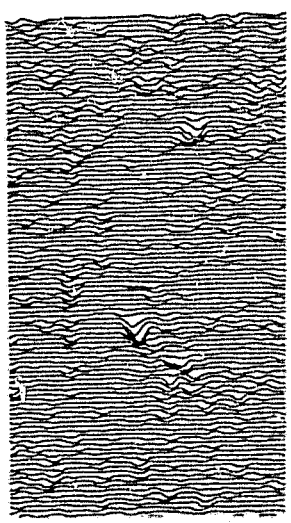

*Conventional reflected ultrasound scan*

Joseph S. Heyman, 3418 (505-33-23)

## A New Interferometer for Surface Acoustic Waves

A wideband differential interferometric optical probe for the detection of ultrasonic surface waves in solids is insensitive to ambient acoustical noise. The probe was developed by in-house and grant-supported research (Virginia Polytechnic Institute) for assessment of properties of aerospace materials. Light from a 2-mW helium-neon laser is divided into two parallel and slightly separated collimated beams of equal intensity by a fixed beamsplitter. The beams are partially transmitted by a second beamsplitter and focused to points separated by a distance on the surface of the specimen. Upon reflection the beams are partially reflected by a second beamsplitter and superimposed to form a straight-line interference pattern which is spatially filtered and focused on a wideband optical detector. The new system is sensitive to differential changes in the optical pathlengths of the two beams which cause relative motions of the output fringe pattern with respect to the fixed spatial filter.

One advantage of this technique over other techniques is its insensitivity to ambient acoustical noise which can mask small-amplitude high-frequency signals. The new interferometer has applications in the nondestructive characterization of surface and near-surface defects in solids, in ultrasonic transducer calibration, and in the study of adhesive bonds using interface waves.

John H. Cantrell, Jr., 3418 (505-33-23)

## Threshold Parameters for Burn Injuries

As part of Langley's effort to continue to expand on technologies developed for space and aeronautical programs and utilize prior employee experience in critical areas of national interest, cross-fertilization of ultrasonic nondestructive testing research and burn research has increased the understanding and assessment of total burn injury. Knowledge of the *in vivo* threshold parameters for burn injuries is important in the design of safety equipment and protective clothing. A new mathematical model of thermal injury in skin tissue has been developed which is based on the solution of the one-dimensional heat equation with time-dependent boundary conditions. The model predicts the burn depth as a function of exposure time to damaging temperature. The threshold temperature for irreversible tissue death is calculated to be 65.3°C for exposures at 100°C and is in agreement with experimental observations. The energy of transformation from a state of tissue viability to a state of tissue death is calculated to be 886 J/g. The model also allows, for the first time, the ability to determine the molecular weight of the chemical constituent of the cell whose thermally induced inactivation at the threshold level is responsible for cellular death. The molecular weight is calculated to be 710.

John H. Cantrell, Jr., 3418 (505-33-23)

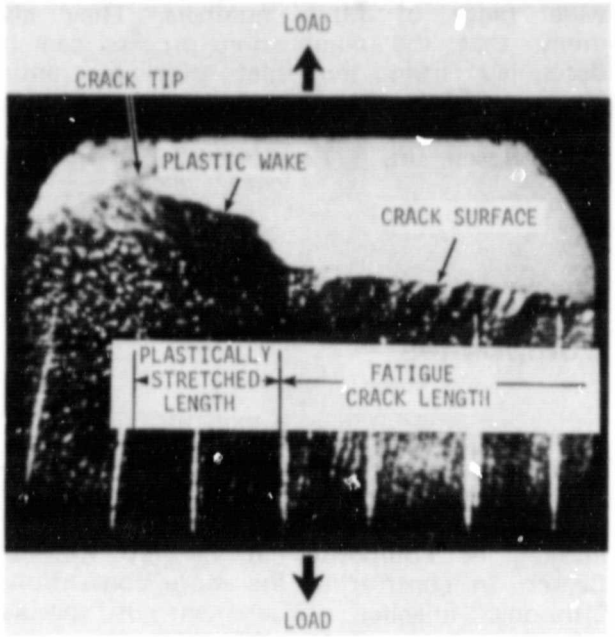


*Plastic wake formed in ductile copper*

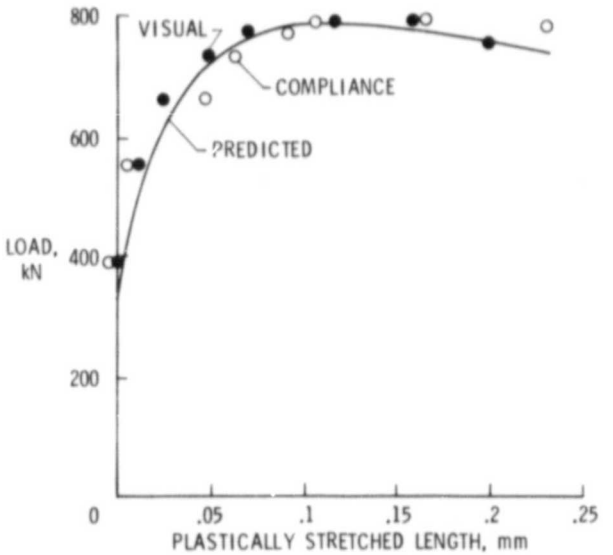


*Plastic wake model prediction of stable crack growth*

## A Plastic Wake Concept of Model Failure Prediction

Under an increasing load, a crack growing in metal leaves plastically stretched material behind. The stretching is very dramatic in ductile materials, as is shown in the photograph of a copper specimen failing. An arrow indicates the plastic wake of material formed during the final load cycle of a fatigue test. Although the plastic wakes are much smaller in aerospace structural materials, their formation still controls stable-crack growth and instability. If the plastic wakes were not there, any crack extension would precipitate unstable growth and catastrophic failure.

Finite-element analyses of the crack-growth process have confirmed the importance of the plastic wake concept. A simple strip-yield model has recently been developed which includes the effects of plastic deformations around the crack tip as well as those of residual plastic deformations left in the wake of the moving crack. The simple model requires only a desk-top calculator. As illustrated, the model was able to predict both stable-crack growth and the load at

instability (maximum load). The fracture parameters (critical crack-opening displacement and a plastic-wake constant) used to predict the curve were determined from a small laboratory-type compact specimen. The symbols show experimental results from visual and compliance methods. The agreement between predicted and experimental results was very good.

J. C. Newman, Jr., 2093 (505-33-23)

## Improved Solvent Resistance of Thermoplastics

Thermoplastics are a class of polymeric materials which generally exhibit attractive mechanical properties, but their use for aircraft structures has been precluded due to severe degradation when exposed to aircraft fluids and solvents, especially in a stressed condition. In addition, thermoplastics often creep under load at temperatures below their heat distortion temperature. In an attempt to overcome the shortcomings of thermoplastics without severely compromising their attractive features, work was initiated using a model system (polyphenylquinoxaline, PPQ) to demonstrate a general concept. Latent pendant crosslinking groups (e.g., ethynyl and phenylethynyl) were incorporated on the linear molecules. Upon heating, these groups react to provide controlled crosslinking. In this way, molecules are tied together such that there is a significant improvement in their elevated temperature performance (e.g., creep resistance) and, more importantly, in their fluid and solvent resistance.

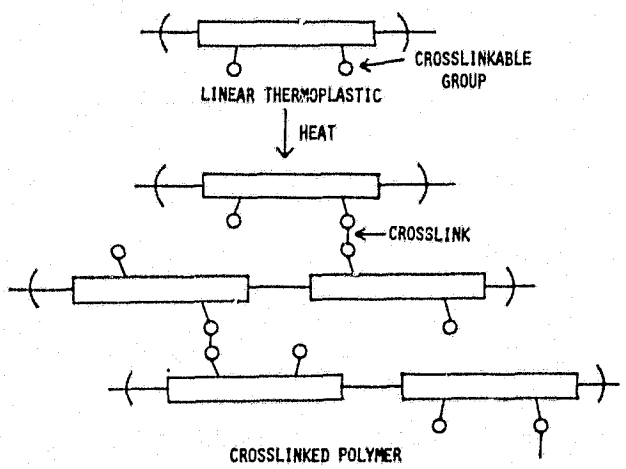


*Controlled crosslinking of thermoplastics*

Test results show that the 288°C lap shear strength of a cured PPQ containing crosslinking groups was substantially higher than the parent PPQ void of crosslinking groups. At the 10-percent crosslinking group level, the cured crosslinked PPQ was totally insoluble. This novel route offers the potential of modifying existing thermoplastics, particularly polysulfones, to improve their performance and make them acceptable for structural uses on future aircraft and spacecraft.

P. M. Hergenrother, 3041 (505-33-33)

## A Multipurpose Thermoplastic Polyimide

LARC-TPI is a linear thermoplastic polyimide which was developed for a variety of high-temperature applications. This polymer is an outgrowth of basic research and development and has been used in-house as an adhesive in the NASA Supersonic Cruise Research and Solar Sail Programs. LARC-TPI has been further developed as a thermoplastic adhesive in the preparation of high-temperature large-area film laminates. In its fully imidized form which eliminates volatiles, LARC-TPI has successfully joined large pieces of polyimide film to produce flexible, 100-percent-void-free laminates for flexible circuitry, communications devices, and electronic packaging applications. This thermoplastic polyimide has also demonstrated potential as a molding powder and composite matrix resin due to its high ductility.

LARC-TPI was recently recognized by Industrial Research & Development magazine as one of the 100 most significant technological developments of 1981. Initial stages of the commercialization of LARC-TPI are presently underway by Gulf Research and Development, Pittsburgh, Pennsylvania.

Anne K. St. Clair, 3041 (505-33-33)

## Tailoring Polymer Structures to Control Properties

The oxidative stability and color (transparency) of linear aromatic polyimides

can be tailored by altering chemical groups that bridge the aromatic rings. As illustrated,



the -c- (carbonyl) bridging group is in the dianhydride-derived portion of the polymer and the -o- (oxygen) bridging group is in the diamine-derived portion of the conventional polyimide. When this polyimide was tested at 350°C, the polymer film lost half of its initial weight in 80 hours. Other experimental polyimides were prepared and tested in the same manner, but the bridging groups were altered as shown. With the carbonyl bridge in both components (LARC Polyimide I), oxidative stability was improved by a factor of 2 without affecting the color transparency. Altering the structure by placing the oxygen bridge in both components (LARC Polyimide II) provided a polymer film with good transparency (colorless) and oxidative stability comparable to the conventional polyimide.

These results indicate the progress being made in understanding how to control properties by tailoring the chemical structure of the polymer. For polymer coatings good transparency can be achieved without sacrificing oxidative stability, or the structure can be altered to achieve excellent gains in thermoxidative stability.

T. St. Clair, 3041 (505-33-33)

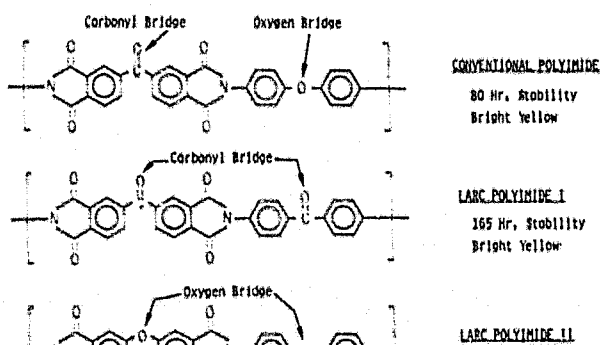


*Conventional and tailored polymer structures*

## Strain Limit for Composite Structures in Compression

Research at Langley has revealed the importance of damage tolerance considerations in the design of filamentary composite structures. Prior to this research the importance of damage tolerance for compressive loading on composite structures was not appreciated. In metal structures fatigue, crack initiation and growth, and failure of damaged structure are generally critical for tension loading only. The Langley research clearly showed that defects, holes, and impact damage can seriously degrade the strength of composite structures under compression. In addition to first calling attention to this situation, Langley researchers performed carefully executed experimental work which bounded the problem and defined the limits of strain sensitivity of damaged structural panels. As a direct result of this pioneering work, research on damage tolerance of composites increased at Langley, other government agencies, and industry.

Results of this work are being applied by manufacturers of composite aircraft components. A maximum-strain damage-tolerance criterion was applied to the design of composite structures for the Boeing 757 and 767 aircraft. Boeing established a compressive limit-load strain of 0.0027 based primarily on Langley data supplemented by Boeing tests using test techniques developed at Langley. The Lear Avia Corporation, which recently designed, constructed, and flew an all-composite executive aircraft, also adopted a limit strain criterion based on work done at Langley.

James H. Starnes, Jr., 2552 (505-33-33)

## Postbuckling Failure of Graphite-Epoxy Plates

Using composite materials to reduce the mass of structural components requires that structural response characteristics and failure modes be understood. One potential application of composites is to structural components designed to operate with buckled skins. The postbuckling response and failure characteristics of graphite-epoxy laminates loaded in compression are now being studied at Langley. A typical specimen is shown loaded into the postbuckling range using a Moiré fringe technique to show the buckle pattern. The center of the concentric circles on the photograph represents a point of maximum out-of-plane deflection, and the closely spaced lateral fringes represent nodal lines (or out-of-plane displacement gradients).

Typical load-displacement results are shown for a specimen where the applied load is plotted versus measured end-shortening. Initial buckling is represented by an open circle and failure is represented by a cross. Failure for all of the composite specimens tested so far occurred along a nodal line of the buckle mode. The high membrane strains occurring near the sides of the specimen couple with the out-of-plane displacement gradients to induce large enough shearing forces normal to the specimen to cause the shear failure mode shown. This failure mode does not occur with metal structures and could be a major contributor to the stiffener pull-off failure mode which limits the amount of load carried by stiffened composite panels designed to operate with buckled skins.

James H. Starnes, Jr., 2552 (505-33-33)

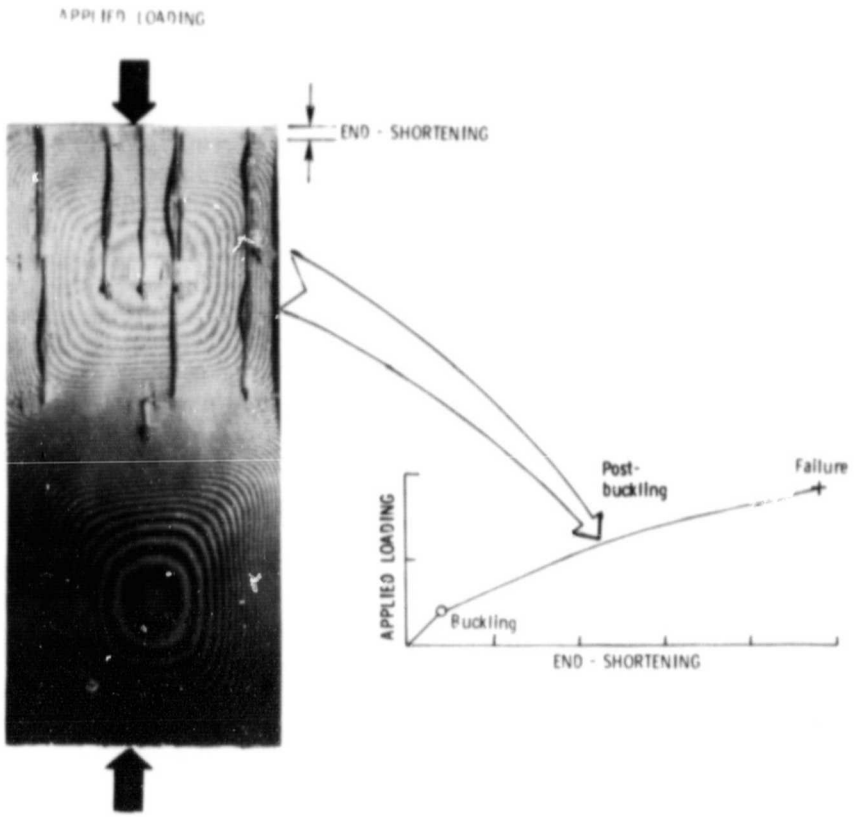


*Typical load-displacement results*

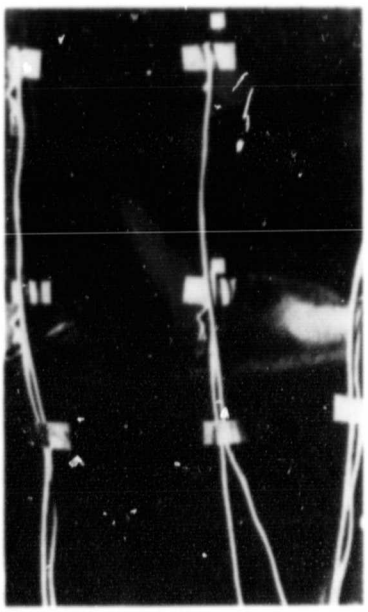

*Induced shear failure mode*

## Optimized Low-Order Control Law Synthesis

The mathematical model of an aeroelastic system requires a large number of high-order equations to accurately represent the flexible structure and unsteady aerodynamics. The order of the system poses a significant problem when synthesizing active control laws. For example, a widely-used optimal control law synthesis technique (linear quadratic Gaussian method) required that the control law be of the same order as the system being controlled. Not only is this unnecessarily complex, but this high-order control law can be very difficult to implement in a flight computer.

A new approach has been developed for synthesizing lower-order optimal control laws for high-order systems. The basic concept is to begin the synthesis process with an

assumed low-order control law and use a nonlinear programming algorithm to optimize the control law. Two problems arise when applying this approach — the choice of a proper set of design variables and their initial values. The contribution of the new approach is the development of the methodology, utilizing the theoretical basis of the linear quadratic Gaussian method, for choosing the design variables and their initial values. The resulting low-order control law is optimal and is much easier to implement in a flight computer. The method is completely generic and can be applied to many control problems.

J. Newsom, 3169 (505-33-63)

## Active Control Law Synthesis Package

A preliminary version of SYNPAC (synthesis package for active controls) has been developed for the design of multi-input/multi-output control laws. SYNPAC employs constrained optimization techniques which allow explicit consideration of design criteria. The constrained optimization approach is complementary to the more commonly employed classical and LQG (linear quadratic Gaussian) design techniques. SYNPAC automates the search for free parameters in a candidate classical control law and can be used to simplify a control law developed using LQG techniques while, in either case, explicitly considering design criteria.

SYNPAC has been applied to the design of a combined RSS/GLA (relaxed static stability augmentation/gust load alleviation) control law for a drone aircraft. Pitch rate and incremental normal acceleration were measured from a point near the center of mass. This sensed information, appropriately filtered, was fed to the horizontal stabilizer and two wing control surfaces to provide load alleviation and stability. Feedback gains and filter parameters were sought by SYNPAC which minimized wing root bending moment subject to handling quality, torsional moment, and control power constraints. A reduction in the standard deviation of incremental wing root bending moment of 39 percent was achieved, demonstrating the successful application of this constrained optimization technique to the design of a multi-input/multi-output active control law.

William M. Adams, Jr., 2013 (505-34-33)

## Parameter Estimation in Nonlinear Flight Regimes

The inherently nonlinear nature of the aerodynamic forces and moments in post-stall and spin flight regimes creates difficulties both for the design of flight test programs and also, because the airplane mathematical model structure is unknown, for the application of parameter estimation algorithms. One must have a method of extracting information from maneuvers in such transient operating regimes in order to construct a nonlinear mathematical model which encompasses all operating regimes.

An algorithm consisting of a modified stepwise regression (MSR) and several information criteria has been developed for application to maneuvers anywhere in an airplane's operating envelope. For example, the MSR was applied to flight data generated by a single large-amplitude longitudinal

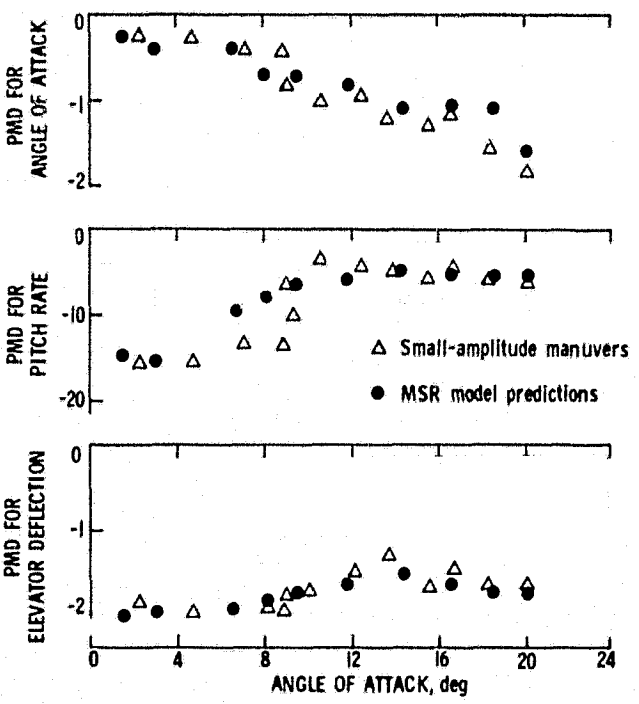


*MSR estimated pitching moment derivatives*

maneuver over a range of angles of attack. The results of that application are illustrated by comparing the pitching moment derivatives (PMD) estimated by applying the MSR model (shown as closed circles) with a baseline set of results (shown as triangles) from several small-amplitude maneuvers by the same airplane. This single example verifies the applicability of MSR to the modeling of aircraft over a large range of angle of attack.

J. G. Batterson, 4591 (505-34-33)

## Decoupled Controls for Improved Safety in Wind Shear

The approach and landing phases of flight can be quite demanding for pilots of transport aircraft in the presence of wind shear. In fact, wind shear has been a significant factor in several airplane accidents which occurred during final approach, such as the Eastern 66 crash which occurred at Kennedy Airport in 1975.

A decoupled longitudinal control system has been developed at Langley to improve a pilot's ability to make safe landings in severe wind shear. The control system uses constant gains to avoid onboard computation and combines changes in thrust, elevator position, and symmetric spoilers to provide independent or decoupled control of flight-path angle, pitch angle, and forward velocity.

The effectiveness of the decoupled control system has been demonstrated using a fixed-base simulation of the NASA Terminal Configured Vehicle (TCV). The simulation modeled a typical twin-engine jet transport. The conventional control system and the advanced TCV control system pitched to high angles of attack, stalled, and crashed approximately half of the time in simulated Kennedy wind shears. When the decoupled control system was used, the airplane did not stall, all landings were successfully completed, and there was no evidence of any impact on pilot performance due to reduced control authority.

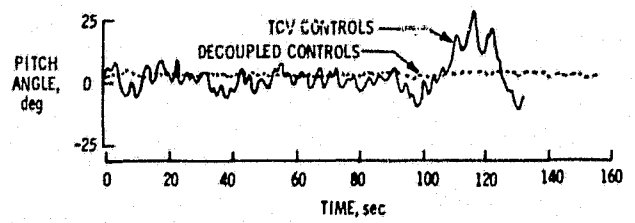


*Pitch performance in severe wind shear*

G. K. Miller, 4591 (505-34-33)

## Multiobjective Insensitive Design of Airplane Control Systems

A multiobjective computer-aided design algorithm has been developed which minimizes the sensitivity of the design objectives to uncertainties in system parameters. The more important uncertain parameters are described by a Gaussian random vector with known covariance matrix, and a vector sensitivity objective function is defined as the probabilities that the design objectives will violate specified requirements constraints. Control system parameters are found which

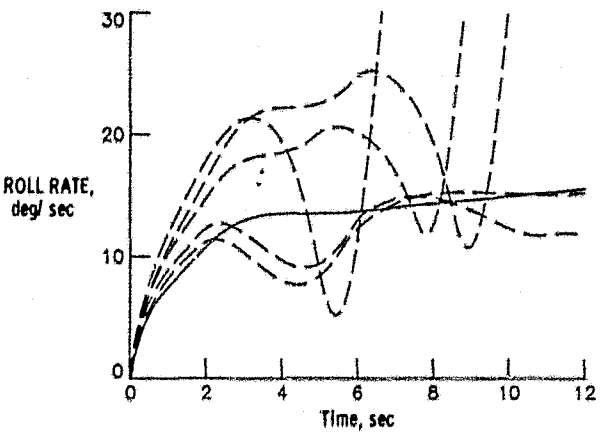


*Deterministic design*

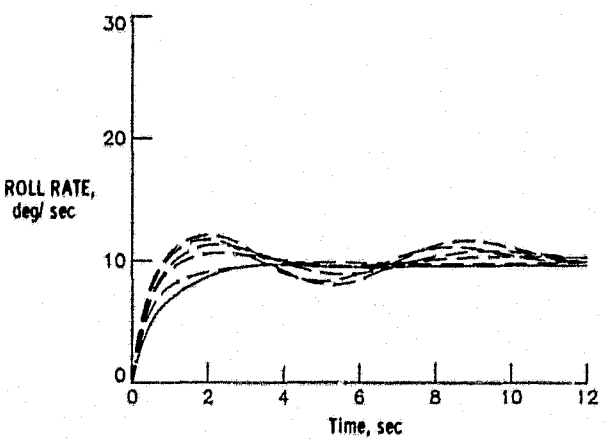


*Stochastic-insensitive design*

*Comparison of responses for deterministic and stochastic-insensitive design*

minimize the sensitivity vector in a Pareto-optimal sense, using constrained minimization algorithms.

Results have been obtained for the example problem of designing a lateral stability augmentation system for three Shuttle flight conditions. The multiple objectives are taken to be the probabilities of satisfying handling qualities criteria and avoiding control limiting, with aerodynamic derivatives as the uncertain parameters. Validity of the method has been verified by comparison with deterministic Pareto-optimal designs, using 1000 random samples of the uncertain aerodynamics. The figure compares roll-rate responses at a Mach number of 2.5 with the new insensitive design and a deterministic design. The solid lines are responses for the nominal system and the dashed lines are for five off-nominal cases at the 99th percentile of the random sample. The unstable roll rate responses are caused by limitations in control deflections and rates. The new design method provides much less sensitivity to off-nominal parameters with little loss of effectiveness in the nominal case.

Albert A. Schy, 3917 (505-34-33)

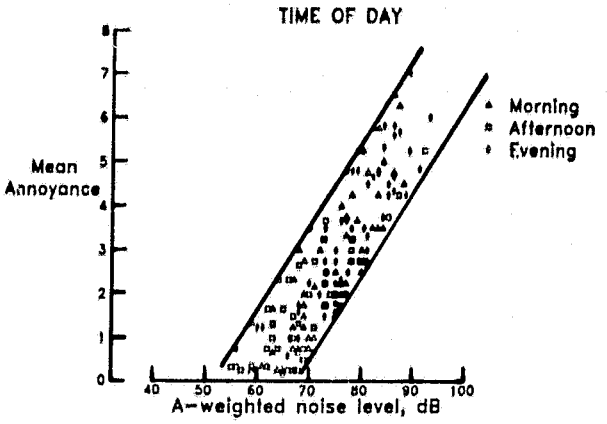


*Effect of time of day on human response to noise*

## Time-of-Day Weighting for Aircraft Noise Measurements

Human response to noise is assumed to be dependent upon the time of day. The usual practice is to penalize noise events which occur at night (10 p.m. to 7 a.m.) by adding 10 dB to weight them with respect to daytime events. The value of this night penalty as well as the time of application is very controversial, however, because of the difficulty of scientifically quantifying this phenomenon. A study was recently conducted at Salt Lake City International Airport to give quantitative insight into noise weighting for aircraft operations. Residents were asked to rate the noise of individual aircraft overflights in tests which were conducted during morning, afternoon, and evening hours. As the results show, the mean responses of the individuals within a given home to an event are seen to be independent of time period. However, in further testing, the residents indicated a preference for aircraft in the daytime hours rather than the evening hours. The results of these two tests suggest that the weighting is not directly related to acoustical phenomena such as ambient noise or aircraft intrusiveness (signal-to-noise ratio) but are related to personal preferences possibly related to the activities of the individual. This finding will greatly simplify the designs of future tests to quantify the time-of-day weighting.

D. G. Stephens, 3561 (505-35-13)

## Motion/Visual Cueing Requirements for Transport Vortex Encounters

A simulation experiment to collect data useful for the specification of motion/visual cueing fidelity requirements for vortex encounters during simulated transport visual approaches and landings was completed by Langley personnel. Highly effective mathematical models to allow simulation vortex penetrations have recently become

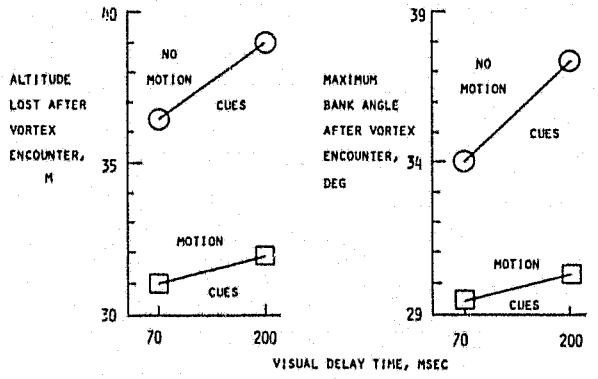


*Effect of visual delay*

available. This is the result of extensive research on wake vortex characteristics to seek a solution for vortex-imposed separation requirements in high-density terminal areas. This study examined the effects of simulator visual system delay with motion/no-motion conditions on control performance for five NASA research pilots. The results, shown as altitude lost and bank angle induced by the vortex upset as a function of simulator cueing condition, indicate a need for motion cueing during simulation studies, and suggest that visual delay characteristics are less noticeable in the presence of motion cueing.

Roland L. Bowles, 3304 (505-35-33)

## An Emergency Egress System for Aircraft

An emergency egress system has been developed which can be utilized in any type of aircraft by allowing designers to create an opening at any desired point on the fuselage. This system is very stable and is activated by predetermined positive actions. It is applicable to military, commercial, and general aviation aircraft and offers improved chances for exiting an aircraft, whether in flight or on the ground. Once actuated, it creates an opening and automatically ejects the structure, thus relieving the pilot or passenger of the responsibility of performing mechanical functions or having to lift and discard a door structure. The particular application for which this system was developed and is now used is to provide emergency egress in flight for the pilot of the NASA Stall/Spin Research Program. As illustrated, the system creates an opening in the left side of the airplane to allow bailout by the pilot should all efforts at spin recovery fail.

This is an add-on system which cuts the airplane's skin and structure to create an opening of approximately 76 by 76 cm (30 by 30 in). The external frame outlines the area to be cut. The metal cutting is accomplished by small quantities (less than 11 g (0.4 oz)) of explosive. The system is actuated by pulling a single handle. On initiation, the explosive cuts the skin around the window to the floor, including the central stringer. The explosive pressure wave then strikes the external frame to provide a jettisoning force. All inboard products of the explosion (products and pressure/sound) are contained by a continuous internal structure. This structure allows the explosive pressure to expand and attenuate within the 3.8-cm

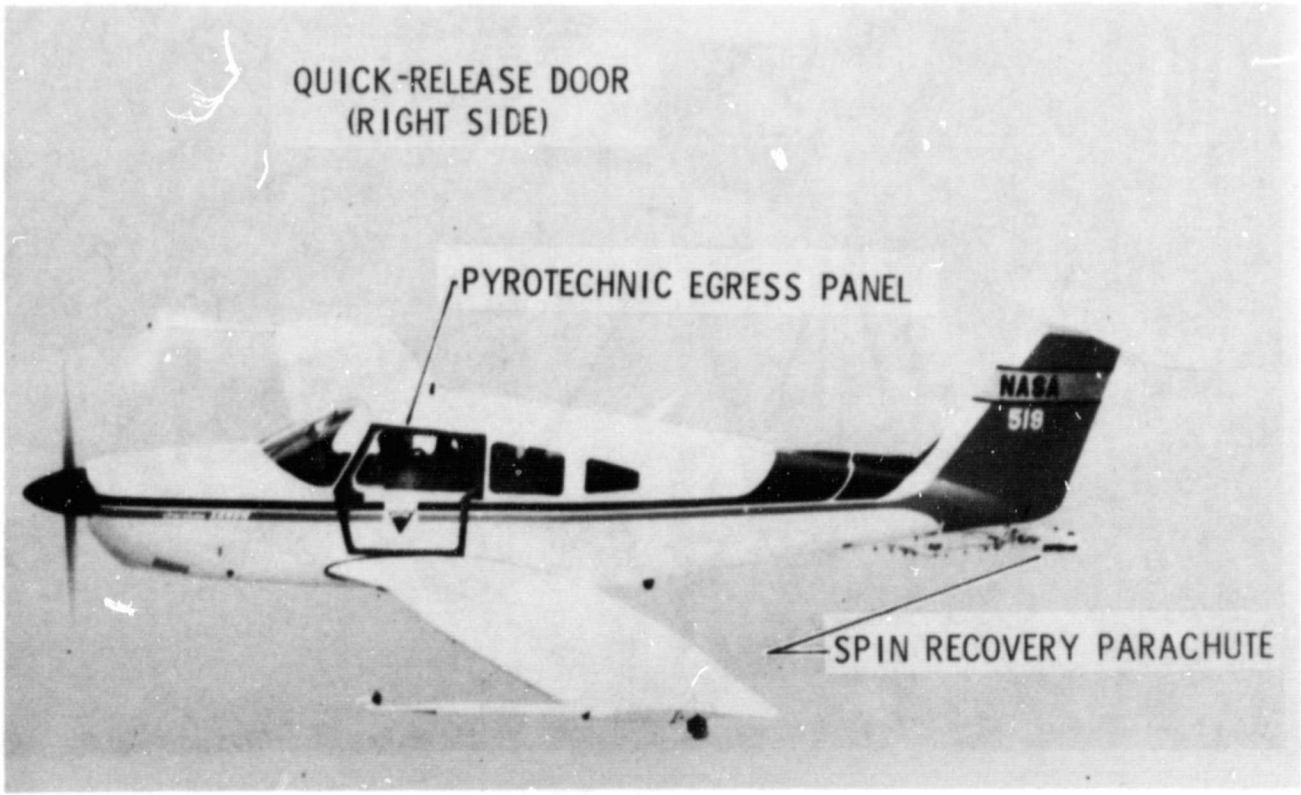


*Piper Cherokee Arrow emergency systems*

(1.5-in) depth of the existing stringers and frames. A 3.8- by 3.8-cm wire mesh stretched across the window prevents the plexiglass window, which flexes and breaks on activation, from entering the cockpit.

The explosive is completely insensitive to mechanical abuse, radio/radar transmissions, lightning, and static electricity. Furthermore, no maintenance or inspection is required, except for a 5-year replacement of the initiators. The total add-on weight is 9 kg (20 lb). The panel which is cut from the aircraft weighs approximately 6.3 kg (14 lb) and is jettisoned at a velocity of 13.7 m/sec (45 ft/sec). The opening is neat and smooth, presenting minimal interference to the pilot during egress.

Laurence J. Bement, 4621 (505-41-13)

## Canard-Configured General Aviation Aircraft

NASA is currently conducting a broad research program to provide a data base on advanced general aviation aircraft. As part of this overall program, wind-tunnel tests were conducted in the Langley 30- by 60-Foot Tunnel to determine the aerodynamic characteristics of a full-scale model of the Vari-Eze, an advanced canard-configured aircraft. The Vari-Eze was chosen for a baseline study because it incorporates many advanced design features. These advanced design features include the use of composite construction which allows the use of advanced airfoils for high performance, use of NASA-developed winglets for increased span

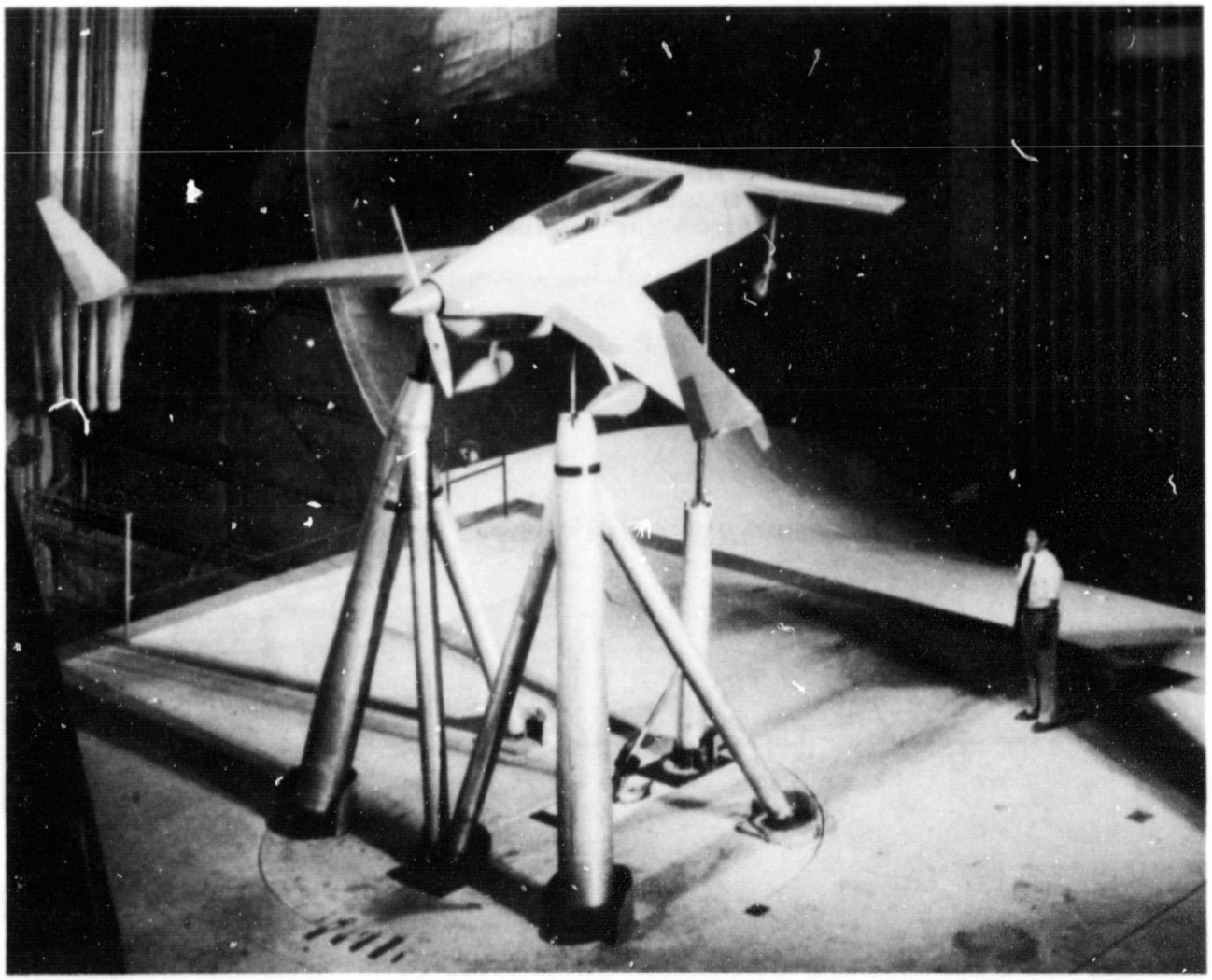

*Vari-Eze configuration mounted in Langley 30- by 60-Foot Tunnel*

efficiency and directional stability, and, most importantly, the use of a canard to limit the aircraft trimmability to below the wing stall angle of attack to insure stall proofing of the concept and to provide increased stall departure and spin resistance.

Preliminary test results indicated that canard stall occurred before wing stall, and therefore the canard was effective in limiting the trimmable model angle of attack. Test results of the canard in a low position indicated that the interference effects on the wing were small. The low-canard position is of particular interest for this configuration to improve pilot visibility. The canard vortex flow field caused the outboard segment of the wing to be highly loaded and to stall prematurely. This premature stalling of the wing tips caused a loss of roll damping which was found to introduce a wing-rock problem in free-flight wind-tunnel tests of 0.36-scale model of this configuration. The wing-rock problem was also identified in full-scale airplane flight tests. The addition of an outboard leading-edge droop to the wing was effective in keeping the flow attached at the wing tip to a higher angle of attack and was found to eliminate the wing-rock problem. Using the chemical sublimation technique, laminar flow was found to occur on the wing and canard to approximately 55 percent of the chord at cruise lift coefficients. The results of simulated rain experiments indicated that water droplets on the canard caused a loss in lift and degradation in laminar flow generally similar to that obtained by the use of grit to fix boundary-layer transition at 5 percent of the chord. The laminar flow results of the lower Reynold's number wind-tunnel experiments were substantiated by flow-visualization experiments conducted in flight tests of a Vari-Eze aircraft at a Reynold's number of 4.2 million.

P. F. Coy, 2184 (505-41-13)

## Autopilot Complexity/Benefit Trade-Off Study

Recent research on the use of autopilots in single-pilot IFR (Instrument Flight Rules) terminal area operations has resulted in the documentation of several unexpected results. In comparing five levels of autopilot complexity it was found that the medium level, the heading select mode, made the largest relative difference in decreasing workload and simplifying the approach task. It was also found that the largest number of blunders was associated with the higher levels of automation. The data further show that, regardless of the autopilot mode, performance was highly dependent on the type of approach being flown.

The data show that as the level of automation is increased, pilot workload tends to decrease with a leveling off beyond the heading select mode. However, a disturbing trend was noted at the higher levels of autopilot automation. It seemed that in monitoring the autopilot the pilot would associate instrument readings with the autopilot functions rather than with situational awareness. If an incorrect function was set, this would frequently lead to an incident or blunder. The results of this study indicate that automation is desirable when making IFR approaches in a high-workload environment, but also that some disturbing trends are associated with the higher levels of automation as presently implemented in state-of-the-art autopilots. A better man/machine interface could possibly alleviate these difficulties.

Hugh P. Bergeron, 3917 (505-41-73)

## "Follow Me" Box Display for General Aviation

The development of cathode-ray-tube and microprocessor computer technology has generated proposals for a wide variety of pictorial aircraft display formats of the path-in-the-sky nature. The "follow me" box display is one of these formats which combines great simplicity with many useful advantages. Whereas the typical path-in-the-sky format shows a continuous line to be followed, the "follow me" box shows only a short segment of the path which stops at a selected distance ahead of the aircraft. The box therefore provides a target which is equivalent to a flight director signal. The three-dimensional shape of the box also provides raw data in that any time either the side, top, or bottom of the box is visible, a very sensitive indication of small displacement errors is provided. The square shape of the box provides roll attitude information, and the location of the box in the display frame provides pitch and heading information. Since all of the flight director and raw data

ORIGINAL PAGE IS
OF POOR QUALITY

information required for the control of the aircraft is provided by the box symbol, very tight control of the aircraft can be achieved. By changing the distance that the box is ahead of the aircraft in the direction of the commanded path, control of the tightness of the pilot-aircraft system response can be exercised.

The box display can therefore be used for both enroute navigation and terminal area control. The two-box format shown has been tested and documented in a general aviation context with simulator and flight tests. The enroute box was located 4 nautical miles ahead of the aircraft to provide ease of finding and following the box, and a final approach box was located 300 meters ahead of the aircraft for precise control of a curved, descending final approach to a 30-meter decision height.

James J. Adams, 3917 (505-41-73)

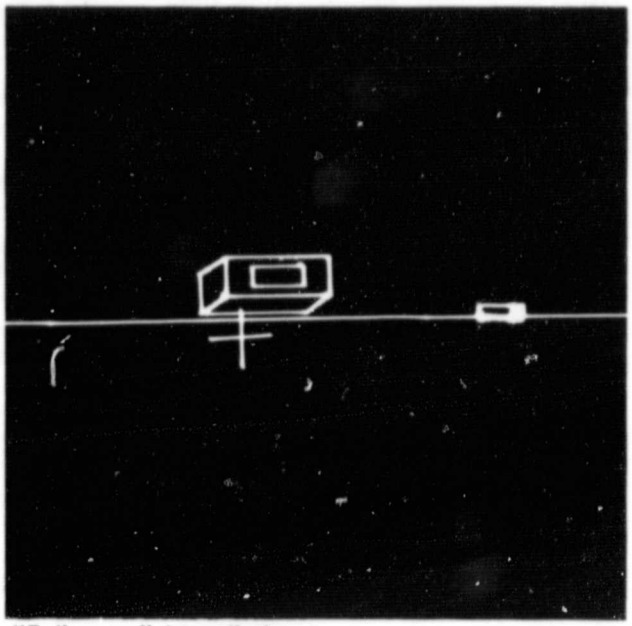

*"Follow-me" box display*

## Wake Vortex Alleviation

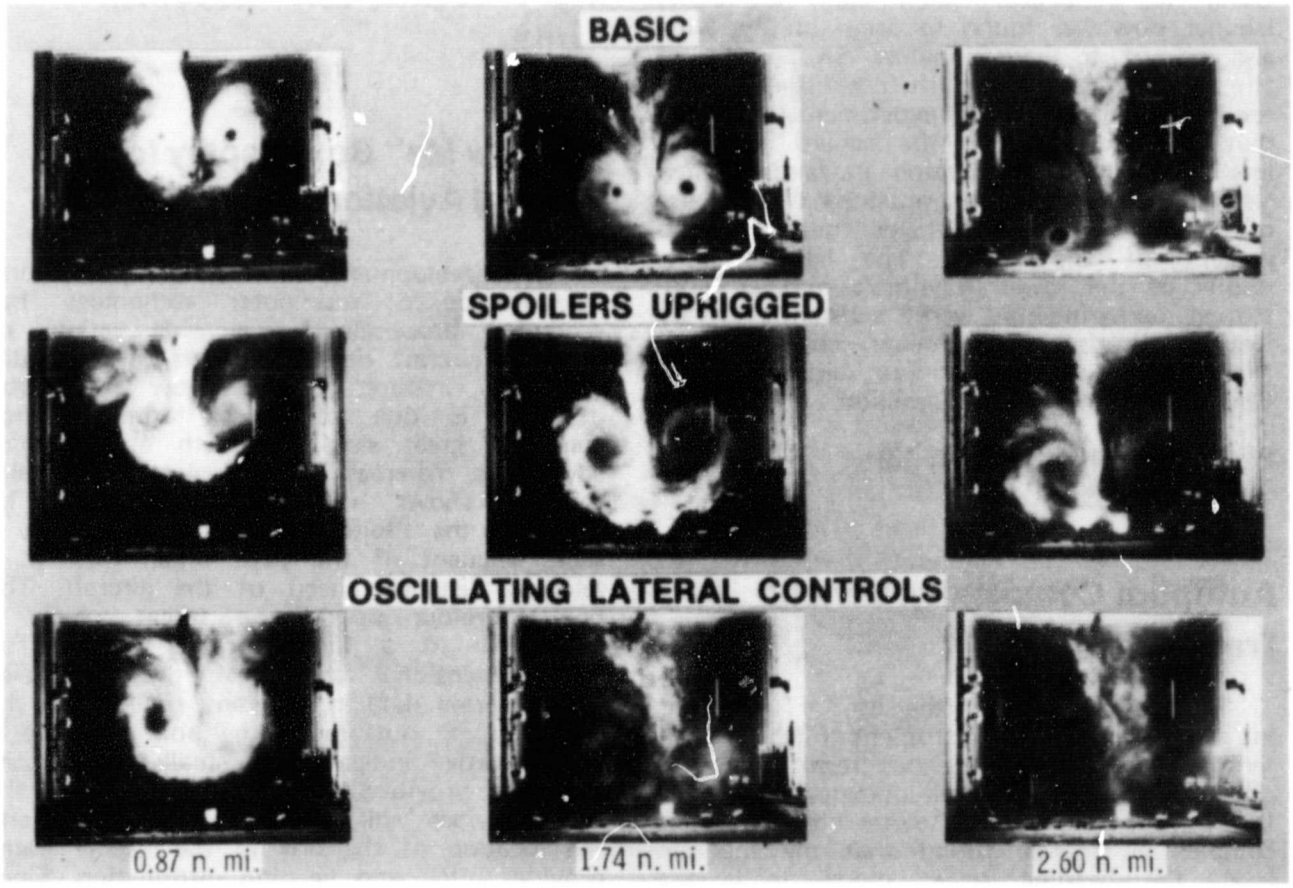


*Wake vortex alleviation by oscillating lateral controls*

Tests conducted with a scale model of the Boeing 747 transport aircraft in the Langley Vortex Research Facility have demonstrated the effectiveness of lateral-control oscillations on wake vortex alleviation. When the control surfaces were oscillated with the flight spoilers uprigged, the rotary motion remaining in the wake after a separation distance of about 2 nautical miles was very small. The flow visualization photographs compare the alleviation obtained by oscillating lateral controls with that obtained by uprigging the spoiler segments without oscillation. In the tests, both spoilers and ailerons were oscillated through their full range asymmetrically, as in a normal roll control input, at a rate corresponding to a full-scale frequency of about 1/4 cycle per second. These results correlate very well with previous NASA/FAA flight test results which indicate that essentially total vortex alleviation can be achieved at a 3-nautical-mile separation distance by oscillating the lateral controls.

Analysis of the visual data from these model tests has provided insight into the flow dynamics contributing to the rapid vortex decay rate observed for the oscillating case. As would be expected, the periodically changing wing spanload distribution and turbulence injection produce an extremely complex wake. Large flow nonuniformities are produced longitudinally in the wake during each cycle of oscillation, and in addition large lateral interactions are produced because of the asymmetrical nature of the oscillation. It is hoped that these studies will lead to the development of more practical alleviation concepts.

The test results are of considerable technical interest because they demonstrate that nearly total vortex alleviation can be achieved as close as 2 to 3 nautical miles behind a large transport aircraft in the landing configuration. Since current terminal area Instrument Flight Rules (IFR) governing separation requirements for aircraft following such large transports are from 4 to 6 nautical miles, depending on following aircraft size, near-total vortex alleviation at 2 to 3 nautical miles could permit a significant reduction in separation requirements without compromising safety.

F. L. Jordan, 2543 (505-41-83)

## Propfan Noise Measured and Predicted

A flight test to measure fuselage sidewall acoustic pressures from a model of a high-speed propfan model is being conducted by NASA Dryden Flight Research Center. A Jetstar aircraft is used with the propfan model operating on a fuselage-mounted pylon. Langley had made predictions of the expected noise several months before the first flight test. Some of the acoustic data from the first test have been analyzed and compared with the pretest predictions. The graph shows the measured data for one test condition together with pretest predictions corrected for fuselage reflection. The microphone array is parallel to the propfan axis. Operating conditions of the flight test were altitude = 9.15 km (30 000 ft), flight Mach number = 0.8, helical tip Mach number = 1.07, and advance ratio = 3.5. The blade angle in the test was set at a slightly higher value than that used in the calculations, resulting in about 80 percent higher horsepower absorption during the test than was assumed for predictions. This could influence predictions for microphones which are far from the propfan plane. However, the predictions are in substantial agreement with measured data — within 4 dB of the measurement.

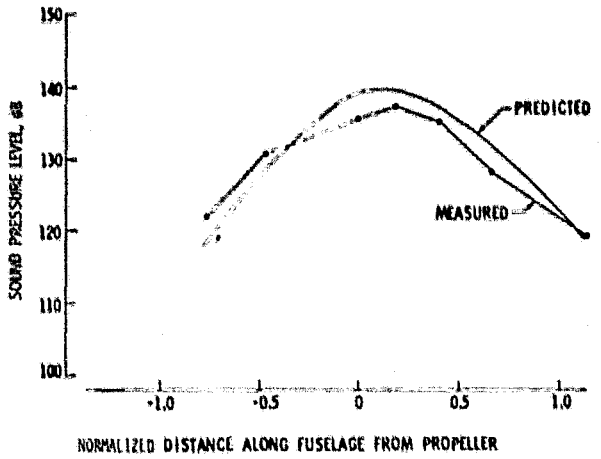


*Measurement and prediction of propfan noise*

F. Farassat, 2645 (505-42-23)

## Helicopter Vibration Reduction

A higher harmonic control (HHC) system for the reduction of helicopter fuselage vibrations has been developed and tested in the Langley Transonic Dynamics Tunnel. This method of reducing vibrations is achieved by superimposing nonrotating swashplate motions upon the basic flight controls at the blade passage frequency. The blade passage frequency is defined as four times the rotor rotational frequency for a four-bladed rotor

(4P). Helicopter model tests demonstrated that by choosing the correct amplitude and phase of 4P input, rotor oscillatory airloads were altered to achieve up to 90-percent reductions in the forced 4P fuselage vertical and longitudinal vibration levels.

The unique components developed for higher harmonic control include an electronic control unit (ECU) and an optimum controller. The ECU extracts the 4P component of the fuselage vibrations from the accelerometers for use by a digital computer. The optimum controller is an algorithm in the computer which calculates the "optimum" 4P magnitude and phase to be implemented through the control system. The controller adapts to changes in the speed of the helicopter (or the wind-tunnel speed) and applies update commands once every rotor revolution.

The success of this joint program with the Army Structures Laboratory will lead to a full-scale flight test on an OH-6A helicopter. The preliminary design, submitted by Hughes Helicopters, was successfully reviewed by a joint NASA-Army committee and hardware for the flight test is being fabricated. The figure designates the major components to be installed on the testbed aircraft.

John H. Cline, 2661 (505-43-13)

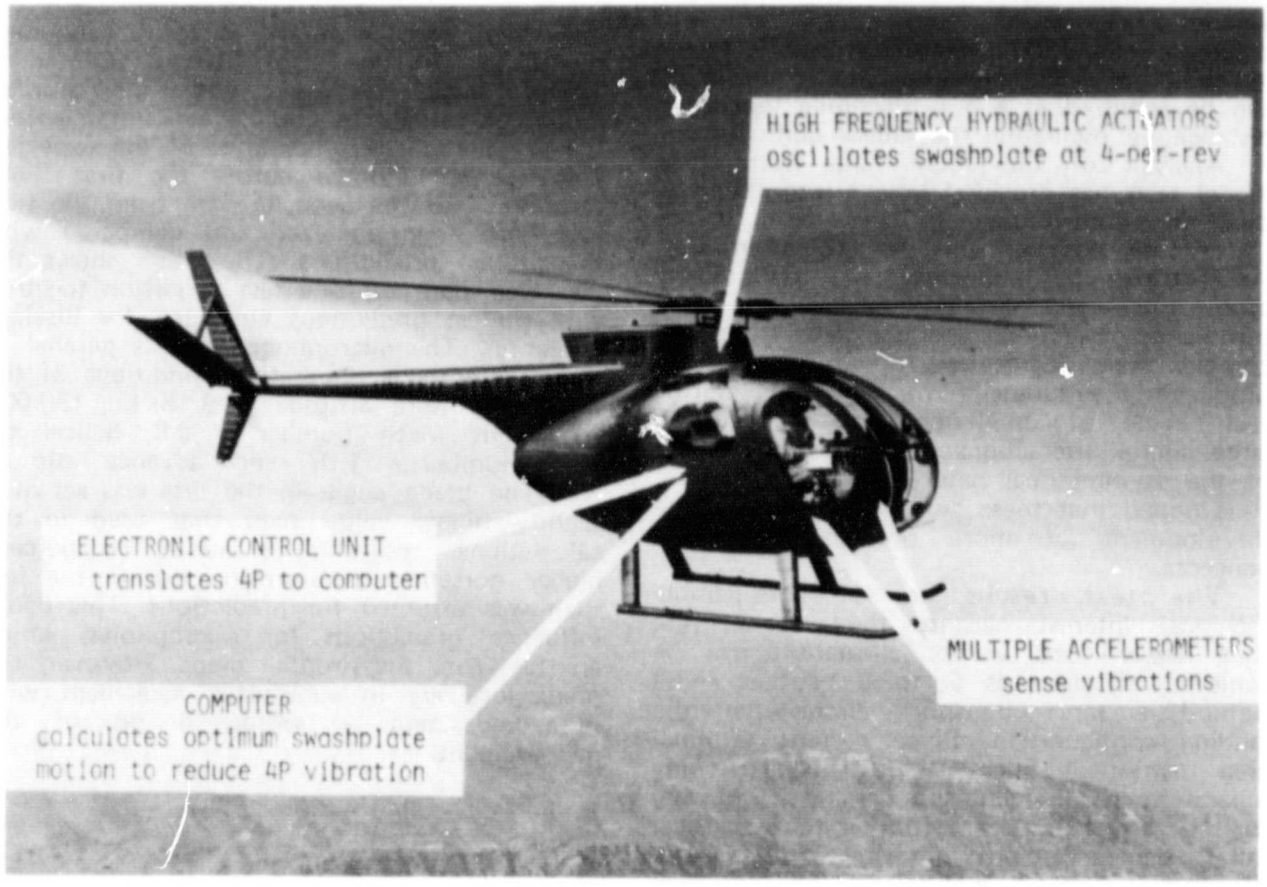


*Major components of higher harmonic control system*

## Military Stall/Spin Research

Military stall/spin research is conducted at Langley to provide the United States with the technology needed to develop high-performance military airplanes having satisfactory stall/spin characteristics which enhance, rather than limit, tactical effectiveness. During the past year, accomplishments have included continued

ORIGINAL PAGE IS
OF POOR QUALITY

analysis of the F-18 airplane, study of several advanced fighter designs, and investigation of the high-angle-of-attack aerodynamics which causes undesirable wing-rock characteristics in fighter airplanes.

Additional tests and analyses conducted on the F-18 design have identified potential adverse effects of external stores at high angles of attack and have defined small airframe refinements which could provide needed improvements in high-angle-of-attack pitch stability. Wind – tunnel tests of the forward-swept-wing fighter design, proposed for prototype flight tests by the Defense Advanced Research Projects Agency (DARPA), have revealed that the airplane fuselage forebody aerodynamics seem to dominate the high-angle-of-attack stability and control characteristics more so than the forward-swept wing feature. High-angle-of-attack investigations of a fighter design incorporating the arrow-wing concept have identified several airframe changes which are needed to provide acceptable pitch stability and lateral stability, and have provided the aerodynamic data now being used to conduct a piloted simulator study of this design on the Langley Differential Maneuvering Simulator (DMS).

Further wind-tunnel studies of the high-angle-of-attack dynamic phenomenon of limit-cycle rolling motions, known as wing rock, have employed unique dynamic test methods to identify the nonlinear aerodynamic damping characteristics causing wing rock. Specific wing-rock studies of a highly-swept delta wing have revealed the flow-field mechanisms producing the motion and have culminated in the development of a mathematical model capable of predicting the oscillatory behavior observed in experiments. Extension of this testing and analysis to complete fighter configurations is now in progress.

W. P. Gilbert, 2184 (505-43-13)

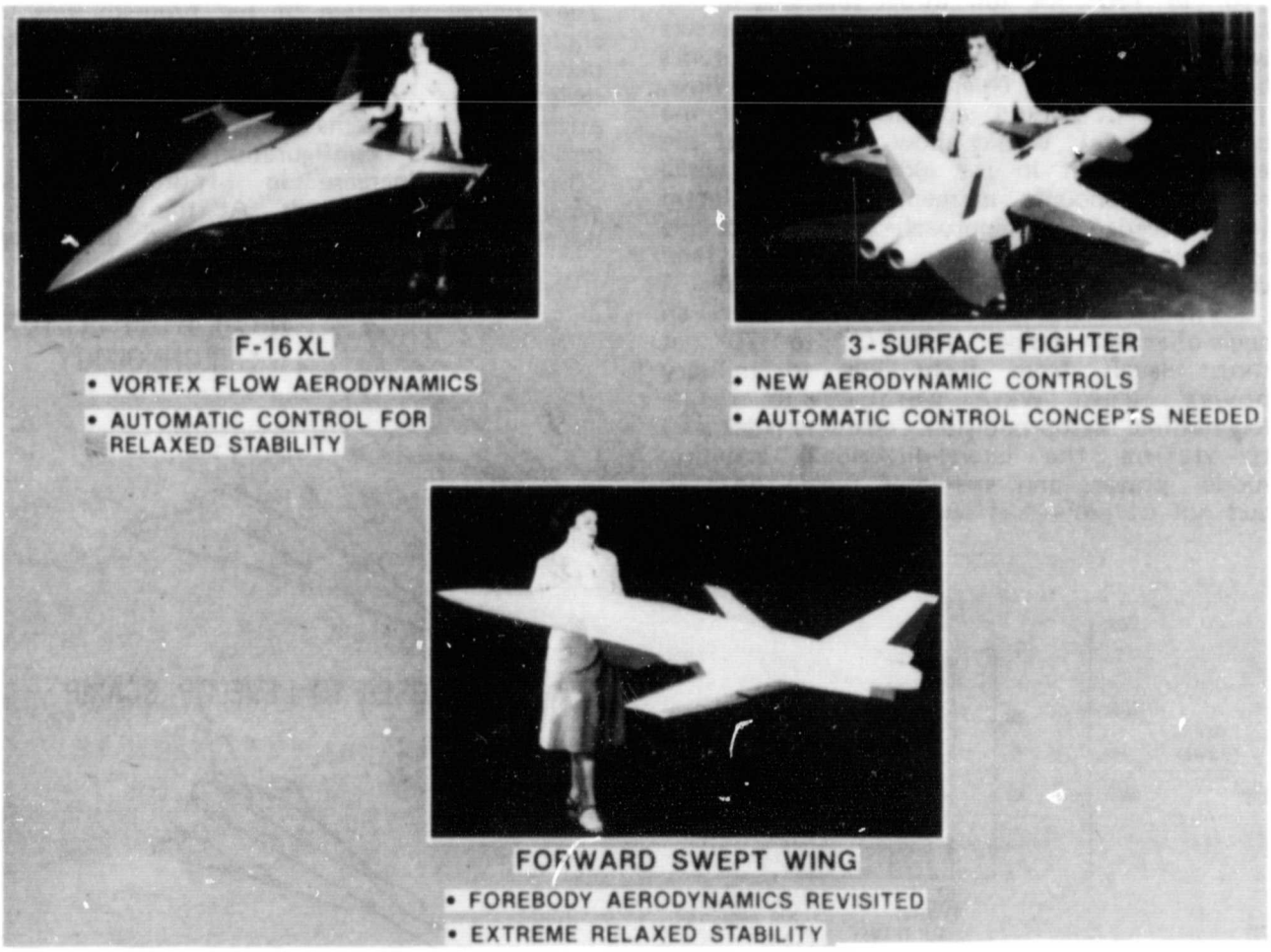


*High-angle-of-attack research on advanced designs*

## Effects of Thrust Reversing on Fighter Aerodynamics

A cooperative investigation involving NASA, U.S. Air Force Wright Aeronautical Laboratory (AFWAL), and McDonnell Aircraft Company was conducted in the Langley 4- by 7-Meter Tunnel to determine the effects of thrust reversing on the low-speed aerodynamics of a 13-percent F-15 fighter configuration. Three thrust reverser concepts were tested. The reversers were designed to spoil thrust in a manner which permits military power settings to be maintained in the approach configuration and also to obtain full reverse thrust for reduced ground rolls once the configuration is on the ground. The first reverser configuration was an upstream rotating vane concept in which the reverser was installed ahead of the basic F-15 nozzle. Four sets of vanes were used to vector the exhaust flow from $50^{o}$ to $90^{o}$ for partial thrust reversing during approach and from $110^{o}$ to $130^{o}$ for full thrust reversing during landing roll. The second and third reversers were both a three-door type. Clam-shell doors both blocked and reversed the exhaust flow. This concept would completely replace the basic nozzle. It would allow a portion of the exhaust to exit in the axial direction while reversing enough momentum to maintain thrust needed for approach with the engine at military power settings. The flow is then completely reversed during the landing roll.

These tests were conducted over an angle-of-attack range from $0^{o}$ to $20^{o}$ at thrust levels from flight idle to military power. Data were obtained to define longitudinal aeropropulsion characteristics and to define the lateral-directional stability, rudder power, and stabilator power both in and out of ground effect.

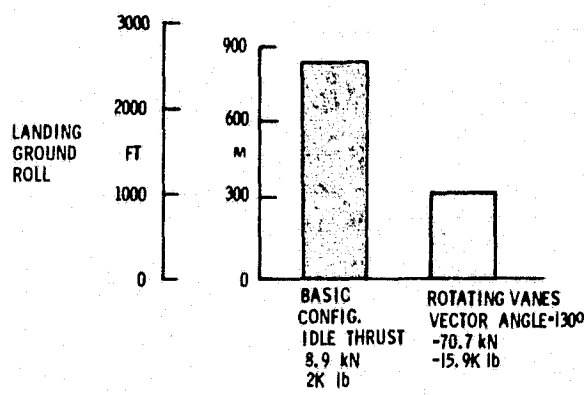


*Effect of thrust reversing on landing roll*

Preliminary results indicate that the best configuration was the upstream rotating vane. The data show that the landing distance can be reduced from about 760 m (2500 ft) to less than 300 m (1000 ft). This concept had acceptable levels of aerodynamic interference on approach and appeared to be significantly better than the three-door concept in the full reverse mode in ground effect.

John W. Paulson, Jr., 3611 (505-43-23)

## Fighter Technology Research

A cooperative research program has been conducted over the last 4 years in which a Langley team of aerodynamic researchers and personnel from the General Dynamics Corporation have applied their latest technology to the development of an efficient supersonic wing for the basic F-16 airplane. The original objective of the program was to apply advanced supersonic wing technology to develop an efficient supersonic wing and maintain the fuselage, propulsive system, and aircraft subsystems intact. This research resulted in a configuration which has a 30-percent increase in lift-drag ratio at supersonic cruise speeds. At the same time, research was being conducted to design an

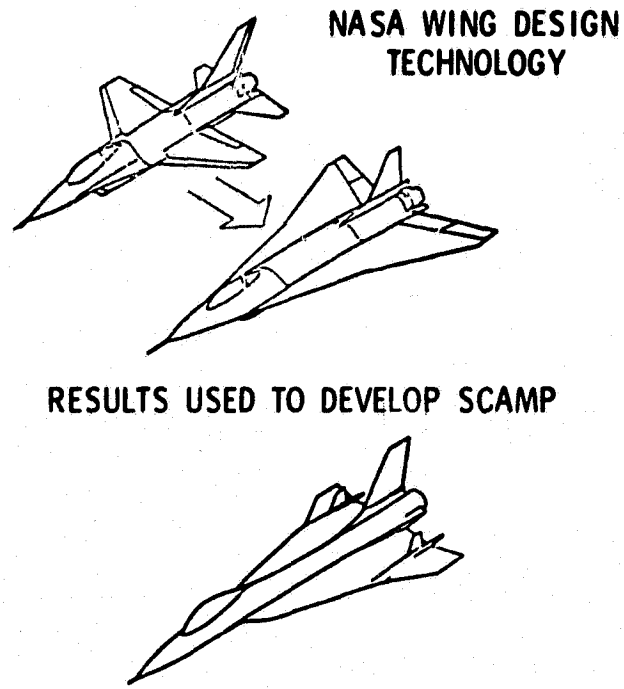


*NASA/industry cooperative fighter research*

efficient, transonic maneuver camber surface for the new wing planform. This work showed significant potential for improved transonic performance. With these possibilities of a major improvement in the basic F-16, the General Dynamics Corporation initiated a Supersonic Cruise and Maneuver Program (SCAMP) to develop an advanced F-16. The Langley team continued to contribute to the technology of this concept by providing improvements to the low-speed characteristics.

Based on the technology improvements provided by the Langley team of researchers, General Dynamics has taken the SCAMP study into the prototype development stage. Two prototype aircraft (designated F-16E) are being built and the current schedule calls for flight by July 1982.

W. C. Sawyer, 3134 (505-43-23)

## Aeropropulsive Performance of Nonaxisymmetric Nozzles on the F-18

Recent studies of nonaxisymmetric nozzles installed on twin-engine fighter aircraft have identified several potential benefits of this nozzle concept. These include improved integration for installed drag reduction, thrust vectoring for maneuver enhancement and short take-off and landing, and thrust reversing for improved agility and ground handling. An investigation has been conducted on a 0.10-scale model of the F-18 airplane to determine the performance of nonaxisymmetric nozzles relative to the aircraft's baseline axisymmetric nozzle at Mach numbers from 0.60 to 2.20. The performances of a two-dimensional convergent-divergent (2-D C-D) nozzle, a single-expansion ramp nozzle (ADEN), and a wedge nozzle were compared to the baseline axisymmetric nozzles. The nonaxisymmetric nozzles were designed for vectoring and reversing (except ADEN). The axisymmetric nozzle did not have these capabilities. An incremental afterbody thrust-minus-drag parameter is presented which is the difference between performance for the F-18 with nonaxisymmetric nozzles and that for the baseline axisymmetric nozzles. A positive increment indicates higher performance for the F-18 with nonaxisymmetric nozzles installed. The comparisons presented here are for the nozzles in their full-forward-thrust mode at dry or cruise power and for the aircraft at zero angle of attack.

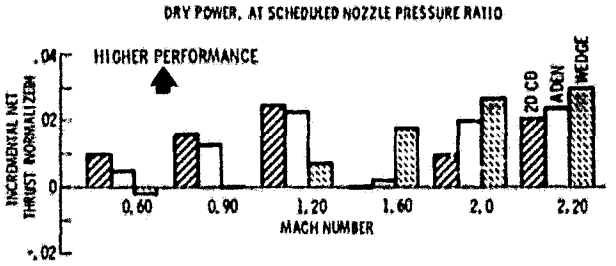


*Afterbody aeropropulsive performance (incremental over axisymmetric nozzle)*

These results demonstrate that 2-D C-D nozzles can be installed on twin-engine aircraft with equal or higher performance than axisymmetric nozzles. Similar results were found for the 2-D C-D nozzle in an afterburner mode. Under dry power conditions, the ADEN and wedge nozzles also showed advantages.

Francis J. Capone, 2674 (505-43-23)

## Computer Management of Product Design Information

The Integrated Programs for Aerospace Vehicle Design (IPAD) project is developing computer-based technology to support product design in the aerospace industry. A computer program package developed under IPAD provides for the first time a high-speed interactive capability to manage engineering data. This software package is denoted Relational Information Management System (RIM) and has proved very effective at Langley in computer-aided analysis and design activities. RIM manages data in a convenient fashion for engineering use and is capable of interfacing with FORTRAN-based engineering applications programs. RIM was used to manage data involved in structural analysis of 8000 thermal protection system tiles on the Shuttle Orbiter. The RIM Shuttle tile data base included 600 000 words characterizing geometry loads, materials, and resulting stresses and deflections. It was a vital tool in certifying the tiles for the first flight of the Shuttle.

R. E. Fulton, 2887 (510-54-13)

## Laminar Flow Control (LFC) Technology

Important goals of laminar flow control (LFC) technology include maintaining laminar flow and delaying or preventing turbulent eddies from disrupting the flow field about a wing. Preliminary designs of two LFC wing structures for commercial transport aircraft have now been completed. One design employs an approach in which the surface suction slots and suction ducting are integrated into an advanced composite material wing structure. The other design employs porous outer panels attached to the primary wing structure. The porous panels are a sandwich construction with an electron-beam-perforated titanium outer face sheet (0.635 mm thick with 0.066-mm-diameter perforations) and a fluted core for collection of suction air. Design studies have also been completed which address the packaging problems of LFC systems in the leading edge of commercial transports, with new concepts evolved for storing suction ducts, deicing systems, anticontamination systems, and leading-edge high-lift devices. Packaging difficulties can be resolved by functionally integrating the required system; for instance, the Krueger shield, a leading-edge high-lift device, can also function as an anticontamination component.

Parametric studies have also been completed to determine the characteristics of a high-lift system for the NASA design advanced LFC airfoil. With appropriately chosen leading-edge Krueger gap and overlap, a short-chord Krueger and a trailing-edge flap have been found which produce adequate high lift in the takeoff and approach configurations. Finally, a contract study conducted by The Boeing Company has demonstrated that the super plastic formed diffusion-bonded (SPF/DB) process for titanium structure fabrication can be adapted to fabricate thin-gage LFC porous panels. Small demonstration panels were fabricated to verify attainable surface smoothness and wave-free requirements. In a parallel effort, the feasibility of SPF/DB fabrication of thick sandwich skin primary wing structure with integral molded suction passages was also demonstrated.

Richard D. Wagner, 2045 (534-01-13)

## Control Surface Unsteady Aerodynamics

Wind-tunnel model tests have been conducted in the Langley Transonic Dynamics Tunnel on a 10.8-aspect-ratio semispan wing with leading-edge and trailing-edge control surfaces which can be oscillated over a wide range of frequencies and amplitudes. The wing has a supercritical airfoil section and a planform representative of energy-efficient transport designs of current interest. The model is shown mounted on the tunnel

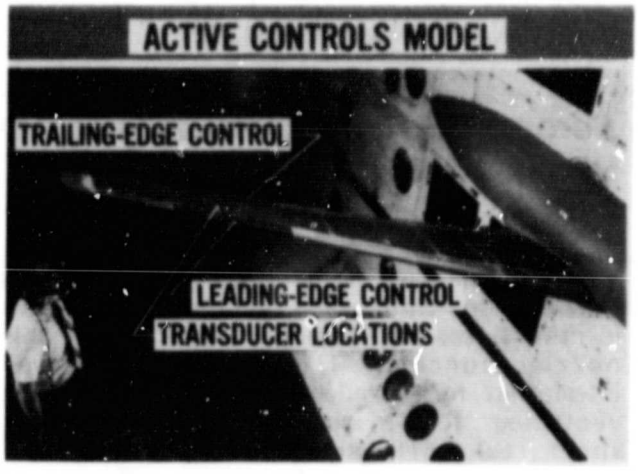


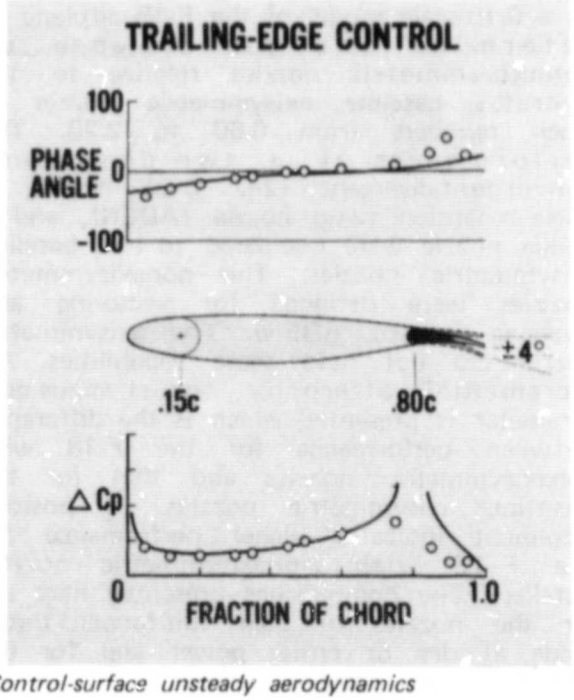


*Control-surface unsteady aerodynamics*

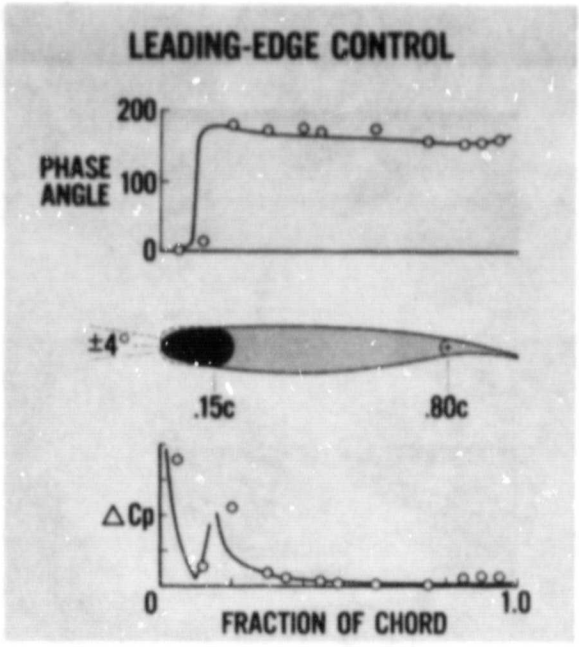


*Control-surface unsteady aerodynamics*

sidewall. The two outboard (leading-edge and trailing-edge) control surfaces were oscillated about their hinge lines to generate the unsteady airloads on the wing, and pressure transducers measured chordwise distributions of lifting pressure.

High-quality unsteady pressure data have been obtained at several Mach numbers. At moderate subsonic Mach numbers, where there are no transonic shock waves, good agreement is obtained between experimental and calculated lifting pressure coefficients ($\Delta C_p$) and phase angles. Theoretical methods are being developed to predict unsteady pressure distributions at transonic Mach numbers where shock waves are observed, and the experimental data will be very valuable in evaluating these methods.

Maynard C. Sandford, 2661 (534-02-13)

## Energy-Efficient Transport (EET)


*Test aircraft*

Developing techniques and controls for reducing the fuel consumption of transport aircraft is an important goal of the EET program. An active controls-integrated system has been investigated and found to have the potential of reducing fuel consumption by 10 percent. Analysis and wind-tunnel tests have previously indicated that the application of winglets to the DC-10-10 will reduce fuel consumption by 3 to 5 percent. McDonnell Douglas Corporation has designed, fabricated, and installed winglets on a DC-10-10 and begun flight tests which will be continued in fiscal year 1982. Analytical studies and wind-tunnel tests have also indicated that relaxed static stability or aft center of gravity and a smaller horizontal tail on the Lockheed L-1011 airplane would result in a fuel savings of approximately 5 percent. An active controls system has been designed which will allow relaxed static stability on the L-1011. Test aircraft modifications and system tests are currently being performed by Lockheed Corporation and flight tests are scheduled to start in December 1981.

In-service flight evaluations of selected coatings applied to the slats and horizontal tail of a Boeing 727 demonstrated that polyurethane coatings were effective in reducing rain erosion damage to aircraft leading-edge surfaces. Furthermore, additional flight tests using Langley's TCV (Terminal Configured Vehicle) Boeing 737 airplane have indicated a slight reduction in drag due to the coatings as compared to the type of paint currently in use on commercial transports. Extensive in-flight measurements of both the aerodynamic and inertial loads on a Boeing 747 nacelle and pylon have been obtained in order to correlate such loads with changes in engine turbine and fan-blade clearances due to distortion of the engine case. These data will be used by the engine manufacturers to design engines which will be less susceptible to performance deterioration over their life cycle.

Ray V. Hood, 2396 (534-02-13)

## Laminar Flow Control Hardware

Laminar flow control research depends upon localized boundary-layer control over finitely small areas of the upper and lower wing surfaces. Hardware to control this suction has never before been designed or fabricated. Investigations at Langley will include both wind-tunnel and flight research

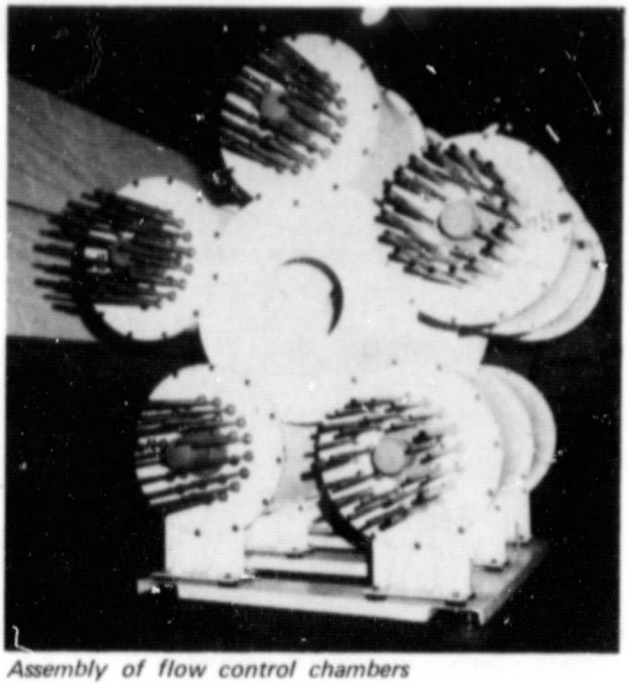

*Assembly of flow control chambers*

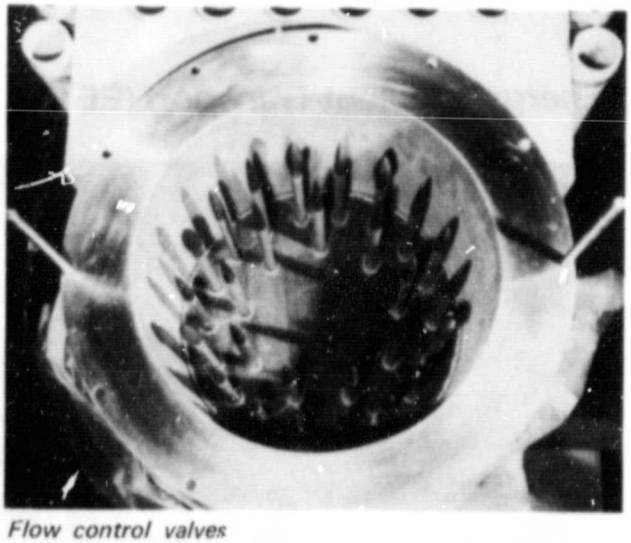

*Flow control valves*

phases. In these investigations, critical wing regions are provided with a porous surface through which air is bled off to ensure laminar flow. This design utilizes five independent flow control chambers, each having 30 precisely controlled bleed orifices.

The design and fabrication of these control valves and flow control chambers required unique combinations of castings, machined parts, and composites. Extensive use of bonding and specially designed manufacturing aids allowed materials unsuitable for machining to be used as primary load-carrying members. Selective low-temperature bonding procedures were chosen to be used on interchangeable items

to allow quick and easy interchangeability without loss of structural integrity. A major component of the valve control mechanism was an investment casting which combined threads, studs, bearing supports, and motor mounting into a single unit. All of these techniques contributed to significant cost savings and easy maintenance.

S. C. Irick, 4621 (534-02-13)

## Composite Components for Commercial Aircraft

Because of their low weight and associated aircraft fuel savings, the use of composite components is expected to grow in the commercial aircraft industry. The first flight of composite primary structure on a commercial transport aircraft was conducted September 26, 1980 with the B-737 composite horizontal stabilizer. Certification of this composite component is expected by March 1982. McDonnell Douglas has successfully completed a rigorous environmental test program for the DC-10 composite vertical fin stub box to assess the influence of moisture and temperature on strain distribution, durability, and residual strength of complex composite structures. Assembly of three full-size DC-10 fins is in progress and flight checkout is expected in February 1982. Segments of the covers and spars of the L-1011 composite vertical fin have now completed 10 years of a planned 20-year simulated service life including flight loads, moisture, and temperature, without incident. The L-1011 composite fin ground-test article experienced premature failure during static tests and is undergoing design modification prior to resumption of static and fatigue tests.

Five shipsets of B-727 composite elevators have accumulated approximately 21 400 flight hours since delivery between March and June 1980. Twelve DC-10 composite rudders in flight service have accumulated more than 164 700 flight hours; the high-time rudder has 21 000 hours. FAA certification of the L-1011 composite aileron was issued in September 1981 and four shipsets of ailerons are to be placed in flight service by the first quarter of 1982.

Herman L. Bohon, 3081 (534-03-13)

## Use of Flight Path Information for Instrument Approaches

A piloted simulation study was conducted by the Flight Systems Division of the Bendix Corporation aimed at evaluating the addition of flight path angle (FPA) symbology to a color electronic attitude director indicator (EADI) for control and monitoring (by the pilot) during flight director instrument approaches. The transport simulator used in the study is a fixed-based cab and modeling is based on the DC-10 airplane. The location of the display is in a primary position on the pilot's instrument panel. Three display formats were evaluated, each made up of a base-line set of display parameters consisting of pitch and roll attitude, indicated airspeed, radar altitude, fast/slow, glide slope, and localizer deviation, and pitch and roll flight director commands. The two format variations about the basic display included the addition of, and specific symbology for, flight path angle, drift angle, and flight path acceleration information. The evaluation was conducted during $3^{\circ}$ straight-in approaches with two different wind profiles characterized by lateral, longitudinal, and vertical shears and turbulence conditions. Flight path tracking data and pilot subjective comments were examined with regard to the pilot's ability to capture and maintain the localizer and glide slope when using each of the three display formats. Four airline pilots were used as subjects.

The results show that the addition of FPA information to a basic EADI format did not significantly improve lateral or vertical tracking performance during the approach to landing under the simulated wind profiles. However, pilot workload required to assess the presence of lateral and vertical wind shears was reduced by the display of flight path and drift information.

Samuel A. Morello, 3621 (534-04-13)

## Improvement of Automatic Flare Control Laws

The present FAA certification criteria for commercial automatic landing systems allow a longitudinal touchdown dispersion of 114.3 meters. In order to reduce runway occupancy time, this dispersion must be reduced to allow aircraft to touch down more accurately

with respect to a high-speed exit location. It is also desirable to control sink rate closely to prevent hard landings for increased safety and reduced maintenance costs. With these goals in mind, three different approaches to improved flare control laws have been taken. The resulting designs have been evaluated in both simulation and flight tests.

The Terminal Configured Vehicle (TCV) Boeing 737 baseline system included the so-called exponential flare law in which the touchdown point and flare initiation altitude are a function of groundspeed. The table gives baseline performance for the TCV baseline law in simulation and during microwave landing systems (MLS) tests in 1976 and 1977. The first attempt to improve performance involved a modification of this control law, called the groundspeed adaptive, in which the exponential path was also a function of groundspeed and the flare altitude was constant. As shown in the table, a substantial improvement in performance was achieved. A version of this flare law is now being implemented by The Boeing Company on the new advanced B-737.

The next tests involved guiding the airplane along a specified trajectory during the flare maneuver. The data in the table form a composite based on several types of landing guidance. During tests with the MLS experimental flare guidance unit this law met the TCV goal. The most recent improvement is the Digital Integrated Auto Land System (DIALS). It is the first modern direct-digital integrated control design to be flown on a commercial transport airplane, and its simulation was closest to the TCV goal with the capability to fly selectable glideslopes up to 6°, approaches at angles up to 4.5° have been achieved in current flight tests.

| Flare Algorithm | Simulation | | Flight | |
|---|---|---|---|---|
| | Longi-tudinal (m) | Sink Rate (m/sec) | Longi-tudinal (m) | Sink Rate (m/sec) |
| TCV B-737 exponential | 77.4 | 0.24 | 78.9 | 0.32 |
| Groundspeed adaptive | 56.4 | 0.31 | 41.8 | 0.19 |
| Specified trajectory | 42.1 | 0.24 | 33.8 | 0.20 |
| Digital integrated | 34.4 | 0.26 | (a) | (a) |
| TCV goal | 30.5 | 0.30 | 30.5 | 0.30 |

(a) Insufficient data at present.

*Touchdown dispersion*

Richard M. Hueschen, 3209 (534-04-13)

## High-Angle-of-Attack Flow-Field Solutions for Orbiter Entry

Calculation of the three-dimensional flowfield about lifting bodies at hypersonic speeds is accomplished at moderate angles of attack by first solving a starting solution encompassing the subsonic portion of the shock layer, and then progressing, or "marching," along the length of the body. Such a method is not applicable at high angle of attack, since the subsonic region may envelop much of the windward side, and the marching technique is only applicable if the flow is supersonic everywhere in the marching direction. Until recently, no solutions of the Shuttle Orbiter flowfield at its entry angle of attack of about 40° were available because of this restriction.

A new computer code designated HALIS (high alpha inviscid solution) provides time-asymptotic solutions of the Euler equations to obtain inviscid flow-field calculations at the desired high angle of

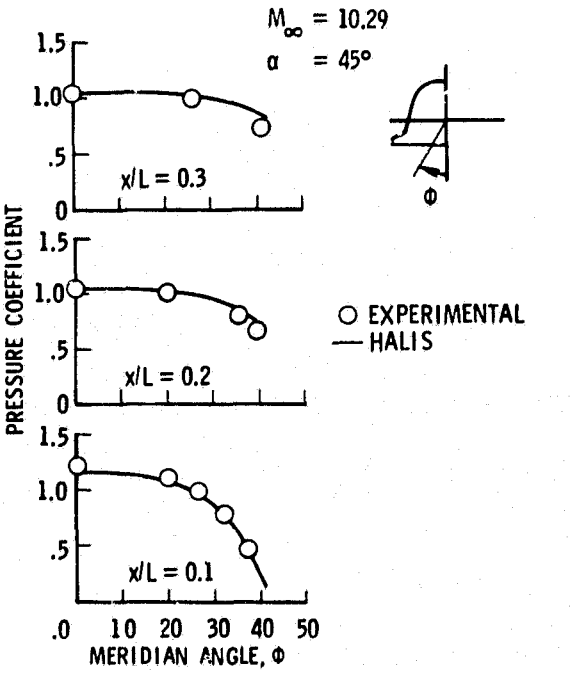


*Meridian pressure distribution at stations (x/L) along Orbiter length*

attack. The code, which is programmed on Langley's Control Data CYBER - 203 vector-processing computer, utilizes a computational grid of over 30 000 mesh points and has been used to obtain solutions for about one-half of the Orbiter length. Combining the results with an approximate boundary-layer method permits description of the heat-transfer rate distributions for comparison to actual flight data.

K. J. Weilmuenster, 3271 (506-51-13)

## Adaptive Grid Code for Complete Flowfields

An adaptive grid finite-volume method has been used to solve the Navier-Stokes equations for complete (forebody and afterbody) flow fields about blunt bodies. The code, which is applicable for axisymmetric or two-dimensional flows, allows the computational mesh to adjust during the computation to provide a closer spacing of mesh points in regions of high gradients, thus minimizing the total mesh size required. The development stage of the study has focused on the Galileo probe configuration, but a wide variety of bodies may be treated.

The solution technique is explicit, utilizing a maximum time step advancement at each grid point to accelerate convergence to the steady state. The code has been fully vectorized for efficient solution on Langley's Control Data CYBER 203 computer.

A very flexible grid adjustment routine can be used to concentrate mesh points anywhere in the field, either by a user-defined algebraic or exponential weighting function or by allowing the high-gradient regions to concentrate the grid. The grid adjustment routine is implicit in nature and represents a very small portion of the total computational cost. Currently, the code runs in approximately $3.4 \times 10^{-5}$ seconds per grid point per iteration.

P. A. Gnoffo, 2921 (506-51-13)

## Hidden-Line Program for Aerospace Vehicle Display

A hidden-line program to display aerospace vehicles has been developed at Old Dominion University under a Langley grant. This program takes advantage of several hidden-line techniques, and the computation time is nearly linear with the number of

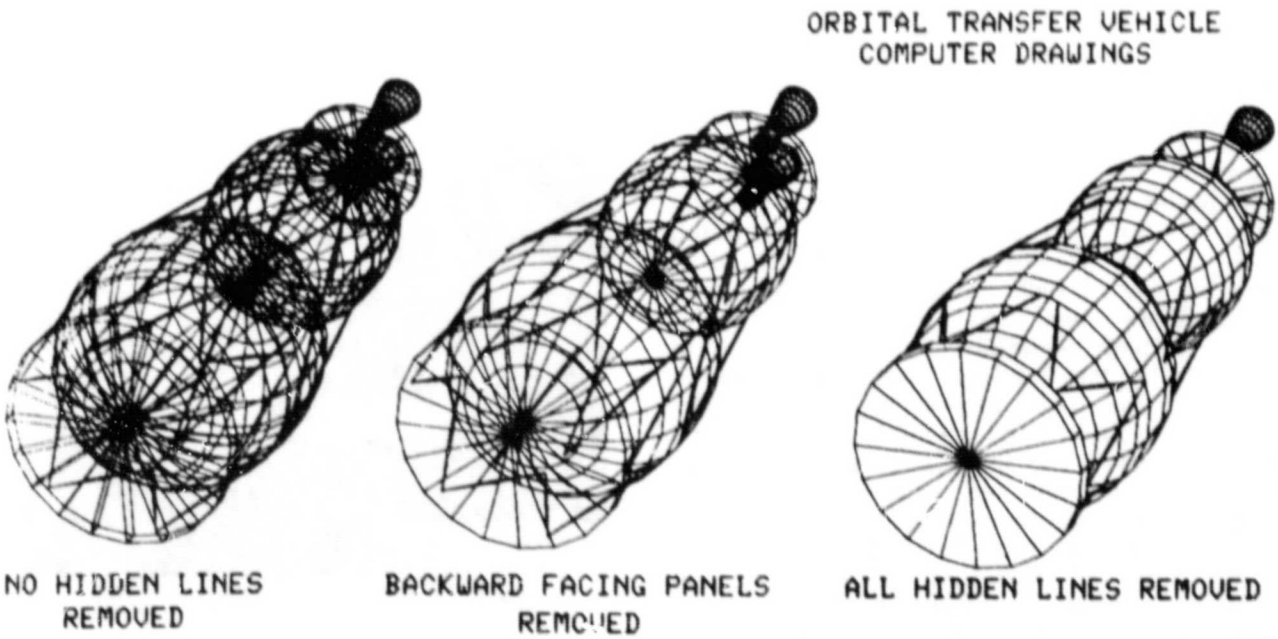


*Hidden-line program for engineering displays*

points defining the surface of the vehicle. Three computer drawings are shown of an orbital-transfer vehicle defined by 4000 points. It takes approximately 1 minute to input the data points and draw the vehicle with no hidden lines. In the second drawing, the panels facing away from the viewer are removed. In spite of the additional computational time to remove the hidden panels, it takes only approximately 45 seconds to complete the drawing since the number of vectors actually plotted is less. In the last case, all the hidden lines are removed. With previous programs, it took on the order of several hours to remove these hidden lines. For the present algorithm, it took approximately 3 minutes on a minicomputer to process the data and plot the drawing on a storage-tube terminal. With this program it is now possible to make a thorough check of a configuration before it is analyzed.

Alan W. Wilhite, 3911 (506-51-13)

## First Measurements of $C_3$ Ultraviolet Band System

The absorption properties of hydrocarbon species are important in determining the extent to which ablation gases emitted from carbon phenolic heat shields are successful in shielding an entry nose cap from shock-layer radiation. Such ablation layer absorption is crucial for the Galileo probe during entry into the atmosphere of Jupiter. In the present investigation, a strong absorption band has been measured in the vacuum ultraviolet (130 to 200 nm) and identified as a transition of the $C_3$ molecule. A portion of this absorption system has been previously reported, but had been tentatively attributed to $C_2H$. The present study was conducted in the Langley 6-Inch Shock Tube. Acetylene and methane were each used as test gas, and the resulting variation in hydrogen-carbon ratio in the test medium was instrumental in determining the absorbing species. The measured absorption strength is in good agreement with a theoretical prediction for the $C_3$ transition and represents the first experimental confirmation of this transition. Incorporation of this new absorption cross section into a flow-field code yields an increase of about 7 percent in ablation layer absorption at Jupiter entry conditions.

Judy L. Shinn, 3786 (506-51-23)

## Silicon Carbide/Titanium Composite Strength Enhancement

The strength of silicon carbide/titanium composites historically has been well below the theoretical limit primarily because of deleterious fiber-matrix reaction during fabrication causing material property degradation. Introducing pure aluminum into the composite system at the fiber-matrix interface by sputtering aluminum directly onto the matrix foils prior to composite consolidation has been found to improve the composite strength. During consolidation, the aluminum reacts with the titanium to form various relatively stable intermetallic compounds which act as diffusion barriers to impede the bulk migration of reactants and as activation energy barriers to the formation of undesirable titanium carbides and silicides.

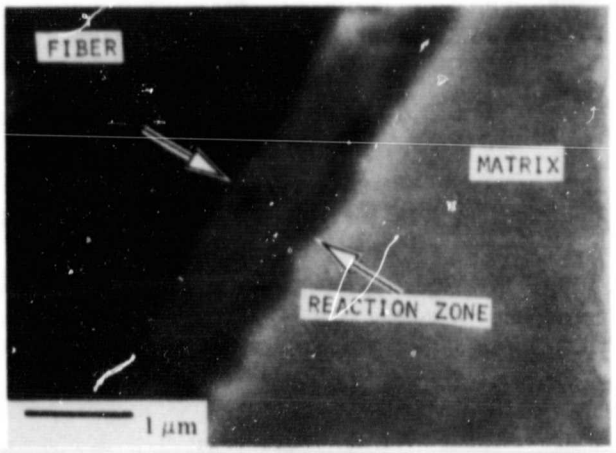


SiC/Ti (Al-COATED) - REACTION ZONE~0.33 μm

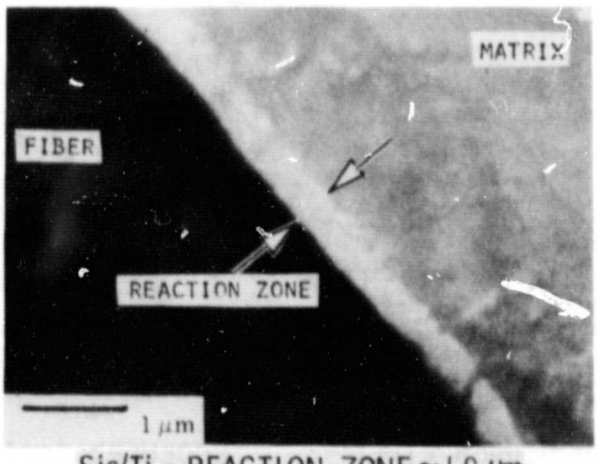


SiC/Ti - REACTION ZONE ~ 1.0 μm

*Photomicrographs of fiber-matrix interface in SiC/Ti composites*

These factors all contribute to the formation of a significantly thinner reaction zone than is typically found in silicon carbide/titanium systems. The coated foil composites have shown increases in strength of up to 50 percent over that of composites with uncoated foils.

William D. Brewer, 3041 (506-53-23)

## Improved Space Shuttle Dynamic Tile Analysis

During a mission of the Space Shuttle Orbiter, the thermal protection system (TPS) experiences dynamic loads arising from acoustics, structural vibration, and transonic shock. The strain isolation pad (SIP) material used in the TPS to attach the reusable surface insulation (RSI) tiles to the Orbiter exhibits significant nonlinear stress-strain behavior. Until recently, tiles were structurally analyzed for dynamic loads assuming a linear SIP material. A more accurate analysis was recently developed at Langley in which the SIP is treated as a nonlinear material with hysteretic and nonlinear viscous damping. Studies using this analysis have revealed significant differences between linear and

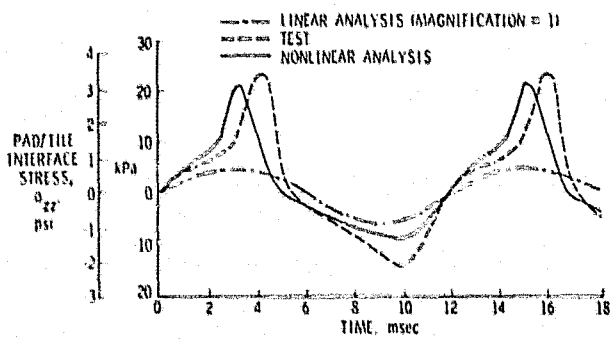


*Dynamic waveform of response to sinusoidal base shake*

nonlinear solutions for peak tensile stresses at the RSI/SIP interface arising from sinusoidal and expected in-flight random dynamic loads. Experiments indicated the capability of the analysis to reproduce the dynamic response of the system. A comparison of the variation with time of the measured and predicted RSI/SIP interface stresses is shown for the case of a sinusoidal substrate excitation. The nonlinear analysis duplicates the high measured stress peaks, whereas the linear solution does not. The dynamic analysis has aided in an examination of the fatigue life of the TPS and has served to demonstrate an in-depth understanding of the dynamics of the system.

Jerry Housner, 2608 (506-53-33)

## Alternate Shuttle Thermal Protection Systems

Recent studies which investigated a variety of alternate thermal protection systems for the Shuttle Orbiter have identified a hybrid system which offers significant improvements in durability, installation, inspectability, and recertification, and is mass-competitive with the current ceramic reusable surface insulation. The hybrid system consists of titanium multiwall tiles for the lower temperature regions, superalloy tiles for the higher temperature regions, and advanced carbon-carbon heat shields for the highest temperature regions. All of the concepts have overlapping lips so that there are no gaps open to airflow and are mechanically attached to the vehicle structure, the tiles with clips and the heat shields with adjustable standoff posts. The all-metal multiwall is formed of alternate layers of dimpled and flat titanium foil; the superalloy concept uses a superalloy honeycomb outer panel, titanium honeycomb inner panel, and corrugated superalloy sides to fully enclose high-temperature fibrous insulation, and the carbon-carbon concept uses a rib-stiffened multipost-supported heat shield to protect encapsulated fibrous insulation.

Verification of the performance and life of each of the concepts through analyses and environmental testing is currently under way at Langley. The evaluation process includes flight testing as part of the Orbiter Experiment (OEX) Program.

Neale Kelly, 3423 (506-53-33)

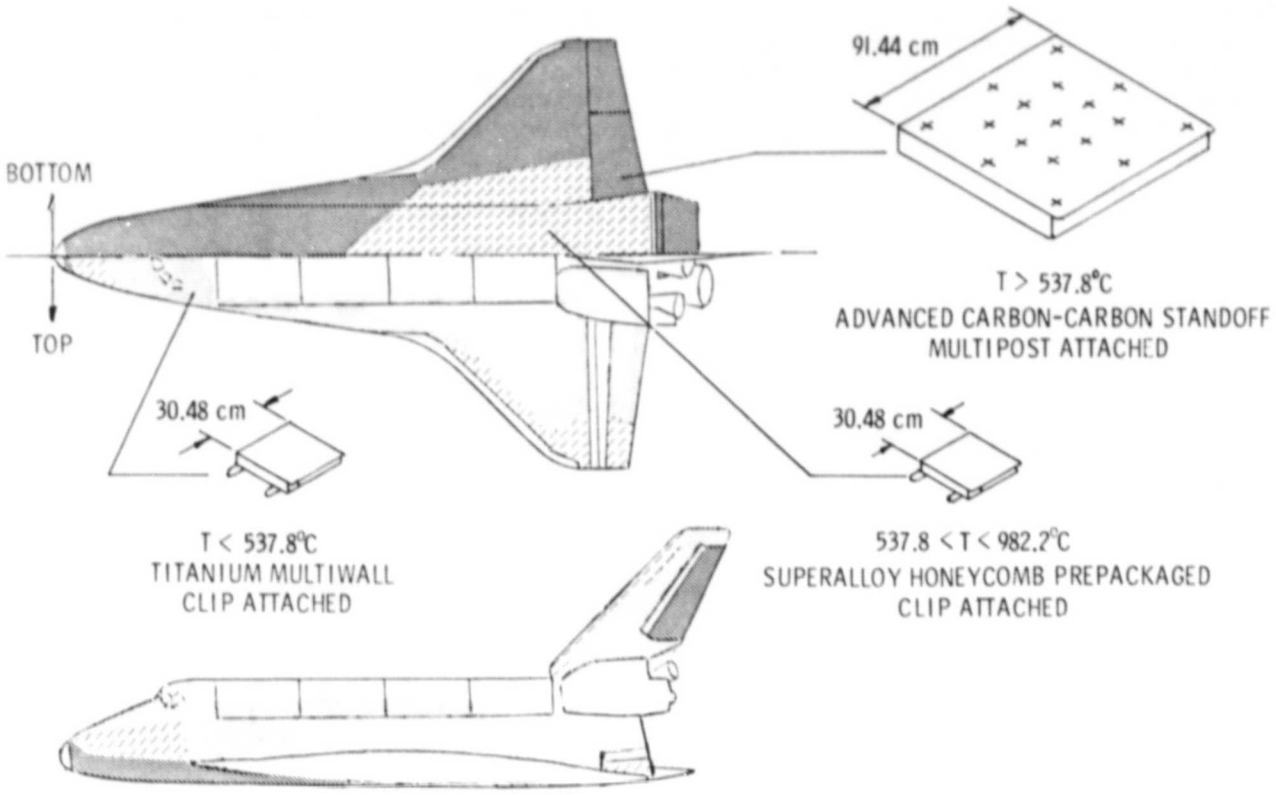


*Alternate TPS concept application*

## Induction Fastening Process

The Langley-developed induction fastening process utilizes an induction heating gun to produce fusion welds in thermoplastic materials. Heating is accomplished by induction coupling to a metal screen located at the tightly joining surfaces. Excellent joints were produced with both acrylic and polyethersulfone adherends. The packaging of this system presents no problem and the power consumption is extremely low (typically 75 W).

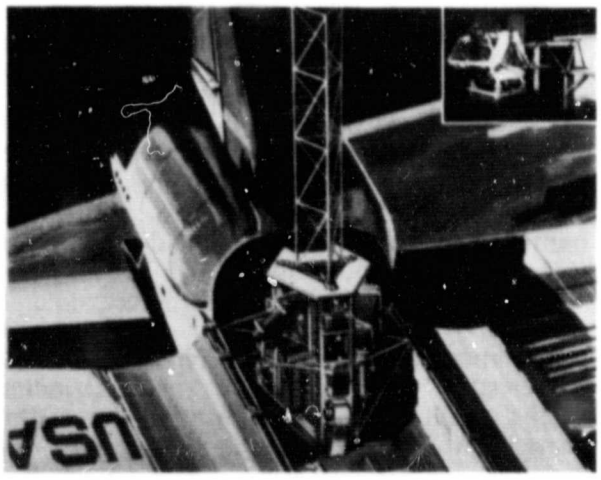

*Toroid induction welding gun used in space manufacturing of beam structures*

John Buckley, 3131 (506-53-43)

## EVA Assembly of a Large Space Structure Element

To assess the potential of manned extravehicular activity (EVA) assembly of erectable space trusses, both manually and with remote manipulator system (RMS) supports, a series of neutral buoyancy tests was conducted under a joint program with George C. Marshall Space Flight Center. Two space-suited test subjects assembled six

5.4-m-long space-weight columns into a regular tetrahedral cell on a mockup of the Shuttle cargo bay. This cell represents the fundamental "element" of a large tetrahedral truss structure. The cell and a simulated equipment module (attached to the cell apex) were assembled under simulated zero gravity, utilizing neutral buoyancy in water. The test setup (assembly aids and tetrahedral cell component) and procedures were modified during the test program to enhance test subjects' performance.

Assembly aids were the greatest contributor to assembly performance by the test subjects in overcoming the restrictions of the suit. These aids provided a fixture on which the cell was assembled and a structure on which the test subjects translated and worked. Foot restraints at each work station freed the test subjects' hands and allowed them to react to their generated forces. Test subjects must learn to accommodate the suit's limits of vision, articulation, and feel. The suit bulk and surface projections limit maneuvers and can make apparently simple tasks difficult, such as inserting a leg into a loop. Furthermore, relatively simple motions of hand-grasping and rotating hardware, such as screws, quickly cause fatigue. The columns were easily manipulated and passed by the test subjects, but once the joints were assembled, verification was difficult. The most difficult maneuver the test subjects faced was positioning and orienting themselves and entering the foot restraints.

The results of the study have confirmed that astronaut EVA assembly of large space structures is well within man's physical capabilities. The time to complete the assembly of the tetrahedral cell, 29 minutes or 5 minutes per column, may be significantly improved by using machines, such as a remote manipulator, to reduce the number of EVA tasks to yield a 3-minute-per-column assembly rate.

Laurence J. Bement, 4621 (506-53-43)

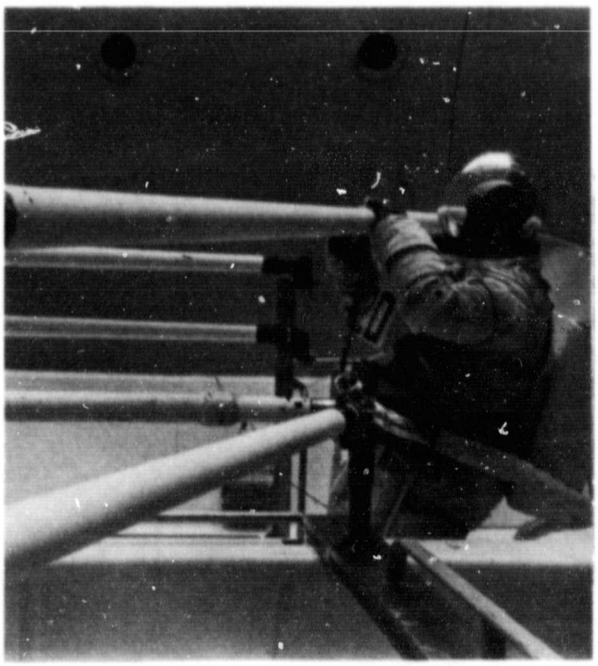

*Column manipulation to installation site*

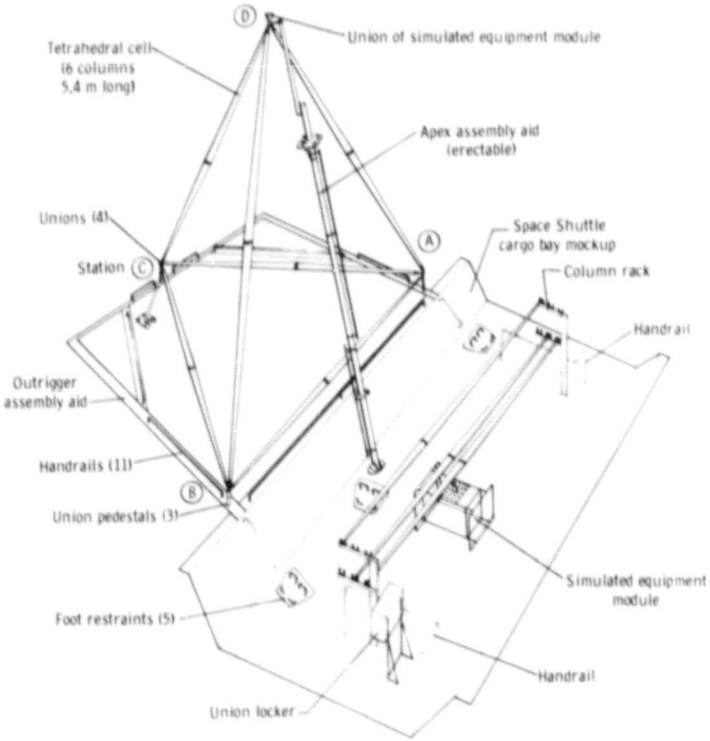


*Simulated zero-gravity EVA assembly of space structure element*

## Space Construction Mobile Work Station Ground Experiments

An assembly concept for large space trusses is being studied at Langley. The concept involves a mobile work station to position a pair of pressure-suited astronauts and move them horizontally and vertically within a prescribed region. The astronauts can

ORIGINAL PAGE IS
OF POOR QUALITY

assemble truss structures which are too large or complex to fold up for transport in the Shuttle Orbiter payload bay. The mobile work station is designed to be located in the payload bay or to be a free flyer operating near the Orbiter.

A large-scale ground test model of the mobile work station has been tested at Langley. The model was used to construct trusses from low-mass, graphite-epoxy conical tubes which can be stacked compactly (like plastic drinking cups) in the Orbiter payload bay for transport into space. A pair of conical tubes is joined at their large ends to form a strut 6 m long. Truss structures are then assembled from these struts by joining their ends without tools, using quick-attachment cluster joints developed at Langley. The concept was tested under Earth gravity at Langley, and two astronauts can assemble a 38-strut truss in about 15 minutes.

W. L. Heard, Jr., 2608 (506-53-43)

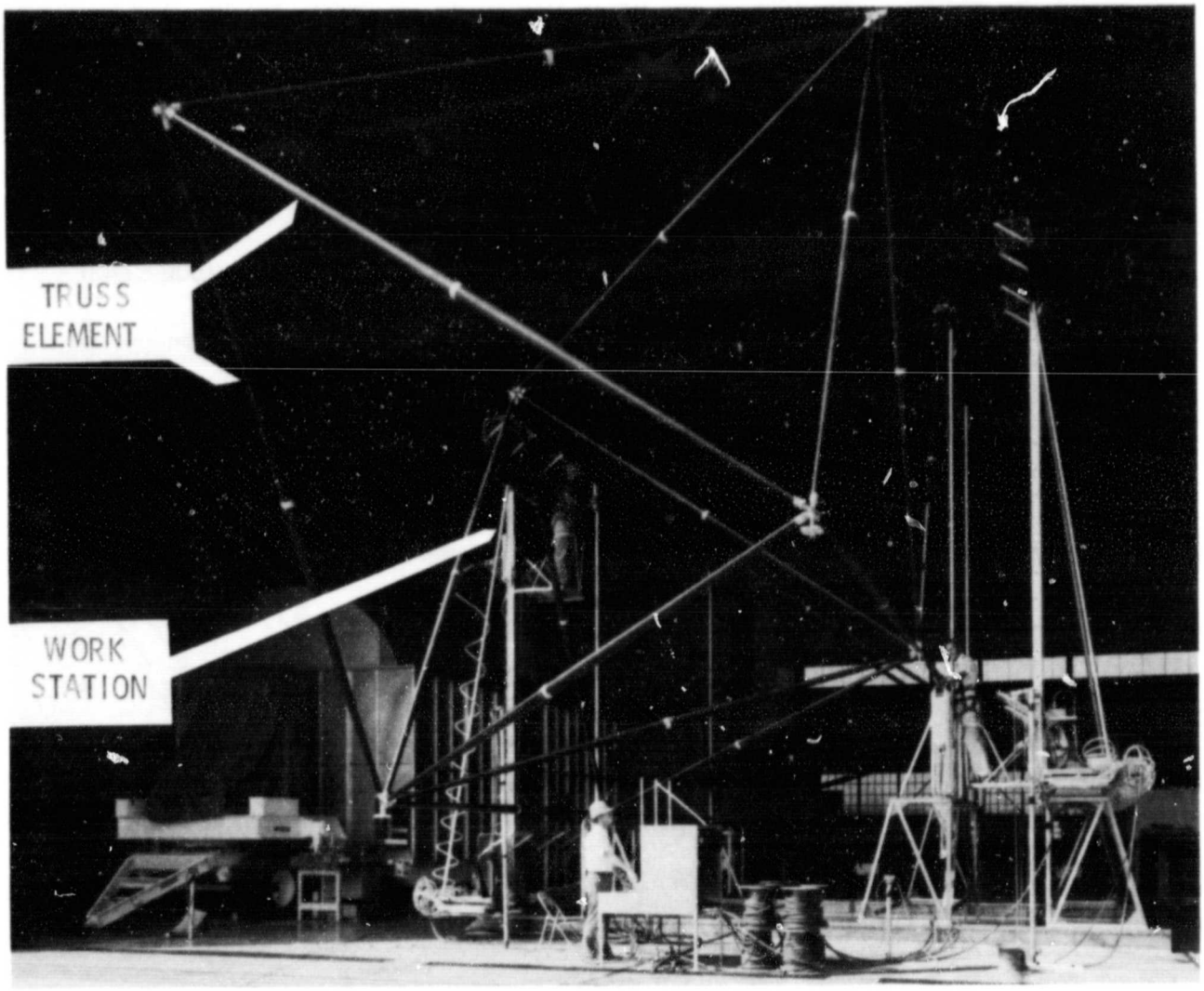


*Test model of mobile work station*

## Aerodynamic Heating on Corrugated Surface

Aerothermal tests were made in the Langley 8-Foot High-Temperature Structures Tunnel on a large $10.2^{o}$ blunted cone having a corrugated surface. The tests were made at Mach 6.7, with a total temperature of 1850 K. The cone was covered by a realistic

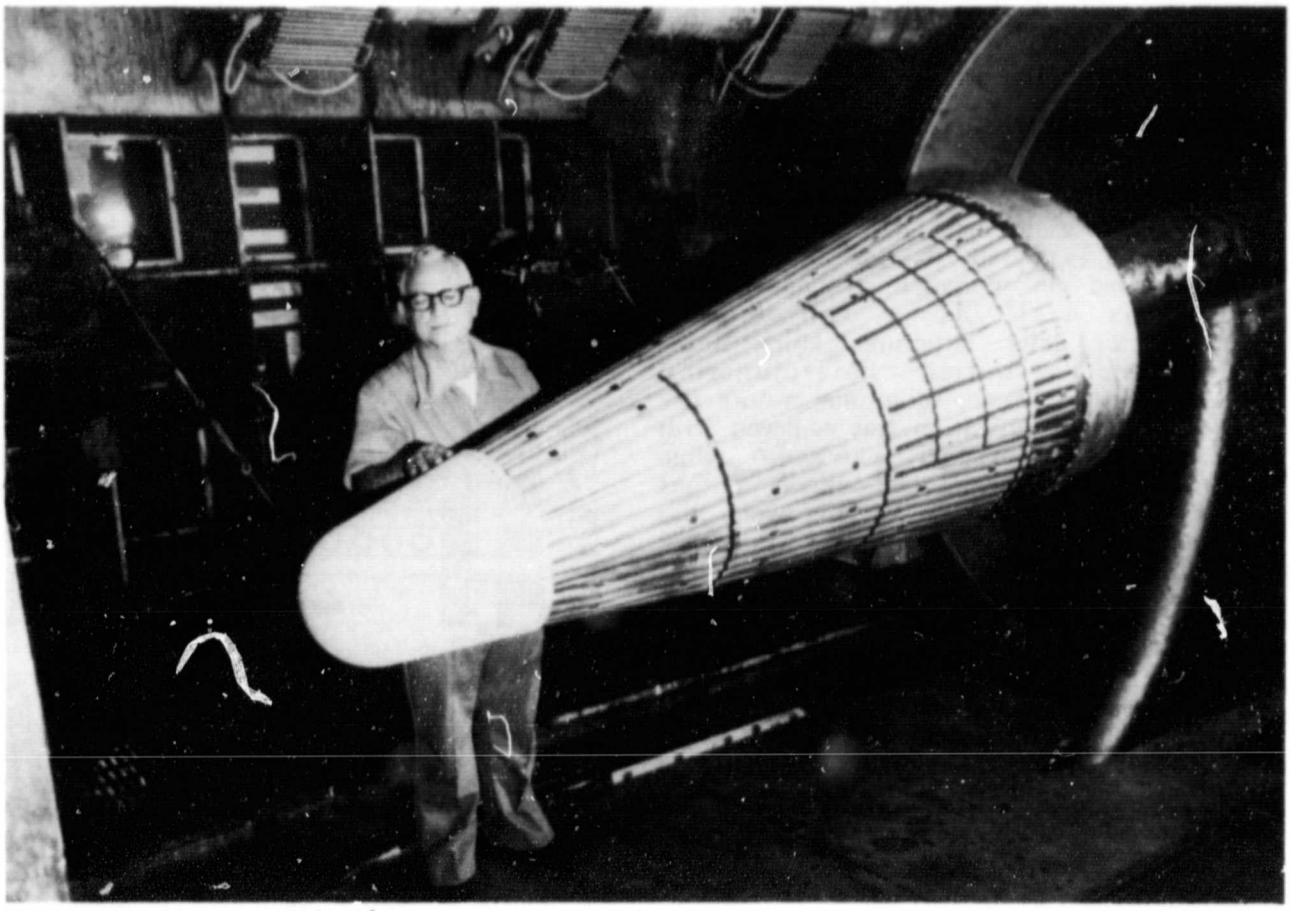

*Test model with corrugated surface*

corrugated thermal protection system (TPS) surface composed of 36 metallic panels.

The longitudinal and circumferential heating distributions show that the heating along the windward meridian of a corrugated cone at an angle of attack of $10^{o}$ is slightly overpredicted by smooth-surface turbulent theory. The heating on the crests appears to be slightly higher than on the flats, probably due to a thinner boundary layer on the crests. The circumferential heating is reasonably well predicted by turbulent theory from the windward meridian to $\pm 50^{o}$ around the body, but the heating then reduces rapidly around to the leeward side as a result of pressure-induced separation produced by adverse tunnel-flow blockage effects. Generally, the heating over a corrugated surface can be reasonably predicted by smooth-surface theory and any discrete effects of the corrugations are probably washed out by flow disturbances due to panel overlap and other minor surface discontinuities. Any effects of the corrugations, however, are small, and there appear to be no excessive penalties imposed due to the use of corrugated surfaces.

Irving Weinstein, 3155 (506-53-63)

## New InGaAs/InP Single-Mode Lasers for Space Applications

Future NASA missions in geosynchronous orbit require devices and components which can operate reliably over long periods of time in a thermally variant radiation environment. In addition, many of the satellite systems must run at high data rates as well as perform at low power levels with overall systems designed for light weight. Optical fiber data systems provide many of the above advantages provided they are operated in the 1- to 1.7-$\mu$m region of the optical spectrum. Development of semiconductor lasers to

provide optical emitters in this region has been pursued by RCA under contract to NASA Langley Research Center. Recently a significant contribution has been made to the understanding of liquid phase epitaxy (LPE) growth kinetics of InGaAsP on the nonplanar surfaces which are utilized in present-day single-mode laser designs. Of four different surface types evaluated, the inverted raised V mesa resulted in complete filling of the region as well as a reproducible semiconductor laser structure. Using these results and a buried heterojunction single-mode laser design, room-temperature CW (continuous-wave) operation was achieved with threshold currents as low as 60 mA while obtaining single longitudinal mode output powers as high as 3 mW. This work has provided better understanding of the LPE growth kinetics involved in the development of improved-performance single-mode InGaAsP/InP semiconductor lasers.

In a related materials growth technology area, a NASA-funded program at North Carolina Agriculture and Technology State University has resulted in the development of a new technique for the growth of epitaxial layers of InGaAs. Epitaxial layers with electron mobilities as high as 8900 $cm^2/V\text{-}s$ have been grown by electrotransport onto both InP and GaAs substrates. This new current-controlled liquid phase epitaxial growth technique appears to be a very promising technology for the deposition of high-quality epitaxial layers of InGaAs onto InP and GaAs substrates.

Herbert D. Hendricks, 3418 (506-54-63)

## Self-Structured Magnetic Bubble Memories

Tape recorders for data storage are one of the most failure-prone subsystems in U.S. spacecraft. This fact coupled with the costs associated with high-reliability manufacture has led to an urgent need to replace tape recorders with an all-solid-state memory. Projected storage capacities and data rates exceed existing solid-state memory technology. For this reason, a research program has been initiated to determine the feasibility of coupling the self-structuring properties of magnetic bubbles with current access techniques to provide up to a tenfold increase in both data capacity and data rate

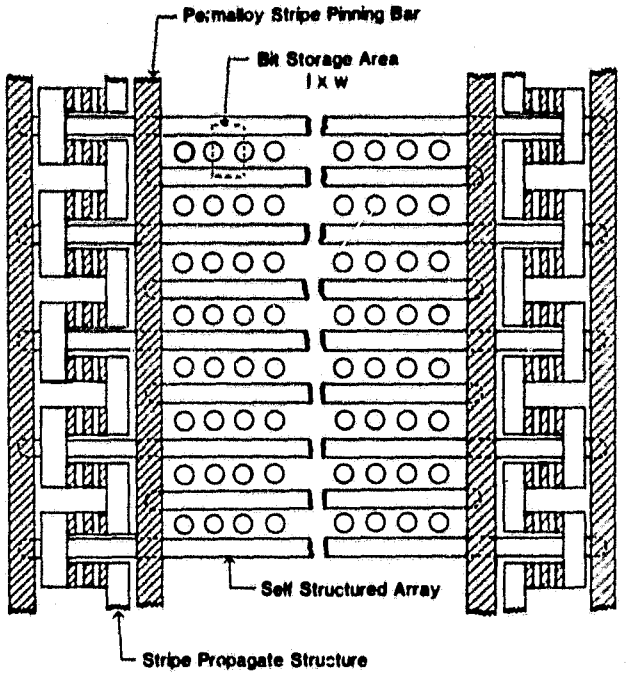


*Self-structured bubble memory*

over conventional magnetic bubble devices. A new bubble lattice has been investigated in which a group of magnetic bubbles are corralled between stripe domains which are pinned to permalloy bars, as illustrated. Data are encoded as the presence or absence of a bubble located under a lattice bubble and in a second ferrimagnetic garnet layer. This lattice configuration provides increased stability and offers significant advantages over the full bubble lattice investigated by others. Specifically, the stripe domains eliminate the possibility of rows of bubbles moving with respect to the rest of the lattice and causing data scrambling.

A test device was designed, fabricated, and evaluated during the past year as a combined in-house and contractual effort. This test device uses the bottom layer as the data layer, which allows planar fabrication methods. The detector utilizes the difference in strip-out threshold between a single bubble and a double bubble to detect the data. The test device was fabricated at Sperry Univac. Though only limited testing could be performed due to processing techniques associated with the glass passivation layer, the tests confirmed operation of all basic functions such as detection, generation, and propagation. An improved glass passivation process has been completed and a more thorough testing program has begun.

Robert L. Stermer, Jr., 3535 (506-54-63)

## Wavelength Division Multiplexing

Recently a data distribution system based on fiber optics has demonstrated a new concept of wavelength division multiplexing/demultiplexing for application in spacecraft and aircraft data communication systems. This concept permits individual data channels to be distributed simultaneously at individual wavelengths on the same data bus/data distribution system and be received without the need for a designator protocol to determine which station is to receive each data channel. The concept was realized through the assignment of a specific semiconductor laser wavelength to each type of data transmission channel, the use of a biconical tapered coupler for multiplexing the four individual wavelengths used onto a common fiber-optic data bus, and the use of beam-splitting interference filters for wavelength demultiplexing at the four receiving stations.

Commercially available electronics, detectors, interference filters, and optics were utilized in the system which was fabricated at Langley Research Center. Single-mode AlGaAs/GaAs semiconductor lasers developed under contract with RCA were used as the wavelength sources. Evaluation of the wavelength division multiplexing/demultiplexing data distribution system was performed with all four transmitters operating simultaneously. With 30 dB of receiver gain no optical crosstalk could be measured or detected between any of the data channels. Bit error rates of less than $10^{-9}$ were achieved for operation frequencies in the 1- to 10-MHz range. This work has demonstrated that the wavelength division multiplexing concept can be engineered into a data communication system with excellent data transmission characteristics.

Herbert D. Hendricks, 3418 (506-54-63/505-34-43)

## Decoupling Control Theory for Large Flexible Space Structures

A technique has been developed which utilizes decoupling and observation theory to control the pitch attitude and the flexible-mode amplitudes of a large flexible structure in orbit. The technique provides a stable and robust control system which has been validated by computer simulations for a 100-m-long flexible beam. Decoupling theory permits the control of one or more modes without affecting the other modes in the model. Observation theory incorporates the Kalman filter in order to estimate the modal state variables (needed for feedback), which otherwise could not be measured.

Complete decoupled control is usually not achievable in practical applications because a large space structure may have an infinite number of flexible modes; hence, procedures were applied to maintain control of the structure with a relatively small number of control actuators. In addition, only one or two sensors were required for the observer. The practical effects of structural- and controller-model error, sensor-location error, inoperative control actuators, and actuator dynamics were of minor significance.

Harold A. Hamer, 3917 (506-54-93)

## First Solar-Pumped Gas Laser Achieved

Continuing research in cooperation with Vanderbilt University into high-power lasers for space applications at Langley produced a significant first with the solar pumping of a gas laser. The figure is a schematic of the experiment which directed broadband simulated solar energy into a laser cavity containing gaseous $C_3F_7I$ to produce a near-infrared beam of coherent laser radiation. This conversion of solar energy into laser energy occurs directly without the intermediate transformation to electricity required for a conventional laser, thus offering great potential for on-board weight reduction and improved overall efficiency compared to conventional schemes.

Between spacecraft, laser power transmission offers the important advantages of small beam divergence and loss, small receiving antenna, and large energy density. Gas and liquid lasers are especially suited for solar pumping because high-temperature operation and lasant recirculation minimize heat rejection requirements and allow scaling to the high powers proposed for future space missions. The present lasant was previously

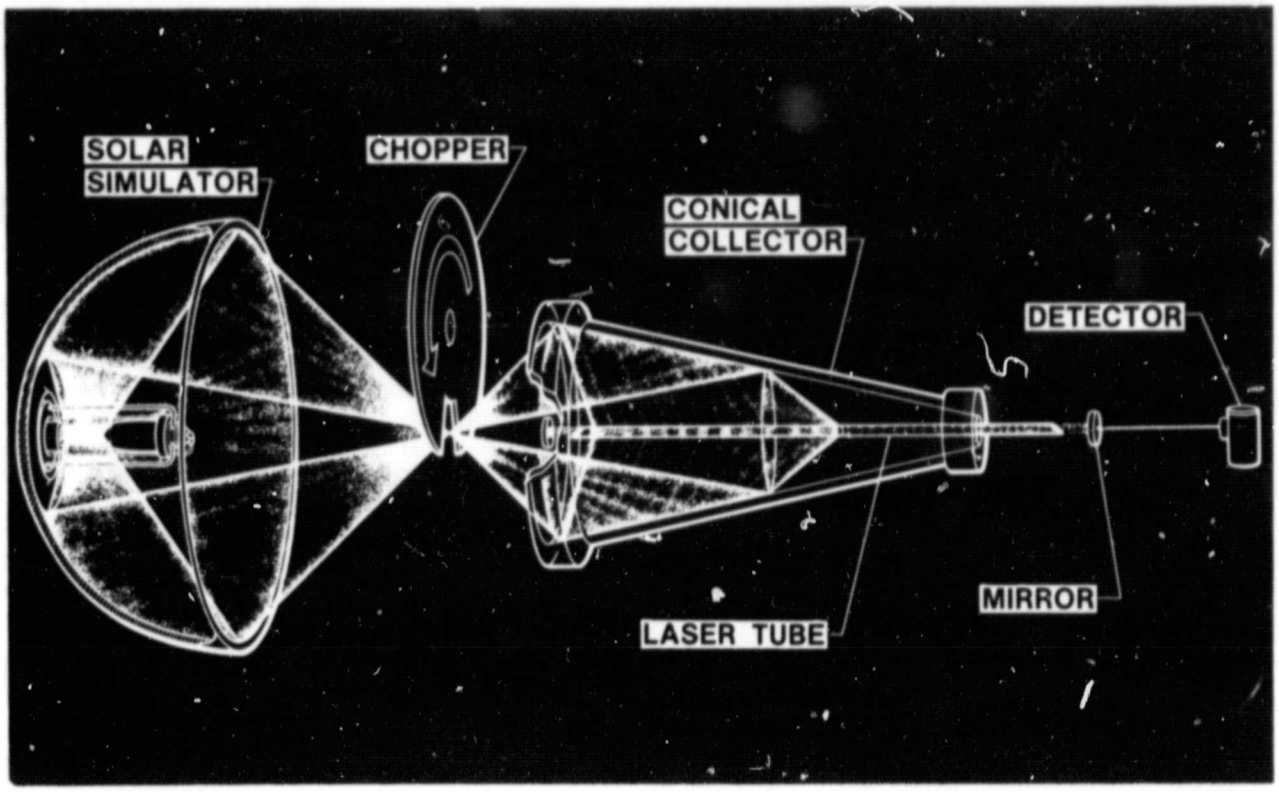


*Solar-pumped gas laser*

shown to have great potential for scaling to high peak output powers ($10^{12}$ W). Since the solar power required for the experiment is obtainable from a collector only 2 m in diameter, advances made in concentrators and large-scale structures programs should permit collector scaling by at least a few orders of magnitude, resulting in potential output powers using the present lasant on the order of tens of kilowatts.

Willard R. Weaver, 3791 (506-55-13)

## Ozone Air-Collisional-Broadening Coefficients

Remote and *in situ* measurements of atmospheric ozone often depend upon the accuracy and availability of infrared spectroscopic data for ozone. While relatively good data currently exist for line position, line strength, and ground-state energies, there has been a conspicuous absence of data for the air-collisional-broadening coefficients, and where experimental data have been reported, major discrepancies exist. Recent laboratory measurements have resulted in the most extensive set of ozone air-collisional-broadening coefficients to date. These measurements, covering the $\nu_1$ and $\nu_3$ bands of ozone (8.8 to 10 $\mu$m) suggest, as expected, transition-dependent coefficients. More importantly, however, the average air-collisional-broadening coefficients for both the $\nu_1$ and $\nu_3$ bands are about 20 percent lower than the currently accepted values given in the Air Force Geophysical Laboratory (AFGL) compilation.

J. M. Hoell, 2818 (506-61-33)

## Annular Suspension and Pointing System (ASPS)

The original ASPS configuration, consisting of two conventional gimbals and a vernier system, utilizing five magnetic bearing actuators (MBA's) and a roll motor for payload isolation and control, has been evaluated analytically and experimentally to

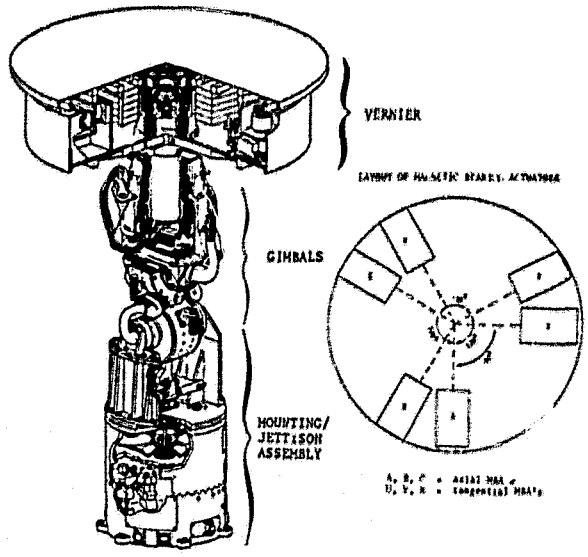


*Second-generation ASPS configuration*

demonstrate the viability of the concept in satisfying the stringent control requirements of a large variety of payloads. To alleviate system operational problems, such as providing backup control in all axes for safeguarding of payloads in case of pointing system component failure, the ASPS configuration has been redefined to include three conventional gimbals and six MBA's in the vernier.

This approach provides highly accurate control capability in all axes via the MBA's and payload protection through the use of the three redundant gimbals. In addition, significant cost savings may be realized in the production of the ASPS hardware since commonality in component designs, such as for the MBA's and the gimbals, may be more widely applied. Using high-fidelity simulations developed from hardware test results, the performance capability of the new configuration has been evaluated and error budgets have been generated to account for all known component characteristics. Results indicate that the 0.01-arc-seconds goal can be attained even in the presence of Shuttle disturbances. These efforts have been performed by NASA and Sperry Flight Systems of Phoenix, Arizona under contract to NASA Langley Research Center.

Claude R. Keckler, 3917 (506-61-43)

## Modeling of Multispectral Sensor System Concepts

To overcome present inefficiencies in worldwide monitoring of resources and the environment by remote multispectral sensing, it is necessary to make such sensor systems "smart" enough so that they can be relied upon to avoid clouds and haze, identify and locate features of interest, and compensate for atmospheric variability. The development of such smart-sensor systems must take into account the complex natural variability of surface and cloud reflectance and atmospheric radiative transfer which the present MSD (mean square distance), techniques do not. To do so, smart-sensor concepts should be developed and evaluated first as models in the computer, and only thereafter, if promising, as actual devices and systems.

A suitable computational model is being developed which accounts for remote multispectral data acquisition and classification as a function of both deterministic and stochastic elements of solar irradiance, atmospheric radiative transfer, surface and cloud reflectance, sensor response, and data processing and classification algorithms. The figure shows preliminary results of a comparative evaluation of the present Landsat multispectral scanner (MSS) and the future Landsat thematic mapper (TM) and multispectral linear array (MLA). The results depict classification accuracy for various agricultural fields and forests as a function of spectral channels (MSS and TM/MLA), classification algorithm (MLH and MSD), and visibility (23, 10, and 5 km); the reference pattern was obtained with 23 km visibility. The MLH (i.e., maximum likelihood) classification algorithm accounts for variabilities of atmospheric radiative transfer and surface reflectance, which the MSD does not, and the classification accuracy of the MLH algorithm is clearly superior.

Friedrich O. Huck, 3535 (506-61-53)

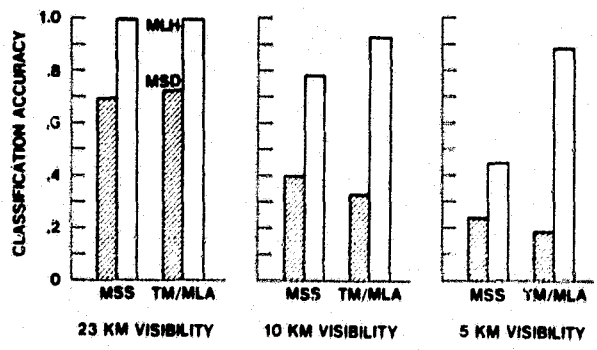


*Simulated classification accuracy for remote sensing systems*

## Electrostatically Controlled Membrane Reflectors

Applications of radiometers on spacecraft typically include environmental monitoring, soil moisture sensing, atmospheric research, and communications. More powerful spaceborne radiometers of the future depend on the ability to erect large reflecting surfaces. A 4.9-m-diameter electrostatically formed reflector has been tested at Langley for surface distortion as part of the Large Space Systems Technology Program. As illustrated, five separate power supplies are connected to five concentric electrodes. The material shown on the ring is 7.62-$\mu$m-thick Kapton polyimide plastic film. Typically, the voltages used in the testing have varied from 40 kV on the center electrode to 60 kV on the outer ring. Several different methods have been used to measure the surface smoothness: photogrammetric photography, triangulation using digital theodolites, and a laser system using a modified Foucault equation.

A systems analysis was completed to determine requirements for a 100-m-diameter electrostatically formed spacecraft antenna reflector. The 4.9-m-diameter ground test article is effectively a 1:20 scale model of the 100-m space reflector. Preliminary test results indicate that a residual roughness of about 0.75 mm (rms) exists with the commercial "off-the-shelf" Kapton film used in these initial tests, and is within the surface quality limits required for radiometer applications.

John W. Goslee, 3666 (506-62-43)

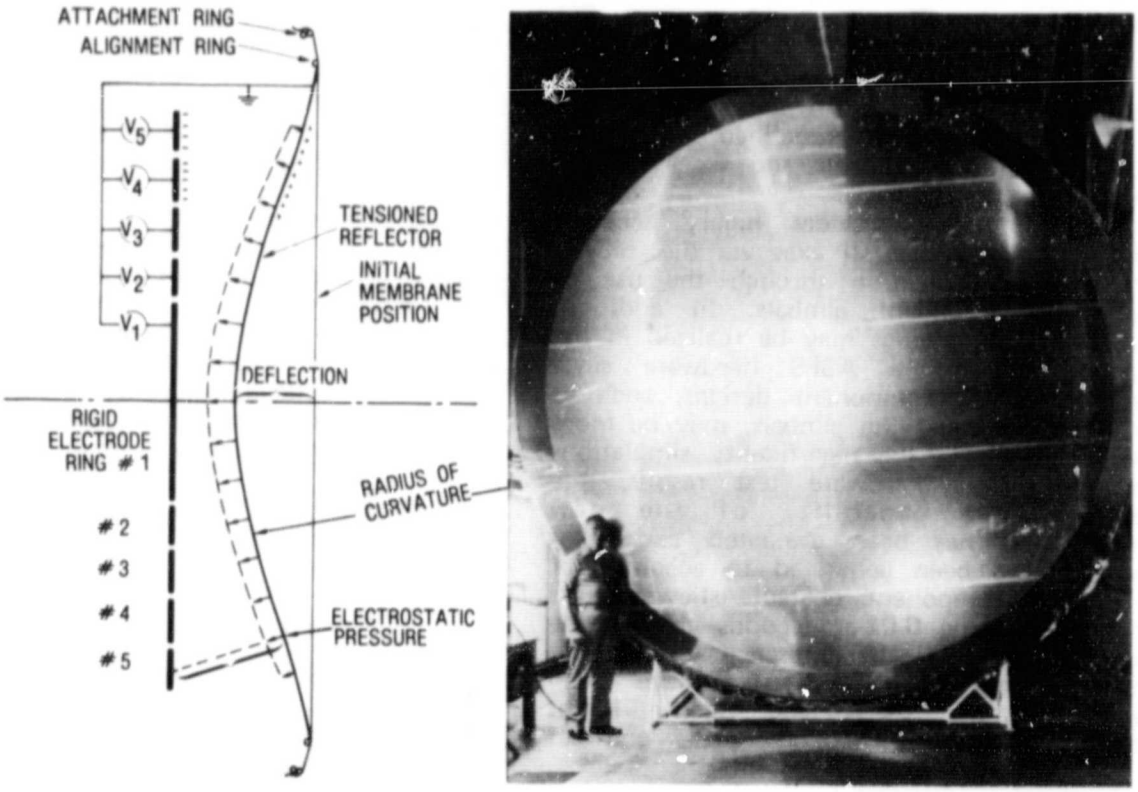


*Electrostatically erected reflector*

## Assessment of Approximated Equations in Unsteady Flow

Several low-frequency time-marching finite-difference methods have been developed in recent years for predicting unsteady aerodynamic loads in the transonic regime. These codes are based on approximations obtained by deleting from the equations

terms whose importance diminishes as the frequency of oscillation decreases. The resulting simplified equations lead to codes which are more efficient than solutions of the full equations. A linear theory has been developed in-house which solves these approximate equations exactly. This theory allows one to assess, for the first time, the accuracy and range of validity of the coded algorithms for the linear case.

The figure compares three analytic methods for calculating unsteady loads on a two-dimensional airfoil oscillating in pitch about a mid-chord axis at Mach number 0.8. The real (in phase with the motion) and imaginary (in quadrature) parts of the lift are shown as functions of reduced frequency over the range of interest in flutter calculations. The solid line represents the exact solution for linear subsonic flow with complete equations. The dashed lines show the new results for two levels of approximation to the equations: (1) the long-dashed curve is the analytic solution of the problem with the second time-derivative of the velocity potential term omitted from the differential equation; (2) the short-dashed curve is the analytic solution with the additional omission of the time-dependent terms from the boundary conditions. Comparison of these three exact results shows the errors that occur as the governing equations are successively simplified. Particularly significant for flutter prediction is the large error in damping (imaginary part) that occurs with the more approximate analysis at quite moderate frequencies.

Comparisons with these exact analytic results verify the accuracy of the finite-difference codes (not shown). Codes based on analysis which neglects time-dependent boundary conditions, such as the widely used LTRAN2 code, are not adequate for flutter prediction.

Samuel R. Bland, 2661 (505-33-53)

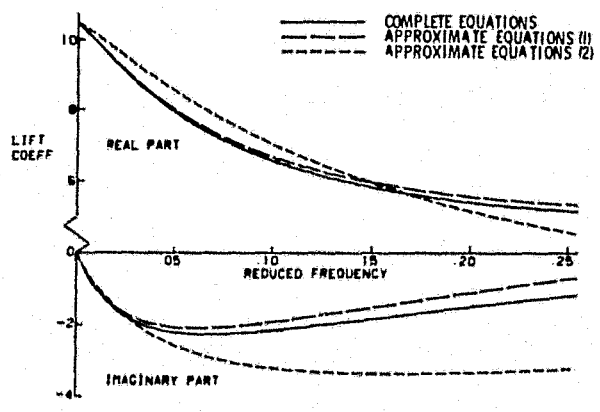


*Calculated unsteady load with various approximations*

## CARE III (Computer-Aided Reliability Estimation)

An innovative, elaborate mathematical model which enables researchers and design engineers to assess the reliability of complex fault-tolerant digital systems has been developed by The Raytheon Company and was successfully installed at Langley Research Center and at the Wright Patterson Avionics Laboratory. The mathematical model is embodied in a computer program called CARE III (Computer-Aided Reliability Estimation). Its development was conceived and technically managed at Langley Research Center and has been jointly funded by the U.S. Air Force and NASA.

CARE III is unique in that it provides a method for modeling very large systems, such as aircraft flight control systems, and it incorporates a universal fault-handling model. A group of national researchers, meeting at the Research Triangle Institute in North Carolina, verified the analytic soundness of CARE III. The group's findings have been published in NASA CP-2167. By request of the U.S. Army at Fort Monmouth, the Hughes Aircraft Company (under contract to the Army) has completed CARE III

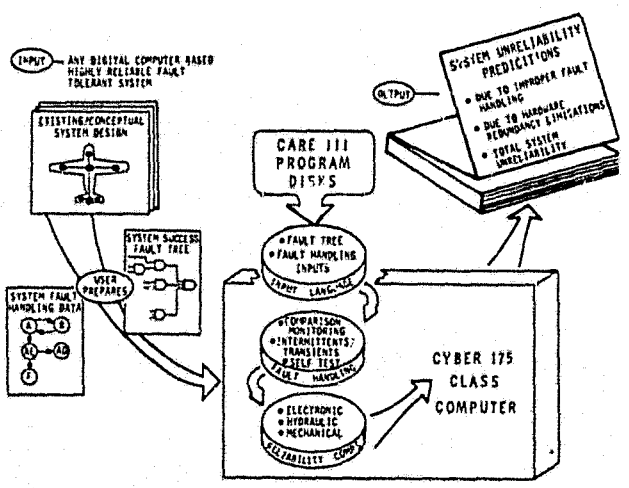


*Computer-aided reliability estimation (CARE III)*

evaluation for incorporation into the Failure Management Design System Development Program. As part of the evaluation, Hughes applied CARE III to a fault-tolerant highly reliable signal processor system comprised of 300 processors.

Sal Bavuso, 3681 (505-34-43)

## Reduction of Aircraft Ground Loads

The capability of an experimental active-landing-gear shock strut has been evaluated in a joint Air Force/Langley study. The active gear is designed to mitigate ground loads experienced by an F-4 aircraft when operating from hastily-repaired bomb-cratered runways. As part of this study a multi-degree-of-freedom flexible-aircraft takeoff and landing computer program is employed to conduct landing simulations of an F-4 aircraft with the original gear and with the gear modified to include active loads control.

Aircraft center-of-gravity acceleration time histories were obtained from computer simulations with both the original and the active gear. The time histories include landing impact and a subsequent traversal of a repaired bomb crater located 328 m (1000 ft) from the point of touchdown. The active gear reduces landing-impact accelerations by 26 percent and crater-traversing accelerations by 70 percent compared with the original gear. These results illustrate the potential of an active gear to reduce ground loads and improve ride quality for the pilot in ground operations.

J. R. McGehee, 2796 (505-44-33)

# Space and Terrestrial Applications

## Ultrasonic System Measures Rock Strain

A cooperative research program between Langley Research Center and the U.S. Bureau of Mines has resulted in a new technology advance in mine safety. The development utilizes a Langley invention for the measurement of changes in acoustic propagation which accompany strain due to loading forces in mine pillars or walls, and which can sometimes warn of cave-ins. The research conducted in the Langley laboratory for ultrasonics shows that a nonlinear stress-induced acoustic phase shift can be measured with a geodynamic accumulated strain sensor ($GAS^2$). The $GAS^2$ is a technology spin-off from the nondestructive evaluation of materials and structures program and has the benefits of an integral large-volume *in situ* strain sensor with resolution of a few parts in $10^6$.

The $GAS^2$ device was recently recognized by Industrial Research & Development magazine as one of the 100 most significant technological developments of 1981. The development and demonstration of this instrument for direct measurement of rock strain should greatly improve and advance mine safety.

Joseph S. Heyman, 3418 (141-20-14)

## Miniature Solar Dosimeter

A low-cost lightweight miniature solar ultraviolet (UV) dosimeter is being developed under the auspices of Langley's Technology Utilization Program. Intended as a tool for research in the fields of medicine, biology, agronomy, horticulture, and dairy science, it has the capability to detect radiation in selected wavebands and time-integrate the intensity variations of the radiation.

The sensitive element consists of a small planar-diffused silicon photovoltaic detector to collect incident radiation after passage through interposed filter(s) selected to block out unwanted radiation. The detector converts the radiant energy into an electrical current which is proportional to the rate of energy absorbed. An electrochemical coulometer (E-cell) measures the electrical charge by plating silver ions onto an electrode at a rate proportional to the input charge.

To quantify the radiant energy absorbed by the dosimeter during an exposure period, a constant-current source is used to deplate the silver in the removable E-cells, restoring them to their initial state for reuse. Radiation dosage is determined by measuring the time required to deplate the silver.

Radiation within wavebands of interest is obtained by selective filtration. In medical research, for use in studies of the relationship between the incidence of skin cancer and the ultraviolet portion of the spectrum, two sets of optics, sensors, and coulometers are utilized, allowing the subtraction of unwanted infrared effects present when glass absorption filters are used. Standardization and calibration of the instrument can be accomplished using known light sources to establish the joule equivalent of the electrical conversion.

Ian O. MacConochie, 3911 (141-20-20)

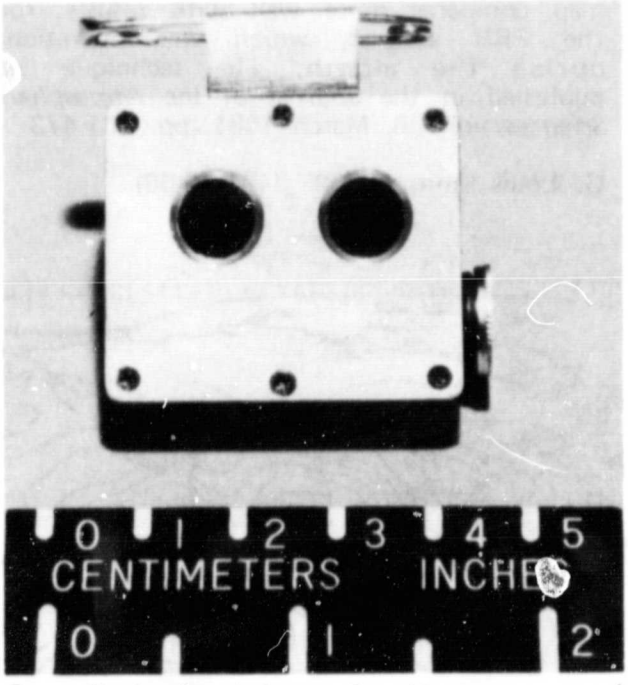


*Personalized solar dosimeter for skin cancer research*

## Clouds and the Radiation Budget

Measurements of cloud cover and its radiative properties are essential to an understanding of the effects of clouds on the Earth's radiation budget (ERB), and ultimately on the Earth's climate. Hourly Geostationary Operational Environmental Satellite (GOES) visible (0.5 to 0.7 $\mu$m) and infrared window (10.5 to 12.5 $\mu$m) digital data from November 1978 have been analyzed with an automated bispectral threshold method developed at Langley Research Center to quantify regional cloud cover. The automated technique eliminates most of the subjectivity of conventional

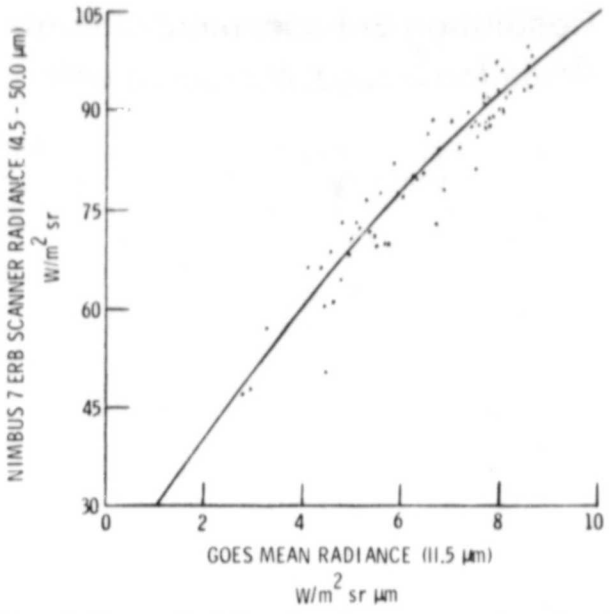


*Correlation of infrared window and broadband radiances*

nephanalyses, computes cloud and surface radiative properties, can cover large areas at a high temporal resolution, and is as accurate as conventional techniques.

This study resulted in the first satellite-to-satellite narrowband/broadband correlations. Empirical spectral transfer functions were derived from nearly simultaneous Nimbus 7 ERB broadband scanner radiances and GOES narrowband measurements. The results indicate a high correlation (0.96) between the infrared window and the longwave broadband data. In comparison, this experimental relationship is almost identical to theoretical approximations. Although the visible-channel albedo was also found to be highly correlated with the shortwave albedo, the two are not equal. These results may have important consequences for ERB estimates derived from narrowband data. Application of the spectral transfer functions to the full GOES cloud data set has also produced some significant results. It was found that systematic diurnal variations of both cloud cover and the radiation budget are generally larger and more widespread, especially over oceans, than was previously suspected. These diurnal cloud oscillations have a substantial impact on the global radiation budget and should be included in the parameterization of clouds for climate models. Analysis of data for other months is continuing in order to study the seasonal and annual variability of regional cloud cover.

Patrick Minnis, 2977 (146-10-06)

## Resolution Enhancement of Earth Radiation Budget Measurements

The Earth radiation budget (ERB) instrument which flew on the Nimbus 6 and 7 spacecraft includes wide-field-of-view (WFOV) radiometers, as does the Langley-managed Earth Radiation Budget Experiment (ERBE) which is scheduled to fly in 1983. The originally intended use of WFOV data was for heat flux measurements at very large scales. However, development of a resolution enhancement technique by Langley researchers now permits extraction of finer details of the radiation field.

The field of view of the WFOV radiometer at Nimbus 6 altitude is a circle on the Earth with a diameter of over $60^{o}$ of great circle arc. Each data point is an integral of the irradiance from all points within the field of view, weighted by the directional response of the sensor. The measurement thus has a very low resolution. In order to enhance the resolution of these data, the measurement is considered to be an integral equation which is to be solved for the emitted radiation leaving the top of the Earth-atmosphere system. Application of the new technique to Nimbus 6 ERB WFOV data has shown that features as small as $12^{o}$ to $15^{o}$ Earth central angle can be retrieved for the first time from such data. A resolution-enhanced map of Earth-emitted radiation is shown for August 1975. This map compares quite well with results from the ERB scanner, which was operational during the month. The technique was published in the *Journal of the Atmospheric Sciences,* vol. 38, March 1981, pp. 461-473.

G. Louis Smith, 2868 (146-10-06)

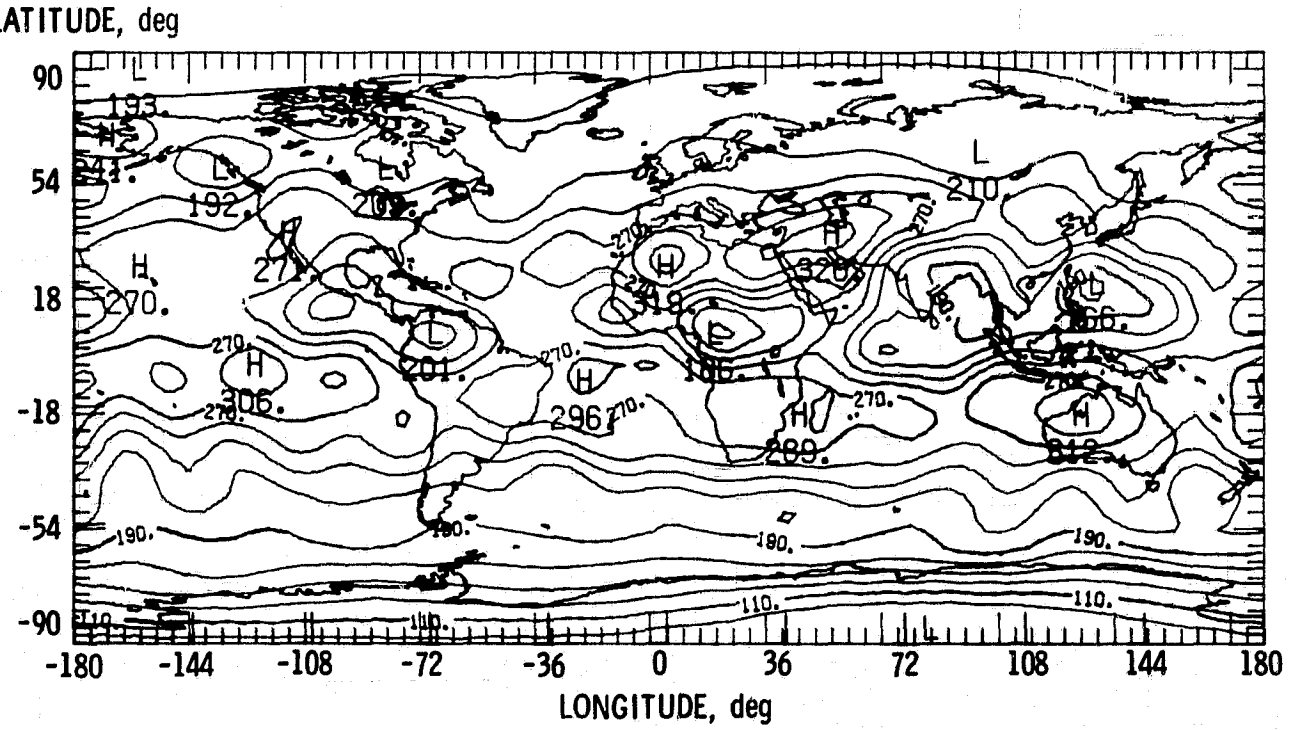


*Map of longwave radiant exitance ($W/m^2$)*

## Annual Cycle of Earth-Emitted Radiation

A knowledge of the annual cycle of the distribution of Earth-emitted radiation is fundamental to the understanding of the annual cycle of climate and its variations. To help define that cycle, measurements taken over a period of a year by the

wide-field-of-view (WFOV) radiometer of the ERB (Earth radiation budget) instrument aboard the Nimbus 6 satellite have been analyzed to study the variation of emitted (infrared) radiation leaving the top of the atmosphere. This study was performed using a new resolution enhancement technique for emitted radiation which was developed at Langley Research Center.

An empirical expression was developed for the variation of emitted radiation flux as a function of $f_0$, the annual average of the emitted energy at some latitude, and $f_M$, the variation about the annual average at that latitude. The annual average $f_0$ is seen to be high at tropical latitudes and low at polar latitudes, as one would expect. The low value at the equator is due to the high band of clouds which is characteristic of the intertropical convergence zone. The high values of $f_0$ on each side of the equator correspond to regions of subsidence which mark the great deserts of the world. The asymmetries of $f_0$ are due to the differences in land-ocean distribution between the Northern and Southern Hemispheres. The $f_M$ curve describes the amplitude of the annual cycle of emitted radiation, which varies sinusoidally with time during the year and was found to lag the Sun's position by 34 days.

T. D. Bess, 3431 (146-10-06)

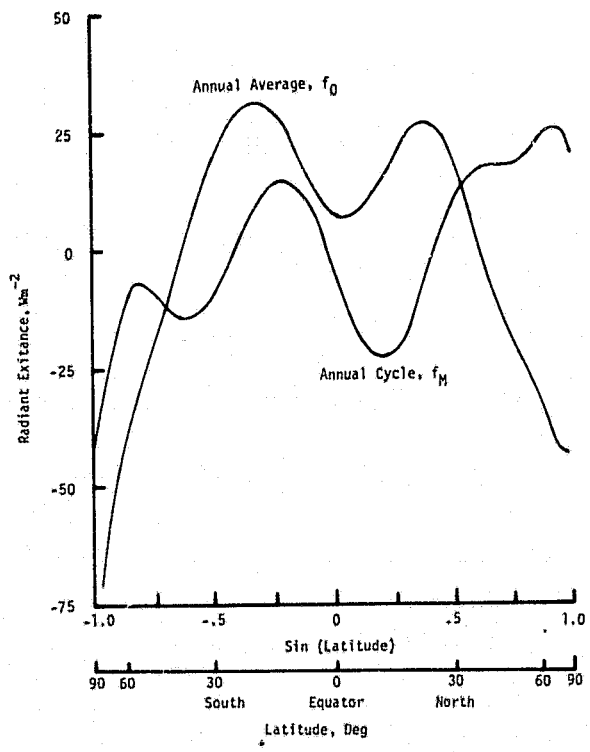


*Variation of Earth-emitted radiation with latitude*

## Origin of Tropospheric Ozone Examined

Changes in tropospheric ozone levels could lead to significant changes in several biogeochemical cycles influencing the Earth's radiation budget, which may in turn lead to climatic and meteorological changes. Thus, it is important to understand the natural cycle of tropospheric ozone so that any perturbations to this system can be properly assessed.

Using available observations of ozone ($O_3$) and carbon monoxide (CO) and a numerical photochemical model of the troposphere, a new theory on the origin of tropospheric ozone was proposed which indicated that anthropogenic activity had greatly perturbed the natural tropospheric $O_3$ cycle. In 1978 researchers hypothesized that the dominant source of $O_3$ in the troposphere was the oxidation of CO by the hydroxyl radical (OH) in the presence of nitric oxide (NO), rather than ozone leakage from the stratosphere as had been popularly assumed. Subsequently, Langley work on the concurrent distributions of $O_3$ and CO using fast-response sensors for both trace gases indicated that the small-scale fluctuations of these two species were generally positively correlated. The most pronounced positive correlations were located in the middle troposphere of the Northern Hemisphere midlatitudes, which is where the largest source due to photochemistry should be observed according to the 1978 theory.

To further clarify the role of the photochemical processes which influence the tropospheric ozone cycle, Langley Research Center is currently developing and testing a new package of aircraft-borne instruments to detect other key trace gases. Initial test flights were completed during the summer of 1981, and the prospects for planning a comprehensive sampling strategy are very encouraging.

J. Fishman, 3109 (146-20-08)

## Remote Sensing of the Troposphere

Langley Research Center and Environmental Protection Agency personnel conducted a field measurement program to measure the vertical distribution of ozone and

aerosols in the upper and lower troposphere using remote and *in situ* sensors. The scientific objective of the program was to study regional and global transport, source, and sink mechanisms for ozone and aerosols. Instrumentation included the Langley airborne ultraviolet differential absorption lidar (UV-DIAL) remote sensor and various *in situ* sensors onboard aircraft, tethered balloon, and sonde platforms. Geostationary meteorological satellite imagery was used extensively for mission planning and real-time implementation. The program was divided into three experiments, each focusing on a particular altitude region within the troposphere.

The first experiment investigated the development of the atmospheric boundary layer as a function of time of day in a complex coastal environment. The effect of the vertical dynamics within the boundary layer on the vertical distribution and horizontal transport of ozone and aerosols was also measured. Measurements performed by the UV-DIAL showed the microstructural entrainment of aerosol-rich air aloft into the boundary layer as convective plumes penetrated these layers from below. The second experiment studied a proposed mechanism for transport of boundary-layer ozone into the free troposphere via convective clouds. Afternoon and evening measurements were made of the profiles of ozone and aerosols in an air mass with cumulus convective activity to search for ozone and aerosol-rich air injected into the stable air above the average afternoon mixing height. The results of the experiment may be incorporated into an ozone-sink module in EPA's Regional Oxidant Model. The objective of the third experiment was to measure the vertical structure of ozone and aerosols in the upper troposphere near the tropopause using the zenith-looking mode of the UV-DIAL. Ozone structure was successfully measured up to 13 km and aerosols up to 14 km. In addition, measurements were made of the horizontal-vertical structure of ozone and aerosols on the north side of the jet stream over Maine. The measurements demonstrated the feasibility of future studies of stratospheric ozone intrusions into the troposphere.

David S. McDougal, 2486 (146-20-10)

## Methane and Hydrocarbons Above the Northern and Southern Atlantic

An automated hydrocarbon analyzer, which had been developed at Langley and successfully applied to regional tropospheric methane and nonmethane hydrocarbon measurements from aircraft, was employed by a Langley researcher on an international science expedition sponsored by the Deutsche Forschungsgemeinschaft (German Research Society) in West Germany. The expedition was formed to characterize environmentally important atmospheric trace gases in the marine boundary layer. Methane and nonmethane hydrocarbon measurements (important in both the global carbon and ozone cycles) were made at hourly intervals aboard the research vessel, which departed Hamburg on October 7, 1980, and arrived in Montevideo, Uraguay on November 8, 1980.

Methane concentrations were found to average about 1.70 ppm in Northern Hemispheric marine boundary-layer air between 40° N and 12° N latitudes. A pronounced change (decrease) in methane concentration was observed during passage through the intertropical convergence zone beginning at about 12° N latitude. The Southern Hemispheric marine air concentrations of methane averaged 1.62 ppm between 10° N and 32° S latitudes. The latitudinal gradient, or difference in methane concentrations between Northern and Southern Hemispheres, is in good agreement with observations made during a Pacific Ocean expedition, suggesting that this is a global phenomenon.

W. R. Cofer III, 2065 (146-20-10)

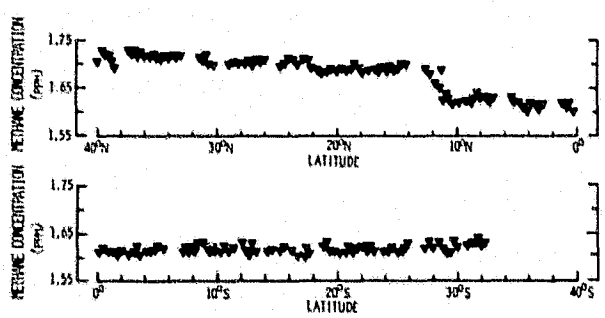


*Measured methane distribution*

## Lidar Regional Measurements of Ozone and Aerosol Distributions

The Langley airborne differential absorption lidar (DIAL) system was used in the study of ozone and aerosols during the Environmental Protection Agency's field experiment conducted in July and August 1980. The objectives of this investigation were the characterization of Persistent Elevated Pollution Episodes (PEPE) and model validation in the Northeast Regional Oxidant Study (NEROS). There were 14 missions flown by the DIAL system on board the Wallops Flight Center Lockheed Electra aircraft. During these missions, a total of 42.5 hours of aerosol data and 32 hours of ozone data was accumulated.

The aerosol data obtained during PEPE/NEROS contain the type of detail shown in the accompanying figure. The picture is made up of 600 nadir-viewing lidar returns representing about 39 km horizontal distance. The stronger scattering (and greater aerosol levels) is indicated by the higher brightness. The ground reflection appears as a bright line at the bottom of the picture with the left side obtained over land (Virginia) and the right side over the Chesapeake Bay. As shown on the left side of the picture, the lidar detects clouds and provides a direct measurement of cloud top height. When the clouds are optically thick, signals are obtained to limited ranges in the cloud, and ground returns cannot be seen. The abrupt increase in aerosol scattering above the cloud tops indicates a mixing height of about 2.5 km over land. As can be seen, there is less vertical mixing and a lower mixing height over the Chesapeake Bay. A catalog of lidar aerosol profiles and mixing height measurements obtained during the PEPE/NEROS field experiment has been generated at Langley. These data will be archived at EPA for future investigations using the complete EPA data set. Boundary-layer processes and tropospheric dynamics are being studied at Langley using the aerosol distribution information available in this extensive lidar data set.

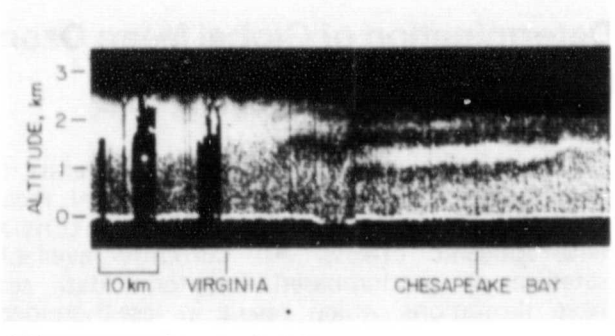


*Lidar-measured aerosol data*

Comparisons between the first airborne remote measurements of ozone profiles by a lidar system and the *in situ* ozone measurements made during the PEPE/NEROS field experiment were found to agree to within ±10 ppb. Ozone profiles were obtained for a vertical and horizontal resolution of 210 m and 6 km, respectively. The variability of ozone above and in the mixed layer is being studied on a regional scale to assist in oxidant model validation and to investigate the relative importance of transport and photochemistry in determining the budget of tropospheric ozone.

E. V. Browell, 2576 (146-20-10)

## Nantucket Shoals Experiment

The Dynamics of Phytoplankton Patches on Nantucket Shoals, a Langley experiment to investigate the distribution and abundance of phytoplankton biomass on the Shoals in relation to rates of nutrient supply, growth, vertical mixing, and advective processes, was performed in May 1981. The thrust of the experiment was to use real-time remote sensing techniques to determine spatial distribution of temperature, chlorophyll, phytoplankton diversity, suspended solids, and salinity at subtidal frequencies over the entire region. The experiment made optimal use of shipboard *in situ* and aircraft and satellite remote sensing techniques to perform the required measurements. Co-investigators included scientists from the Northeast Fisheries Center, Brookhaven National Laboratory, Woods Hole Oceanographic Institution, Marine Sciences Research Center – State University of New York, and Bigelow Laboratory for Ocean Science. They performed shipboard studies of optical properties, phyto- and zooplankton, nutrient chemistry, hydrography, and both Lagrangian and Eulerian current velocity measurements.

The experiment was highly successful, with 100 percent of the planned missions accomplished. Two aircraft flew a total of 39½ hours at altitudes of 0.152, 1.52, and 12.5 km (500, 5000, and 41 000 ft) measuring distributions of chlorophyll, fluorescence, salinity, and ocean color

parameters. The six participating surface vessels occupied about 160 complete oceanographic stations during the experiment and provided continuous water temperature, salinity, and fluorescence sampling.

Due to the cold weather and high winds during the experiment, the delineation between well-mixed and stratified regions was not as sharp as in past years. Surface nutrient concentrations were highest in the cold regions and showed good inverse correlation with temperature. Chlorophyll varied by a factor of five across the Shoals, with a clear maximum downstream from the colder, highly nutrient regions. It appears that there is excellent agreement between measured phytoplankton growth rates, nutrient supply rates, chlorophyll abundance, distances between sources and patches, and observed current velocities. More detailed analysis will include accounting for tidal excursion effects and a more complete nitrogen and carbon/chlorophyll budget.

W. E. Esaias, 2871 (146-40-15)

## Satellite Evidence of Global Ozone/Solar Activity Relation

There has been considerable interest in determining whether there is a relationship between global mean ozone and solar activity, since the existence of such a relationship might mask any effect of chlorofluoromethanes on stratospheric ozone. Evidence has accumulated from ground-based ozone measurements of variations in ozone with a period on the order of 11 years at various locations, but there has been a lack of consensus as to whether these variations are related to the 11-year solar activity cycle. Satellite instruments now provide the potential for obtaining improved global trends because of their more extensive coverage. By evaluating global trends with satellites, many of the local and regional dynamical effects measured by ground stations which could disguise the smaller effects of possible solar variations are filtered out.

Analysis of global ozone variations for the period from April 1970 to December 1975 was performed using the reprocessed Nimbus 4 backscattered ultraviolet (BUV) measurements of total ozone. A correlation coefficient of 0.97 is found between the

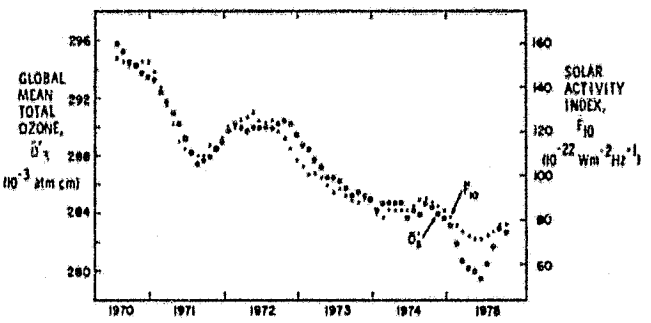


*Correlation of mean (filtered) ozone with solar activity*

6-month running mean of global mean total ozone (filtered for mean semiannual, annual, and quasibiennial variations) and the 10.7-cm solar activity index. The study was performed by a Langley researcher and his colleagues at Systems and Applied Science Corporation, and is being published in the *Journal of Geophysical Research.*

Correcting the satellite ozone data for a time-dependent latitudinal bias relative to ground-based Dobson ozone measurements reduces to 2 to 3 percent the global mean ozone variation over the solar cycle. This still substantially exceeds the decrease in ozone from 1970 to 1975 expected from anthropogenic sources. A study with a one-dimensional time-dependent radiative photochemical model has shown that the ozone variability can be accounted for assuming a 10- to 20-percent ultraviolet (UV) variability (over the solar cycle) of solar radiation between 0.18 and 0.21 $\mu$m. This variability appears to be consistent with recent solar UV observations. Thus, based on the photochemical model and this empirical study using Nimbus data, accurate knowledge of solar UV variability may be important in separating the variations in ozone related to natural and anthropogenic effects.

Gerald M. Keating, 2084 (146-60-01)

## Determination of Global Mean Ozone With Limited Spatial Sampling

There is currently considerable interest in determining natural variations of global mean ozone and in searching for potential anthropogenic effects. All currently available satellite or ground-based long-term data sets have limitations which result in less-than-ideal spatial distributions for determining the global

mean. The error due to sampling can become a significant and, in some cases, dominant source of error.

A technique has been developed for evaluating the errors in the estimated ozone field due to the spatial distribution of the data. The ozone field to be estimated from the data is expanded in a set of spherical harmonic functions. Due to various data limitations, only a finite number of coefficients in the expansion can be determined. The error due to truncating the series is shown to be equivalent to the error introduced by nonglobal sampling, and is shown to be relatively insensitive to the data noise. The technique permits evaluation of the relative effects of sampling and data noise if the first and second (variance spectra) statistics of the truncated part of the field are known. For the total ozone field, these statistics have been developed using 7 years of Nimbus 4 backscattered ultraviolet (BUV) data.

The technique has been validated using the Nimbus 4 IRIS (infrared interferometer spectrometer) data which provide essentially global coverage for 10 months, from April 1970 through January 1971. One result of the application of the technique is shown in the figure, where monthly mean total global ozone ($C_0$) in Dobson units is shown for the 10 months of IRIS data. Two estimates are shown for each month slightly displaced in time for clarity. The estimates on the right (one error bar) are obtained by directly processing the IRIS data. The error is due to data noise only, which is the dominant error source for the nearly global coverage afforded by the IRIS data. The estimates on the left were obtained by deleting IRIS data to simulate BUV coverage. The BUV instrument can only make measurements in the illuminated hemisphere; hence, there are no measurements in the winter polar regions. Two error bars are shown for these estimates. The smaller bars indicate the error to be expected from data noise only. These are seen to be relatively insensitive to the loss of data in the polar regions. The larger error bars include the effects of both data noise and sampling. They clearly provide a better measure of differences between the two estimates near solstices. The importance of realistic error estimates is evident when it is seen that the error due to sampling can be as large as the natural annual variations in global mean ozone. In addition to data analysis applications, the technique is also applicable in evaluating the relative merits of improving measurement accuracy or sampling density for future satellite measurements.

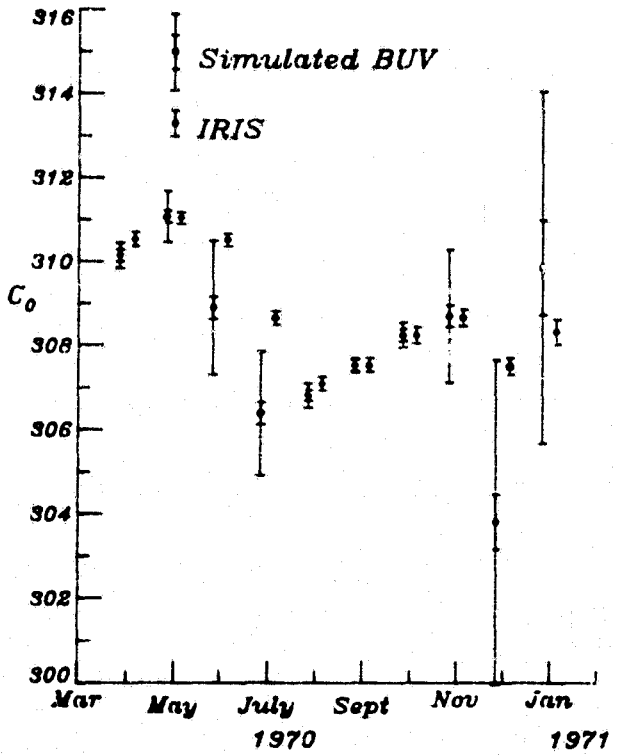


*Comparison of IRIS · data and simulated BUV estimates*

Robert H. Tolson, 2530 (146-60-01)

## Combined Effects of Atmospheric CFM and $CO_2$ Increases

It is well known that increases in atmospheric levels of chlorofluoromethanes (CFM's) may lead to decreases in stratospheric ozone ($O_3$) due to catalytic destruction by the chlorine cycle. Increases in atmospheric $CO_2$ result in a warming of the troposphere and a cooling of the stratosphere with attendant ozone increases at altitudes above 30 km. For a scenario with increases in both the CFM's and $CO_2$, there has been speculation that the $CO_2$ effect on $O_3$ may offer significant compensation for the $O_3$ reductions due to the CFM's.

To resolve this question, a Langley-developed radiative-convective photochemical model was used to calculate the combined effect on atmospheric ozone. The calculations were carried out for a

steady-state situation in which $CO_2$ levels were set at 660 ppmv (twice current levels) and the release rate for the CFM's was taken to be that reported for 1977.

The results show the changes in ozone profiles for several different $CO_2$ and CFM cases. As expected, the effect of the $CO_2$ increases is to reduce the amount of $O_3$ destruction (due to the CFM's) in the vicinity of 40 km. However, within the troposphere the effect on $O_3$ depends upon whether the effect of surface temperature increases due to the "greenhouse effect" of both the CFM's and $CO_2$ is included. With the inclusion of the calculation of the surface temperature, the warming in the troposphere due to the CFM's and $CO_2$ leads to significantly higher levels of water vapor and, hence, hydrogen oxides ($HO_x$). The higher levels of $HO_x$ alter the tropospheric chemical cycles in such a way that tropospheric $O_3$ levels are significantly reduced, offsetting the compensating effects of $CO_2$ in the stratosphere. The net compensation in total $O_3$ due to the inclusion of $CO_2$ is only 0.62 percent in the steady state. More importantly, however, this calculation indicates that perturbations of optically active gases in either the stratosphere or troposphere, which lead to significant surface temperature changes ($\geq 2^{\circ}$C), may have the potential to significantly alter tropospheric chemical processes. Heretofore, this has been a relatively unexplored coupling mechanism.

Linwood B. Callis, Jr., 2985 (147-30-01)

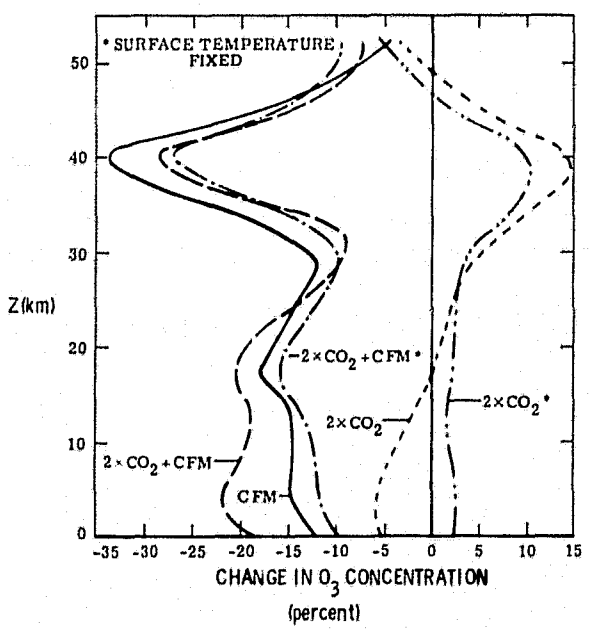


*Steady-state ozone change as a function of altitude*

## Atmospheric General Circulation/Tracer Model

A three-dimensional primitive-equation general circulation model developed at Langley is being used to study stratospheric dynamics and transport. In recent experiments, the model successfully simulated the seasonal transition in the stratosphere with reversal from zonal westerlies in winter to summer easterlies. During the simulation, a midwinter stratospheric warming developed spontaneously in the polar stratosphere with features characteristic of observed warmings. Comparison of the model results with climatological mean data demonstrates the suitability of the model for representing many features of the large-scale circulation. The model has also been used to study the transport of volcanic injected aerosol in the stratosphere. Results have been compared with ground-based lidar data from several stations and show good agreement for the aerosol mixing ratio decay rate.

A chemistry submodel has been formulated for use with the circulation/transport model. Simulations will be conducted to study the spatial and temporal variations of ozone and other chemically active constituents of the stratosphere. Comparisons of the model results with large, global sets of satellite data should prove useful both for interpreting the data sets and identifying model deficiencies.

W. L. Grose, 2039 (147-30-01)

## Observation of Polar Stratospheric Clouds

The Stratospheric Aerosol Measurement (SAM II) satellite experiment was launched onboard the Nimbus 7 satellite on October 24, 1978 to study the stratospheric aerosol layer, which is thought to play a major role in radiative interactions which affect the Earth's climate. Due to the satellite orbital characteristics, SAM II obtains aerosol extinction profiles from $64^{\circ}$ to $80^{\circ}$ latitude in both the Northern and Southern Hemispheres. Background values of peak extinction at the SAM II wavelength of 1.0 $\mu$m are 1 to 2 $\times$ $10^{-4}$ $km^{-1}$ with no clouds for both polar regions. However, in the first

year of operation SAM II observed numerous stratospheric clouds with altitudes of 12 to 23 km and peak extinction values as high as $1 \times 10^{-2}$ $km^{-1}$. Twelve clouds were observed in the Arctic stratosphere and 538 clouds were observed in the Antarctic stratosphere, each during local wintertime. Prior to these observations, such clouds were considered extremely rare, with only 148 sightings documented in the Northern Hemisphere from 1870 to 1973.

The occurrence of these wintertime polar stratospheric clouds appears to be strongly correlated with low temperatures. They are much more prevalent in the Antarctic stratosphere during the colder austral winter and increase the stratospheric optical depths by as much as an order of magnitude for a period of about 2 months. Therefore these clouds could possibly represent a sink for stratospheric water vapor as well as play an important role in the Earth's radiation balance.

M. P. McCormick, 2466 (665-10-40)

## Recent Results from Nimbus 7 LIMS Experiment

The Limb Infrared Monitor of the Stratosphere (LIMS) experiment was launched October 24, 1978 on board the Nimbus 7 satellite. The experiment operated for more than 7 months measuring vertical radiance profiles across the atmospheric limb of the Earth. These profiles were later ground-processed to infer upper-atmosphere temperature profiles and the concentrations of key chemical compounds believed to be important in the stratospheric ozone photochemistry. In addition to temperature, LIMS measured vertical mixing ratio profiles of ozone ($O_3$), nitric acid ($HNO_3$), nitrogen dioxide ($NO_2$), and water vapor ($H_2O$). The LIMS instrument is a six-channel thermal infrared radiometer which uses HgCdTe detectors cooled to ~64 K by a two-stage solid cryogen cooler ($CH_4$ inner stage and $NH_3$ outer stage).

The validation of the LIMS results is now essentially complete. Comparisons were made for each measured parameter with a number of *in situ* soundings of those parameters conducted at the time of the LIMS overpasses. In general, the agreement of the LIMS and *in situ* data sets lies within the overlap of the estimated error bars of both sets of measurements. Scientific investigations of upper atmosphere processes have only just begun in earnest, but there are several points of note which have already been revealed by the data, and although these results are still preliminary, they are mentioned here to indicate the kinds of phenomena which can be observed by LIMS. The results clearly show low nitric acid levels in the tropics and maxima in high latitudes with a poleward and downward slope on the altitude of the maximum. The changeover from winter to summer distribution of $HNO_3$ appears to occur rapidly as evidenced by the fact that the winter maximum has diminished by early April. There appears to be very little variability in the global water vapor horizontal or vertical distribution in springtime at all latitudes. The water vapor profile at this time is virtually constant with altitude at a level of about 4 ppm, as illustrated. The presence of large $NO_2$ diurnal change predicted by models is prominently observed by LIMS. Also, the occurrence of a sharp decrease in $NO_2$ concentration at high winter latitudes in the polar night is observed.

The LIMS data are currently being operationally produced, and results of large data blocks are being evaluated by the experiment team to search for any data dropout or similar anomalies which may not be screened by the software. All data should be in the public archive of the National Space Sciences Data Center by November 1982.

James M. Russell III, 2576 (665-10-40)

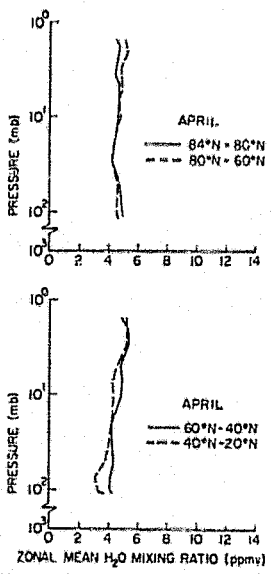


*LIMS zonal mean $H_2O$ mixing ratio*

# Satellite Mapping of Volcanic Effluent in the Stratosphere

The two satellite sensors SAM II (Stratospheric Aerosol Measurement), flown on Nimbus 7, and SAGE (Stratospheric Aerosol and Gas Experiment), flown on AEM-2 (Applications Explorer Mission), have recently demonstrated the ability to detect and track globally the effluent ejected into the stratosphere by volcanic eruptions. The global nature of the data collection also allows estimation of the mass of new material injected into the stratosphere and, therefore, the potential climatic impact of such an eruption.

SAM II and SAGE provide highly resolved vertical profiles of aerosol extinction at 1.0 $\mu$m wavelength. The orbital characteristics of the two satellites are such that together they collect data from 80° N to 80° S latitude. SAM II collects data from 64° to 80° latitude in both hemispheres, while SAGE collects data from 70° N to 70° S latitude.

In the first 1½ years of operation SAGE has detected the injection and mapped the distribution of material in the stratosphere from three volcanoes. The first eruption observed was that of the volcano La Soufriere on the island of St. Vincent in April 1979. In November 1979, SAGE observed the injection of material from an almost unnoticed eruption of the volcano Sierra Negra in the Galapagos Islands. This eruption was observed to have injected at least 10 times more material into the stratosphere than La Soufriere and increased the global stratospheric aerosol mass by approximately 20 percent. In May 1980 SAGE observed the injection of material from Mount St. Helens. During the next 4 months this material was observed by SAM II as well as SAGE to spread northward in latitude and slowly homogenize, resulting in a 50-percent increase in the global stratospheric aerosol mass.

M. P. McCormick, 2466 (665-40-40)

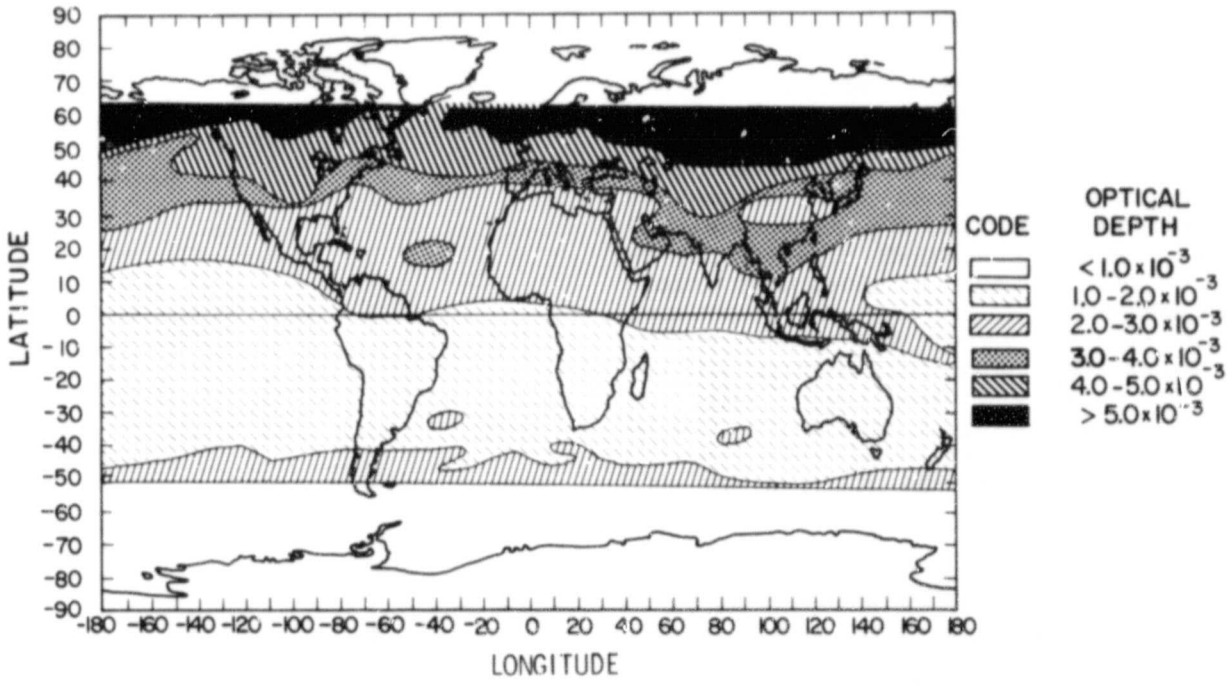


*SAGE measurements of optical depth (September 1980)*

## Environmentally Significant Trace Gases Produced by Lightning

$NO_x$ is a key gas in controlling the ozone budget of the troposphere. Experiments conducted in the Langley Lightning Facility resulted in the first simultaneous measurements of the production of $NO_x$ (nitric oxide, NO, + nitrogen dioxide, $NO_2$), NO, and $O_3$ (ozone) in a laboratory discharge. Chemical analyses of the discharge products indicate that all of the $NO_x$ produced in the discharge was in the form of NO and that there was no detectable enhancement of $O_3$. Combining our experimentally derived NO production rate with atmospheric lightning parameters, we calculate that lightning annually produces about 1.8 megatons of N in the form of NO. This value is considerably lower than previous estimates, which ranged from 35 to 90 megatons. For comparison, the annual global production of $NO_x$ due to anthropogenic activities, e.g., combustion processes, has been estimated to be about 20 megatons.

Recently, the Pioneer Venus Orbiter detected what are thought to be lightning discharges in the atmosphere of Venus. In a series of experiments conducted in the Lightning Facility, the role of lightning was investigated as a source of trace gases in a simulated Venus atmosphere (carbon dioxide, 95 percent, nitrogen, 5 percent, and smaller variable concentrations of water vapor and sulfur dioxide). Photoelectric and photographic spectra as well as gas chromatographic measurements were obtained during the laboratory discharge. It was found that very large amounts of carbon monoxide were produced during the discharge. The analysis of these Venus experiments is continuing as a collaborative effort between scientists at Langley, the NASA Ames Research Center, and the State University of New York at Albany.

In a flight program to assess the production of nitrous oxide ($N_2O$) in lightning, the Atmospheric Chemistry Experiment aboard the NASA Langley Storm Hazards Project F-106B Delta Dart obtained samples of air prior to and during exposure to the lightning environment of thunderstorms. These samples were then analyzed for their $N_2O$ content using a gas chromatograph/electron-capture detector. Analysis indicates that about one-third of the more than 100 thunderstorm samples showed $N_2O$ levels enhanced more than 10 percent above the clear air background level of about 308 parts per billion. $N_2O$ is environmentally important since it controls the destruction of stratospheric ozone, which protects the Earth's surface from lethal solar ultraviolet radiation. The F-106B samples constitute the first direct and unambiguous measurements of the production of a trace gas by atmospheric lightning and indicate a new localized natural source of atmospheric $N_2O$.

J. S. Levine, 2187 (146-20-10)

# Space Transportation Systems

## Combined Loads Orbiter Tests (CLOT)

A large variety of tests were made to determine the strength and fatigue characteristics of the thermal protection system of the Shuttle Orbiter. Included were tests of the individual components, single-tile systems, and tile arrays. Materials, vibroacoustic, aerodynamic load, and aerodynamic heating tests were conducted with models of varying size and complexity in the laboratory and in many types of wind tunnels. Simulations of the time histories of Shuttle ascent loads on tiles bonded to "real" structures were conducted in the Langley 8-Foot Transonic Pressure Tunnel, a type of test never before attempted in a wind tunnel of this size. Simulation concepts and hardware were developed for three separate areas on the bottom of the Shuttle; only the two declared critical for the first flight were tested. The two areas are located ahead of, and behind, the forward external-tank/Shuttle yoke bipod and are among the most critical on the Shuttle. Not only are local heating rates extremely high, but if a smooth surface is not maintained over this region through ascent, the heat of entry will be increased over the downstream areas and the structural integrity of the aerospacecraft will be jeopardized.

The test panel behind the yoke was selected because of the high buffet loads induced by the unsteady wake of the yoke, the high vibroacoustic loads, and the

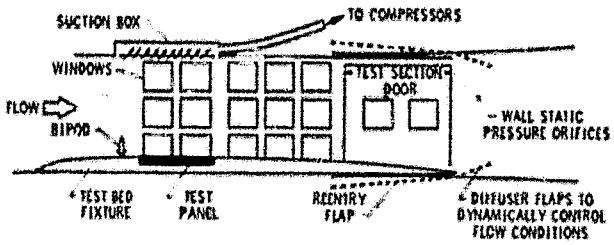


*Test setup for panel behind yoke*

possibility of a "step and gap" problem between the tiles due to these loads. The structure on this area is of the skin/stringer variety.

The panel ahead of the yoke includes the doors of the forward landing gear compartment. These doors are constructed of a thick honeycomb sandwich material and are so rigid that structural vibrations were not a concern in this area. However, buffet loads due to extremely high unsteady pressure levels caused by the supersonic bow shock were a concern.

The successful completion of these tests not only contributed greatly to the degree of confidence for the first Shuttle flight, but also marked a major milestone in the application of a large transonic tunnel to conduct tests on flight articles such as the Shuttle tiles with the following features: (1) combination of structural aerodynamic and acoustic loads, (2) time simulation of loads, and (3) diagnostic loads and response data.

Percy J. Bobbitt, 2961 (986-12-40)

## Aerodynamic Loads Assessment for Shuttle Orbiter Tiles

The major effort of the Langley Baseline Thermal Protection System (TPS) Life Assessment Task was an independent evaluation of the undensified tile loads and stresses which would occur during the ascent portion of STS-1 (Space Transportation System) mission. In support of the life assessment, Langley has developed an analytical three-dimensional internal flow model which systematically predicts the internal pressures and the steady aerodynamic loads acting on the tile system. This model is capable of analyzing a nine-tile array when the tile outer moldline pressure distributions and tile geometry are given. This model features various types of flows (laminar gap flow, flow through porous media, and preferred flow direction through filler bar to tile gap) and variable tile-gap and strain isolation pad (SIP) flow conductances. An iterative solution accounts for the tile movement and changes in the flow conductances. The model predicts the pressure distributions in the tile gaps, SIP, filler bar, and tile internal. The appropriate pressure distributions are numerically integrated to predict the steady aerodynamic loads acting on the tile during ascent.

George W. Ivey, Jr., 4656 (986-15-10)

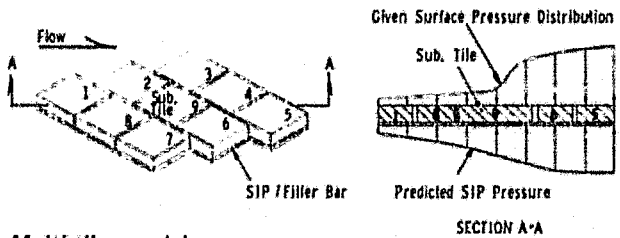


*Multi-tile model*